

编号	
----	--

江苏省成人高等教育精品资源共享课程建设

申报书

学校名称 南京农业大学

课程名称 兽医寄生虫学

课程层次 高起专 高起本 专升本

课程类型 公共基础课 专业基础课 专业课

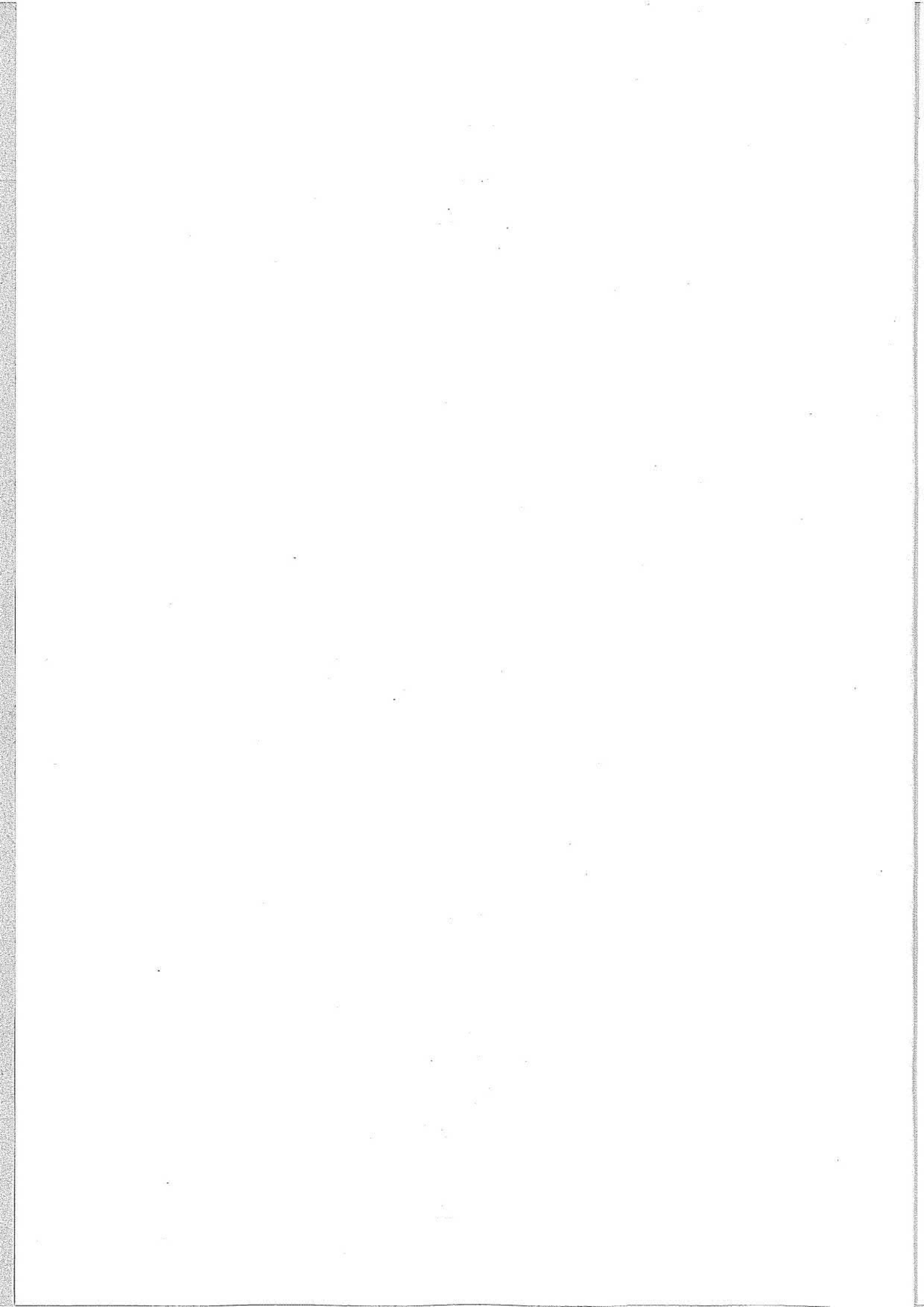
课程基础 校级精品 省级精品

所属一级学科名称 农学

所属二级学科名称 动物医学

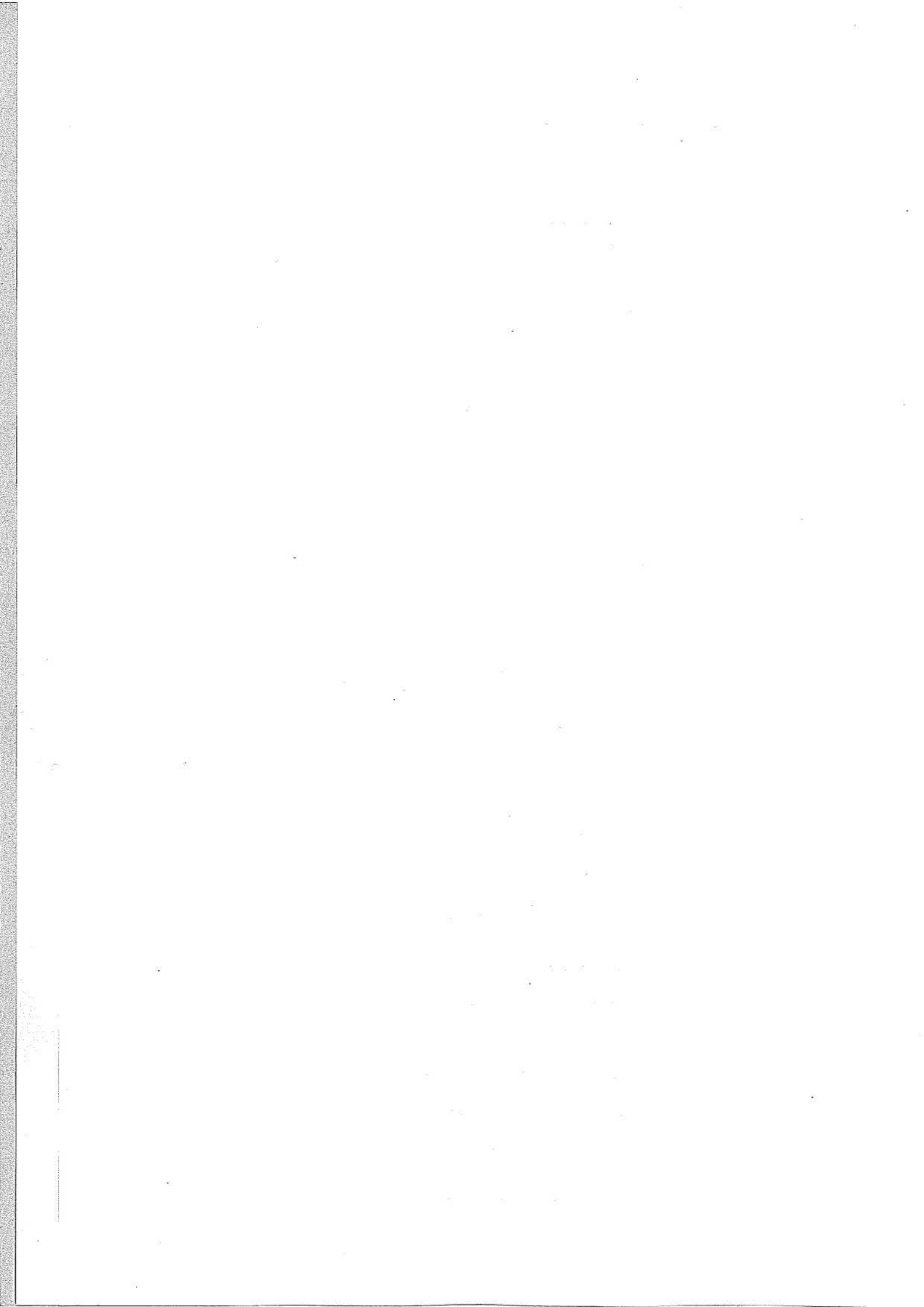
课程负责人 李祥瑞

申报日期 2016年12月08日



填写要求

1. 本表限用 A4 纸双面打印。
2. 表格文本中外文名词第一次出现时，要写清全称和缩写，再次出现时可以使用缩写。
3. 涉密内容不填写，有可能涉密和不宜大范围公开的内容，请在说明栏中注明。
4. 课程所属学科按教育部规定的方式分类：本科专业按照《普通高等学校本科专业目录》（教高〔2012〕9号）填报，专科专业按照《普通高等学校高等职业教育（专科）专业目录》（教职成〔2015〕10号）填报。
5. 本表中填写内容可以根据情况进行扩充；本表有关统计内容截止时间为 2016 年 8 月 31 日。



1. 课程负责人

基本信息	课程负责人	李祥瑞	性 别	男	出生年月	1958.12
	最终学历	博士研究生	专业技术职务	教授		
	学 位	博士	行政职务	无		
	所在院系	南京农业大学动物医学院				
	通信地址(邮编)	江苏省南京市卫岗 南京农业大学 (210095)				
	研究方向	预防兽医学				
教学情况	<p>近五年讲授本课程情况:</p> <p>2012年, 兽医寄生虫学, 动医 81-82 班, 62 人共 54 学时, 课程负责人授课 22 学时</p> <p>2013年, 兽医寄生虫学, 动医 91-92 班, 63 人共 54 学时, 课程负责人授课 19 学时</p> <p>2014年, 兽医寄生虫学, 动医 01-02 班, 65 人共 54 学时, 课程负责人授课 19 学时</p> <p>2015年, 兽医寄生虫学, 动医 11-12 班, 75 人共 54 学时, 课程负责人授课 19 学时</p> <p>2016年, 兽医寄生虫学, 动医 21-22 班, 59 人共 54 学时, 课程负责人授课 19 学时</p> <p>近五年来讲授的主要课程:</p> <ol style="list-style-type: none"> 1、兽医寄生虫学 (总学时 54), 本科专业课, 每周 5 学时, 5 届 324 人 2、兽医法规与专题讲座 (总学时 32), 研究生专业课, 每周 3 学时, 4 届 213 人 3、寄生虫分子与免疫学 (总学时 32), 研究生专业选修课, 每周 3 学时, 5 届 65 人 4、常见人兽共患病防治 (总学时 32), 本科公共选修课, 每周 2 学时, 2 届 87 人 5、兽医学专题 (总学时 32), 本科专业课, 每周 2 学时, 2 届 375 人 <p>承担的实践性教学任务:</p> <ol style="list-style-type: none"> 1、兽医寄生虫学实验, 学生人数 60-65 人/年, 5 年共指导 324 人 2、兽医寄生虫学实习, 学生人数 120-140 人/年, 5 年共指导 623 人 					

学术
研究

近五年来承担的学术研究课题:

1、捻转血矛线虫重组 Galectin 抑制山羊外周血淋巴细胞细胞因子转录的通路研究, 国家自然科学基金, 2012.1-2015.12, 主持人

2、鸡艾美耳球虫侵入部位特异性关键分子研究, 国家基金面上项目, 2014-2017, 主持人

3、鸡球虫树突状细胞刺激性抗原的确定及其应用, 国家自然科学基金委员会与巴基斯坦科学基金会合作研究项目, 2016-2019, 中方主持人

发表学术论文 (*示通讯作者):

1 GuangWei Zhao, Bo Shen, Qing Xie, Li Xin Xu, Ruo Feng Yan, Xiao Kai Song, I.A. Hassan, Xiang Rui Li *Detection of Toxoplasma gondii in free-range chickens in China based on circulating antigens and antibodies. *Veterinary Parasitology*, 2012, 18, 572 - 577 doi:10.1016/j.vetpar.2011.10.031

2. Wang Wang, Cheng Yuan, Shuai Wang, XiaoKai Song, LiXin Xu, RuoFeng Yan, I.A. Hasson, XiangRui Li. Transcriptional and proteomic analysis reveal recombinant galectins of *Haemonchus contortus* down-regulated functions of goat PBMC and modulation of several signaling cascades in vitro. *Journal of Proteomics*, 2014, 98, 26:123 - 137

3. Qing Xie, Julia Klesney-Tait, Kathy Keck, Corey Parlet, Nicholas Borcharding, Ryan Kolb, Wei Li, Lorraine Tygrett, Thomas Waldschmidt, Alicia Olivier, Songhai Chen, Guang-Hui Liu, Xiangrui Li & Weizhou Zhang. Characterization of a novel mouse model with genetic deletion of CD177. *Protein Cell*, 2014: DOI 10.1007/s13238-014-0109-1

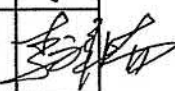
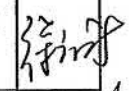
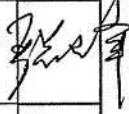
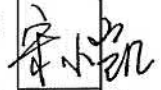
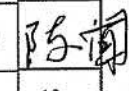
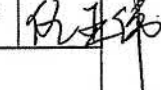
4. ZhenChao Zhang, JingWei Huang, MengHui Li, YuXia Sui, Shuai Wang, LianRui Liu, LiXin Xu, RuoFeng Yan, XiaoKai Song, XiangRui Li*. Identification and molecular characterization of microneme 5 of *Eimeria acervulina*. *PLOS ONE* | DOI:10.1371/journal.pone.0115411 December 22, 2014

5. Javaid Ali Gadahl, Bu Yongqian, Muhammad Ehsan, Zhen Chao Zhang, Shuai WANG, Ruo Feng Yan, Xiao Kai Song, Li Xin Xu and Xiang Rui Li, *Haemonchus contortus* excretory and secretory proteins (HcESPs) suppress functions of goat PBMCs in vitro.

学术研究表彰/奖励:

1、Induction of protective immunity against *Eimeria tenella*, *Eimeria necatrix*, *Eimeria maxima* and *Eimeria acervulina* infections using multivalent epitope DNA vaccines 被评为中国畜牧兽医学会兽医寄生虫学分会第十三次学术研讨会优秀学术报告一等奖, 2015.7

2. 课程团队

	姓名	性别	出生年月	单位	职称	学科专业	在课程建设中承担的工作	签字
主讲教师、教学辅助人员基本信息	李祥瑞	男	1958.12	南京农业大学	教授	预防兽医学	课程建设与教学	
	徐立新	男	1968.2	南京农业大学	讲师	预防兽医学	课程建设与教学	
	严若峰	男	1976.8	南京农业大学	教授	预防兽医学	课程建设与教学	
	宋小凯	男	1979.10	南京农业大学	副教授	预防兽医学	课程建设与教学	
	陈 闻	女	1981.2	南京农业大学	实验师	预防兽医学	辅助教学	
	仇亚伟	男	1981.2	南京农业大学	实验师	预防兽医学	辅助教学	
	教师队伍整体素质	<p>知识结构：</p> <p>承担本课程教学固定人员 6 人。其中教授、博士生导师 2 人，副教授、硕士生导师 1 人，讲师 1 人，实验师 1 人，助理实验师 1 人。均为兽医专业毕业，并长期从事兽医寄生虫学教学科研工作。另外每学期配置 1-2 名研究生助教。师资队伍中，具有博士学位 3 人，硕士学位 1 人，学士学位 1 人。主讲教师均承担着国家级和省部级科研课题，并在兽医寄生虫学研究中取得了明显成绩。</p> <p>年龄结构：</p> <p>50 岁以上 1 人，40-50 岁 2 人，30-40 岁 1 人。该团队是一支年富力强、教学经验丰富的教学队伍。教师年龄结构和知识结构合理，优势互补，其中课程负责人拥有 30 年教学经验和丰富的兽医寄生虫学研究经验，其他主讲教师均有 5 年以上的教学经历。</p> <p>学缘结构：</p> <p>教学队伍的学缘结构多元化，有在中国农业大学、南京农业大学、安徽农业大学、河南农业大学等多所不同高校学习经历。4 名教师中 3 人具有博士学位，其中从中国农业大学取得博士学位 1 人，从南京农业大学获博士学位 2 人；4 名教师中 4 人获得硕士学位，其中从安徽农业大学取得硕士学位 1 人，从南京农业大学获硕士学位 3 人。主持人有在美国、韩国、英国、丹麦等国学习和进修的经历，团队成员严若峰教授在加拿大留学一年，另一团队成员宋小凯副教授在丹麦留学进修。</p>						

学术研究 与教学 研究	<p>(1) 主持南京农业大学创新性实验实践教学项目“动物弓形虫等寄生虫病的人工复制、诊断与治疗”。</p> <p>(2) 参加国家精品课程建设与教学。</p> <p>(3) 参加国家精品资源共享课建设与教学。</p> <p>(4) 参加《兽医寄生虫学》多媒体课件制作,获教育部“第五届全国多媒体课件大赛”优秀奖(高教组)。</p> <p>(5) 指导本科毕业论文,7-12人/年,多人获优秀本科毕业论文。</p> <p>(6) 近5年来,项目成员参编、副主编教材10多部。其中《动物寄生虫病彩色图谱(第二版)》为国家出版基金项目现代农业科技专著系列图书。</p> <p>(7) 近5年来,先后指导30多名学生从事10多项SRT研究,其中2项获国家大学生实验计划资金资助、1项获江苏省大学生科技创新基金资助,其他项目均由南京农业大学专项资金资助。</p> <p>(8) 获希尔思、生泰尔、回盛、森楠等奖教金7人次。</p>
-------------------	---

3. 教学理念与课程设计

3-1 教学理念

课程定位:

兽医寄生虫学是动物医学专业、动物药学和动物健康与动物生产强化班的必修课,为专业核心课程。该课程包括寄生虫病原生物学和寄生虫病学两部分,既是一门基础课,更是一门临床课。动物寄生虫病是国家法定动物疫病,是国家执业兽医资格考试的必考内容。人畜共患寄生虫病不仅危害动物健康,对人类健康和公共卫生也产生巨大影响。因此,《兽医寄生虫学》是动物医学专业学生知识结构中必不可少的重要组成部分,是动物健康养殖、动物疫病防控的重要内容,是执业兽医必须具备的知识与技能,在保障人类健康和促进公共卫生方面也发挥着重要作用。

3-2 课程总体设计

教学方法:

*理论教学

(1) 理论课以教师课堂教学为主,辅以课堂练习和课后自学。由于兽医寄生虫学内容多课时紧,课堂教学重点讲授畜禽常见的寄生虫病、危害严的寄生虫病、人兽共患的寄生虫病等,而其他内容以课后自习为主。

(2) 理论教学采用多媒体教学手段,通过大量图片、模式图、视频等资源将寄生虫的病原形态、结构、引起的病理变化等教学内容直观形象的展示出来。

(3) 在讲授临床症状、诊断方法、防治措施等内容时,注重结合典型病例和案例,实施启发式教学。注重培养学生综合、灵活运用知识的能力,同时也大大提高了学生的学习兴趣。

(4) 教学中以具有代表性寄生虫病为“点”,而以同一类寄生虫病为“面”,注重其病原结构特点、生活史、寄生部位进行“以点带面”的教学模式,减轻学生们的记忆压力和学习负担。

*实验教学

(1) 实验教学以学生动手操作为主,辅以教师简单讲解和演示操作,重点培养学生动手能力。

(2) 教学过程中,每次实验教师一般用 0.5 学时对实验目的、实验原理、实验操作、注意事项等进行讲解或演示;学生用 2.5 学时动手操作,此间,教师进行课堂巡视,对学生操作不当随时进行纠正,对学生提出的问题进行答疑。

(3) 每次实验后学生提交实验报告,教师批改,对共性问题在下一实验前统一讲解。

*综合性实践教学(教学实习)

(1) 要求学生自主设计实验,主要以学生动手操作为主,辅以老师讲解和演示,培养学生综合、灵活运用理论知识的能力,提高学生发现问题、分析问题和解决问题的能力。

(2) 学生先写出试验设计方案,老师修改;设计方案通过后,学生开展实验,实验中和老师讨论、交流,解决实验中出现的的问题;实验结束后,学生分析实验结果,提交完整的实习报告。

(3) 采用新的评价体系,主要评价学生试验设计是否合理、试验准备是否充分、试验操作是否规范、试验结果是否可信、数据分析是否正确等。对学生的评价“不以成败论英雄”,即允许失败,让学生明白科学必须讲究实事求是,但要求认真分析失败的原因,真正理解科学的严谨性。

4. 课程建设规划

4-1 课程建设目标及预期效果

教学目标:

(1) 专业教育 主要针对兽医专业在校学生,起到替代或半替代线下课程教学的作用,作为线下教学的有效补充,帮助学生预习和复习该课程,习题和试题可以自我检验学习效果。

(2) 科普教育 主要面对社会大众,普及人兽共患寄生虫病等大众医学知识,对因饲养宠物、不良饮食方式、旅游、过度生产与开发等问题所引发的人类寄生虫病的相关知识进行介绍,提高公众疾病预防意识和能力。

受众定位:

(1) 高等院校兽医相关专业学生 该部分人群是本课程的主要听众,他们具有兽医学相关的理论基础和一定的实践能力。

(2) 普通社会大众 希望了解兽医寄生虫病相关知识的群体,可通过专题讲座、诊断

检索系统、图片资料等获得其所关心的知识。

学习效果：

(1) 提高学习兴趣 该课程相比其他课程来说比较难学，主要表现在寄生虫的病原形态多样、结构复杂、生活史不尽相同、有特定的宿主范围和寄生部位等。本课程提供了大量图片、病理标本、模式图、录像、动画、视频，使得学生对病原的认识更加直观和生动。

(2) 提高学习效果 课程资源提供了各个章节的知识点、重点和难点，提高了学习效率。此外，课程资源中提供了大量的练习题和试题，能及时检验学生学习效果。

预期成果：

(1) 建成学校在线精品课程。

(2) 培养青年教师 2-3 名。

4-2 课程建设实施步骤、方法

按照相关要求于 2017 年 6 月底上线。

- PPT 制作，按照课程章节制作，格式统一。
- 完善更新教学视频，按照课程章节录制视频，剪辑加工。
- 典型寄生虫病案例教学。
- 寄生虫病例分析。
- 寄生虫病原结构模式图。
- 不同动物常见寄生虫病检索系统。
- 不同动物常见寄生虫病诊断参考方法。
- 练习题。
- 试题库。
- 拓展资源建设。

4-3 课程建设的创新点

(1) 资源内容丰富，层次分明

课程资源分为理论教学和实践教学资源两部分，每一部分又分基础和提高两个层次，为不同的学习对象提供相应的学习材料。

(2) 资源类型多样，形式各异

课程资源包括教学大纲、教材、课件、练习题、试题、教学视频、寄生虫形态结构等，以文字、图片、视频、动画等多种形式呈现给读者。

5. 课程基础及教学资源

5-1 课程建设基础（含课程现状、课程评价及教学效果）

《兽医寄生虫学》是动物医学专业的核心课，寄生虫病是国家法定动物疫病。《兽医寄生虫学》在动物医学专业学生知识结构构建、动物疫病防控和学生职业生涯发展中具有不可替代的作用。随着科学进步和学科的发展，《兽医寄生虫学》在改革中不断发展，特别是近 10 年来，改革成效显著，建立起了较为成熟的教学体系。

（1）更新教材，与时俱进

本课程以中国农业大学孔繁瑶教授主编的《家畜寄生虫学》第二版修订版为主要教材，参考中国农业大学汪明教授主编的《兽医寄生虫学》第三版（面向二十一世纪教材）。前者的优点是寄生虫种类集中，按寄生虫系统分类编排，后者的优点是便于复习，按寄生虫的宿主动物来分类编排，但也有各自的不足。课程组根据该课程的学时和教学实际情况，将前两种教材进行优化组合，形成了具有自己特色的教材体系。

为了弥补教材文字多、图片少等不足，将本实验室的寄生虫标本和病理标本进行整理拍照，出版了《兽医寄生虫病彩色图谱》（2004 年（第一版），2011 年（第二版）），作为补充教材和参考图书。该书是国内出版的第一本寄生虫病彩色图谱，填补了国内的空白，被很多教学和科研单位作为参考图书。

（2）改革教学内容，强化案例教学

随着我国经济的发展，动物养殖业已发生了很大的变化。养殖规模由分散到集约，动物种类由以役用大家畜为主变为以肉用、蛋用、奶用、毛用、皮用和伴侣等多种动物全面发展。寄生虫病的发生和流行也发生了相应的变化，由过去的以散发为主变为以群发、流行发生为主，所造成的经济损失更大，疾病的控制也由过去的以个体治疗为主转为群体控制为主。针对这种变化，我们对兽医寄生虫学的讲课内容也不断进行更新。如将马属动物的寄生虫病不再作为重点内容，增加水禽、兔、犬、猫、观赏禽类等的寄生虫病的有关内容，适应了经济和社会发展的需要。

此外，近年来，有关寄生虫病的免疫预防和免疫诊断也有了极大的进展，但教材中这部分内容较少。为此，我们结合科研工作，增加了有关免疫诊断和免疫预防研究进展的内容，重点介绍寄生虫免疫诊断方法的实用性和存在的不足，突出寄生虫病的免疫预防特别是有关寄生虫疫苗的研究进展和优缺点，使学生既对学科的发展有所了解，又对存在的问题有所认识。

随着我国经济和社会的发展, 兽医学在保障人类健康和公共卫生中的作用更加重要。在寄生虫病中, 相当一部分是人畜共患病, 具有重要的公共卫生意义, 如猪囊虫病、旋毛虫病、日本血吸虫病、华支睾吸虫病、棘球蚴病、弓形虫病、隐孢子虫病等。对于这些病, 我们始终将之作为重点, 要求学生全面掌握这些病的有关情况, 特别是这些病是如何在动物和人类之间传播的, 以及这些病对人类所造成的危害。并结合近年来发生在我国的案例, 提高学生对这些疾病重要性的认识。

上述教学内容的改革, 拓宽了学生的知识面, 提高了学生毕业后对社会的适应能力。

(3) 实施启发式教学, 改进教学手段

兽医寄生虫学历来被认为是兽医专业课中较难学的课程之一。其原因在于寄生虫种类繁多, 形态结构多样, 生活史复杂, 多数疾病缺乏典型症状等。但寄生虫病也有许多共同之处, 如病原体按动物分类多有共同的特点, 其致病多与其寄生部位及在体内的移行有关等。因此, 我们在教学中多用启发式教学, 引导学生抓住寄生虫共同的地方和不同的地方, 区别病原体; 要求学生掌握寄生虫感染的动物种类、寄生部位和是否在体内移行等, 在已经学过的生理、生化、病理等课程的基础上, 发挥联想、比较, 从而掌握其致病机理、病理变化、症状等。使这门课真正建立在学生已有的知识基础之上, 变的易学、易懂、易掌握、易应用。

与此同时, 我们不断改进教学手段。理论课授课方式包括常规课堂讲授、文献阅读、网络课件浏览、课堂讨论、定期答疑等形式, 以期培养学生正确认识问题、分析问题、解决问题的能力。将教学内容制作成多媒体课件, 配以幻灯片、投影膜和录象带, 形成了多种方式相结合的、系统的教学辅助手段。所制作的《兽医寄生虫学》多媒体课件在教育部“第五届全国多媒体课件大赛”中获高教组优秀奖。

同时, 每一位教师都能够认真听取学生意见, 与学生探讨最佳授课方法, 并且听取教学督导组专家、教授的意见, 及时改进教学方法和手段, 使学生真正喜欢并学好兽医寄生虫学这门课。

(4) 强化实践教学, 提高动手能力和创新能力

实践教学是巩固理论知识、培养学生实际操作能力和创新能力的重要一环。为此, 我们自主编写了《家畜寄生虫学实验指导》, 将实验课单独开设, 加大综合性和设计性实验比例, 增设实验教学实习周, 其中实验教学实习周要求学生自己设计实验, 自己完成。在教学中, 全体教师认真备课, 注重技术基本原理的分析, 提倡学生自己设计试验并自己完成, 启发学生学会分析问题和解决问题的方法。经过几年的摸索, 形成了实验课、实习周并举、

验证性实验、综合性实验和设计性实验共存的实践教学体系。同时，实验室向全体学生开放，取得了很好的实践教学效果，表现为学生参加实验积极性得到提高，学生到本课程组从事毕业论文和科学研究训练（SRT）的人数不断增加。近5年来，课程组先后指导40多名学生从事10多项SRT研究，其中2项获国家大学生实验计划资金资助、1项获江苏省大学生科技创新基金资助，其他项目均由南京农业大学教务处专项资金资助。

（5）尝试双语教学，提高专业英语水平

本课程主讲教师曾在美国、英国、加拿大、丹麦等国进修，英语水平较高。近年来，课程组先后培养了5位外籍留学博士研究生，促进了课程组教师英语水平的提高。为提高学生的专业英语水平，使学生能够更好地查阅寄生虫学研究领域的最新研究进展，授课教师重视在授课过程中对英文专业名词的介绍，并开始尝试在部分教学内容中使用双语教学。

（6）建设教学网站，搭建互动平台

为提高教学效果，培养学生的自学能力，我们建设了教学网站，在网上提供网络课件和相关教学参考资料并及时更新，增强学生自主学习的兴趣和能力。任课教师的电话和邮箱向学生公布，建立每周一次的答疑制度，鼓励青年教师从事班主任工作。通过这些措施，不仅解答了学生在学习遇到的问题，同时，也使学生对教学目标和教师本人有了更加深入的了解，促进了师生互动，促进了教书育人效果。

（7）改革评价方式，注重实际能力

改变过去单一的一张试卷评价标准，采用平时成绩（占总成绩的10%）、期终闭卷考试（占总成绩的70%）、实验课考试成绩（占总成绩的20%）来综合评价学生成绩的标准。平时成绩主要根据课堂考勤、回答问题、实验报告等来评判。期终闭卷考试着重考察学生对基本知识和理论的掌握以及综合分析能力。实验重点考察学生对病原、病变的识别、实习周中自主设计试验的能力和完成情况。

（8）建设基础良好，同行评价优秀

课程组由一支具有较高的政治思想素质，教学水平高，知识结构和学缘结构合理的教师队伍组成。课程组坚持以人为本、教书育人、教学相长的教学理念。在多年的教学中积累了大量的教学经验，不断进行教学改革。对教材及教学内容不断更新和补充，实施启发式教学和案例教学，改进教学手段，注重培养学生动手能力和创新能力。教学效果好，得到了广大学生的好评。

同行专家评价：该学科教研组具有丰富的寄生虫的病原和病例标本，能够使学生有更多的直观和感性的认识，制作的课件图例丰富。任课教师课前准备充分，认真备课，注意学生的创新思维和动手能力的培养，教学内容丰富充实，并即时注意更新和补充相关新的内容。

他们善于利用现有的现代化的教学手段，使学生能充分掌握该课程的知识要点。

5-2 基本资源清单

合计 54 学时，包含所有教学章节和全部知识点。

- (1) 第一章 前言，3 学时。
- (2) 第二章 寄生虫与宿主，1.5 学时。
- (3) 第三章 寄生虫的流行病学和地理分布，0.5 学时。
- (4) 第四章 寄生虫病的免疫与实验室诊断技术，1 学时。
- (5) 第五章 寄生虫病的防治措施，1.5 学时。
- (6) 第六章 寄生虫的分类和命名规则，0.5 学时。
- (7) 第七章 吸虫病，8 学时。
- (8) 第八章 绦虫病，7 学时。
- (9) 第九章 线虫病，11.5 学时。
- (10) 第十章 棘头虫病，1.5 学时。
- (11) 第十一章 蜱螨，2.5 学时。
- (12) 第十二章 昆虫，2 学时。
- (13) 第十三章 原虫概论，1 学时。
- (14) 第十四章 鞭毛虫病，3 学时。
- (15) 第十五章 梨形虫病，4 学时。
- (16) 第十六章 孢子虫病，5 学时。
- (17) 第十七章 猪小袋纤毛虫病，0.5 学时。

5-3 拓展资源建设及使用情况

该课程教学主要围绕指定教材，同时参考了国外兽医寄生虫和人体寄生虫等相关学科教材，不断更新教学资源。建设过程中将注重学科前沿研究，从兽医寄生虫学科权威杂志 *Parasitology Today*、*International Journal for Parasitology*、*Veterinary Parasitology*、*Parasitology*、*Journal of Parasitology*、*Experimental Parasitology*、*Biochemical and Molecular Parasitology*、*Parasite Immunology* 等中获取最新的研究进展，将大量的寄生虫分子生物学和免疫学等内容补充到教学中。拟将课程组在鸡球虫病、捻转血矛线虫病、旋毛虫病、弓形虫病等研究中所取得的最新成果融合到教学中。

6. 自编教材

主编 基本信息	姓名	李祥瑞	性别	男	出生年月	1958.12
	最终学历	研究生	专业技术职务	教授	电话	84399000
	学位	博士	职务		传真	84399000
	工作单位	南京农业大学		E-mail	lixiangrui@njau.edu.cn	
	通信地址(邮编)	江苏省南京市玄武区卫岗1号 南京农业大学动物医学院				
	研究方向	预防兽医学				
教材 基本信息	教材名称	动物寄生虫病彩色图谱				
	出版社	中国农业出版社				
	书号	ISBN 978-7-109-16153-5				
	版次	第二版				
	印数	3000册				
	该教材是否为成人高等教育专门编写? 是() 否(√)					
教材 使用情况	<p>该彩色图谱出版后受到广泛好评,是国内一本系统、完整、图文并茂的介绍动物寄生虫的图书,此书作为该领域的参考书,第一版印制3000本后,2011年又进行了第二版的印制。</p>					

注: 如果本课程使用自编教材, 需要填写本栏目信息。

7. 学校政策支持

学校将对该课程后续建设提供足够的人力、财力、物力保障及政策支持，严格按照江苏省《关于开展成人高等教育重点专业(含精品资源共享课程)建设工作的通知》(苏教高[2016]21号)文件及校发《南京农业大学关于开展江苏省成人高等教育重点专业(含精品资源共享课程)立项申报工作的通知》(校继发[2016]499号)的要求进行后续建设，不断开展教学改革，丰富课程网络资源，及时更新相关内容，确保课程建设的高水平和高质量。

(学校立项建设文件见附件)

8. 承诺与责任

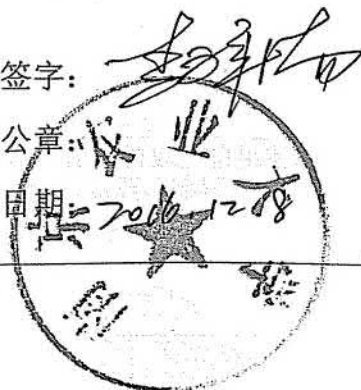
学校和课程负责人保证：

1. 课程资源内容不存在政治性、思想性、科学性和规范性问题；
2. 申报所使用的课程资源知识产权清晰，无侵权使用的情况；
3. 课程资源及申报材料不涉及国家安全和保密的相关规定，可以在网络上公开传播与使用；

课程负责人签字：

学校公章：

日期：2016-12-08



南京农业大学文件

校继发〔2016〕499号

南京农业大学关于开展江苏省成人高等教育重点专业(含精品资源共享课程)立项申报工作的通知

各相关学院及单位:

为贯彻落实《国家中长期教育改革和发展规划纲要(2010-2020年)》关于“加快发展继续教育”的要求和2015年全省高等学校学历继续教育改革发展推进会精神,根据江苏省教育厅《关于开展成人高等教育重点专业(含精品资源共享课程)建设工作的通知》(苏教高[2016]21号)文件要求,不断提高我校成人高等教育人才培养质量,更好地服务“强富美高”新江苏建设,学校决定开展江苏省成人高等教育重点专业(含精品资源共享课程,下同)立项申报工作。现就有关事项转发与通知如下。

一、指导思想

全面贯彻党的十八大和十八届三中、四中、五中全会精神，深入学习贯彻习近平总书记系列讲话特别是视察江苏重要讲话精神，坚持立德树人根本宗旨，以服务经济社会发展和人民群众学习需求为导向，创新成人高等教育人才培养模式，优化专业结构，强化内涵建设，深化教学内容、课程体系、教学方法改革，着力打造一批综合实力强、内涵积淀深、人才培养质量高、社会声誉好的成人高等教育重点专业与精品资源共享课程，切实提高在职从业人员理论知识、职业道德、实践能力和综合素质，更好地发挥成人高等教育在终身学习体系建设中的骨干引领作用。

二、建设目标

今年重点建设3个校级成人高等教育重点专业，每个重点专业至少建成2门主干课程作为精品资源共享课程。充分发挥重点专业及精品资源共享课程的品牌示范效应，促进我校成人高等教育专业建设水平和人才培养质量的整体提升。

三、建设原则

1. 服务发展，需求导向。依据经济社会发展需求和成人高等教育资源状况，集中力量，重点建设具有行业特色、区域优势和符合市场需求，支撑江苏支柱产业、优势产业、新兴产业发展的专业与课程，充分发挥其骨干示范和引领作用，进一步增强我校成人教育的社会服务能力。

2. 彰显特色，打造品牌。引导我校树立品牌意识，强化优势特色，切实加强成人高等教育专业的内涵建设，优化人才培养结构，创新人才培养模式，提升人才培养质量，努力培养经济社会发展急需的高素质、应用型、复合型人才。

3. 标准引领，好中选优。重点专业应以完备的课程体系和优质的资源共享课程为支撑，依据遴选条件和建设标准，同时参考各学院成人教育专业建设的整体水平、建设成效、社会声誉和市场需求，择优遴选。以标准为引领，切实加强我校成人高等教育专业建设。

四、遴选立项

（一）遴选程序

成人高等教育重点专业建设点遴选，按照学院申报、专家评议、结果公示、文件认定的程序进行。学校依据遴选条件和建设标准(见附件1)择优申报。

（二）经费来源

我校成人高等教育专业建设工作纳入学校专业发展整体规划并给予相应的资金支持，对通过学校遴选的专业按不低于20万元/个的标准予以资助，其中精品资源共享课程按不低于平均5万元/门的标准予以资助。

五、申报要求

（一）书面材料

申报材料确保内容真实、数据准确、文字精练、装订规范，按专业或课程装袋（详见附件 7、8）。申报书、汇总表均须加盖学校公章。申报材料不予退回，请自行备份。

1. 成人高等教育重点专业建设点申报材料。请各学院对照申报条件和遴选标准，推荐名额进行申报，并认真准备以下申报材料：

(1) 重点专业建设点申报书(3份，详见附件 3)；

(2) 重点专业建设点申报汇总表(1份，详见附件 5)，并同时 will Excel 格式的汇总表电子文档发送至 lijuan@njau.edu.cn；

(3) 相关证明材料（含教师学历、职称、论文、教学科研成果等）复印件一套。教材、论著，请提供封面及版权页复印件。

2. 成人高等教育精品资源共享课程申报材料。请各院校对照申报条件和遴选标准（详见附件 2），推荐名额进行申报，并认真准备以下申报材料：

(1) 精品资源共享课程申报书(3份，详见附件 4)；

(2) 精品资源共享课程申报汇总表(1份，详见附件 6)，并同时 will 电子文档发送至 lijuan@njau.edu.cn；

(3) 包含课程基本资源与拓展资源的 CD-ROM 光盘。存储路径：一级目录为“申报院校”，如“南京农业大学”等；二级目录为“申报课程”，如“不动产估价”等；三级目录为“基本资源”，如“课程介绍”、“网络课件或演示文稿”、“教学录像”等。

(4) 相关证明材料(含教师学历、职称、论文、教学科研成果等)复印件一套。教材、论著, 需提供封面及版权页复印件。

3. 报送时间。各学院申报材料请集中于2016年11月28日前提交; 联系人: 李娟、周波、徐风国; 联系电话: 84395131、84396043, 13382021215、15850574769; 电子邮箱: lijuan@njau.edu.cn。

(二) 电子材料

1. 重点专业建设点申报书与相关证明材料(附件3, 合并为一个PDF文件, 文件命名规则为“学校名称+专业名称”); 精品资源共享课程申报书与相关证明材料(附件4, 合并为一个PDF文件, 文件命名规则为“学校名称+专业名称+课程名称”)。

2. 重点专业建设点申报汇总表与精品资源共享课程申报汇总表(附件5与附件6, Excel格式)。

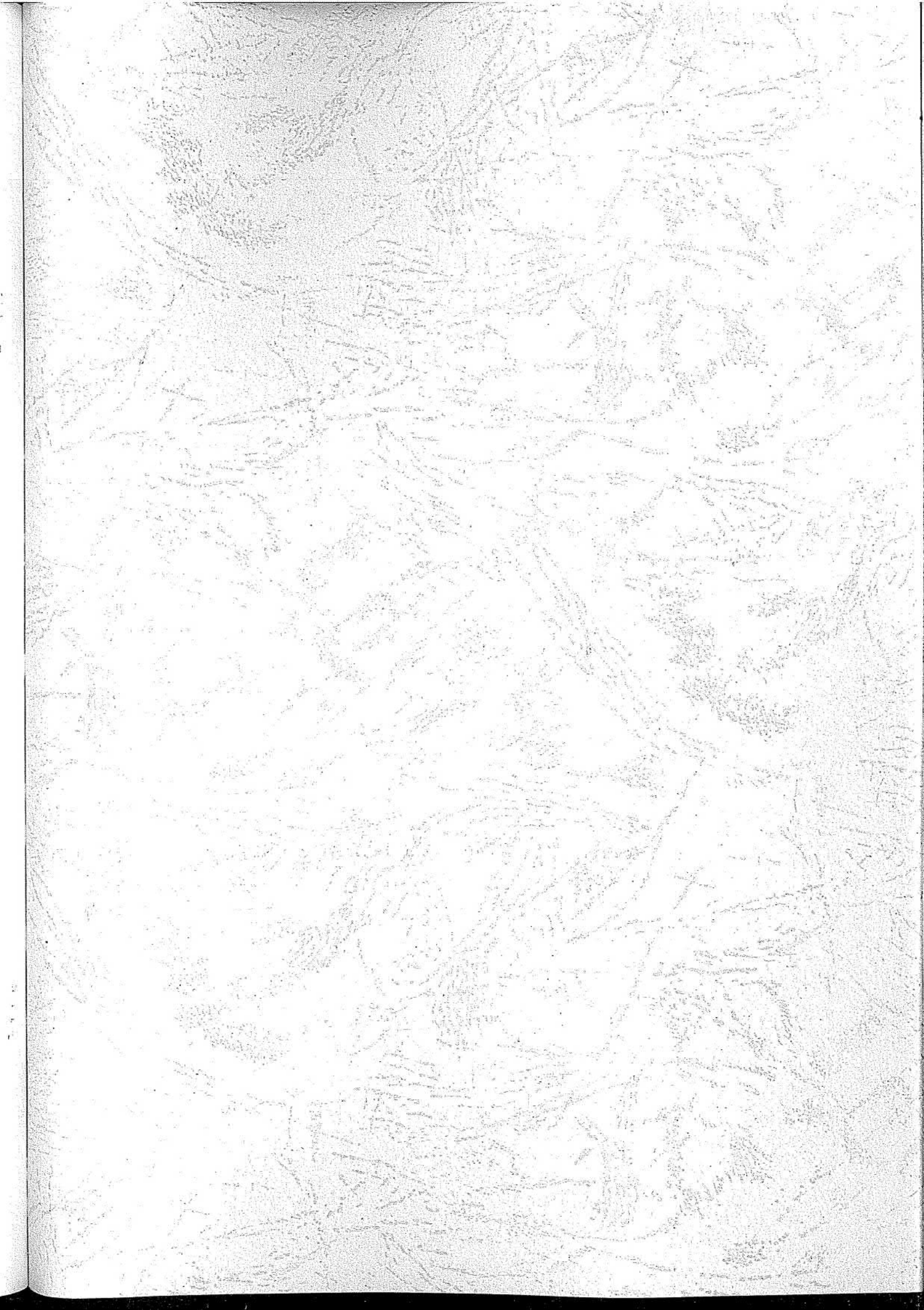
(三) 网站材料

1. 在本校校园网站或继续教育网站上建设成人高等教育重点专业(精品资源共享课程)建设网页(专栏), 采用文字、图片与视频相结合的方式介绍成人高等教育重点专业建设情况。网页(专栏)内容从项目申报、过程管理、阶段性成果展示、总结验收等方面系统考虑, 参照《江苏省成人高等教育重点专业建设标准》一、二级指标设计, 包括项目申报书和相关佐证材料, 便于江苏省教育厅进行过程监控和校际间交流学习。专家通讯评议期间需保证网站畅通运行。

2. 网上精品资源共享课程展示应含课程基本资源与拓展资源,基本资源包括课程介绍、教学大纲、网络课件或演示文稿、作业、参考资料目录和课程教学录像(按照教学单元录制)等反映教学活动必需的资源;拓展资源指反映课程特点,应用于各教学与学习环节,支持课程教学和学习过程,较为成熟的多样性、交互性辅助资源,包括素材资源库、专题讲座库、试题库系统、作业系统、在线自测/考试系统,课程教学、学习和交流工具及综合应用多媒体技术建设的网络课程等。提交的所有课程资源须符合《国家级精品资源共享课建设技术要求》。凡申报江苏省成人高等教育精品资源共享课的全部资源必须具有清晰的知识产权,不存在侵犯其他公民、法人、组织知识产权的问题。

具体附件及相关要求可从继续教育学院网站(chjw.njau.edu.cn)的“资料下载”栏目内下载。





江苏省成人高等教育精品资源共享课程申报汇总表

学校名称 (盖章): 南京农业大学



填表人: 李祥瑞

联系电话: 139520094629

电子邮箱: lixiangrui@njau.edu.cn

序号	学校	课程名称	所属学科专业	所属学科类代码	课程层次	办学形式	课程类型	课程负责人	总课时数	是否为省级成人高等教育精品课程
1	南京农业大学	兽医寄生虫学	动物医学类	090601	专升本	函授	专业课	李祥瑞	40	否

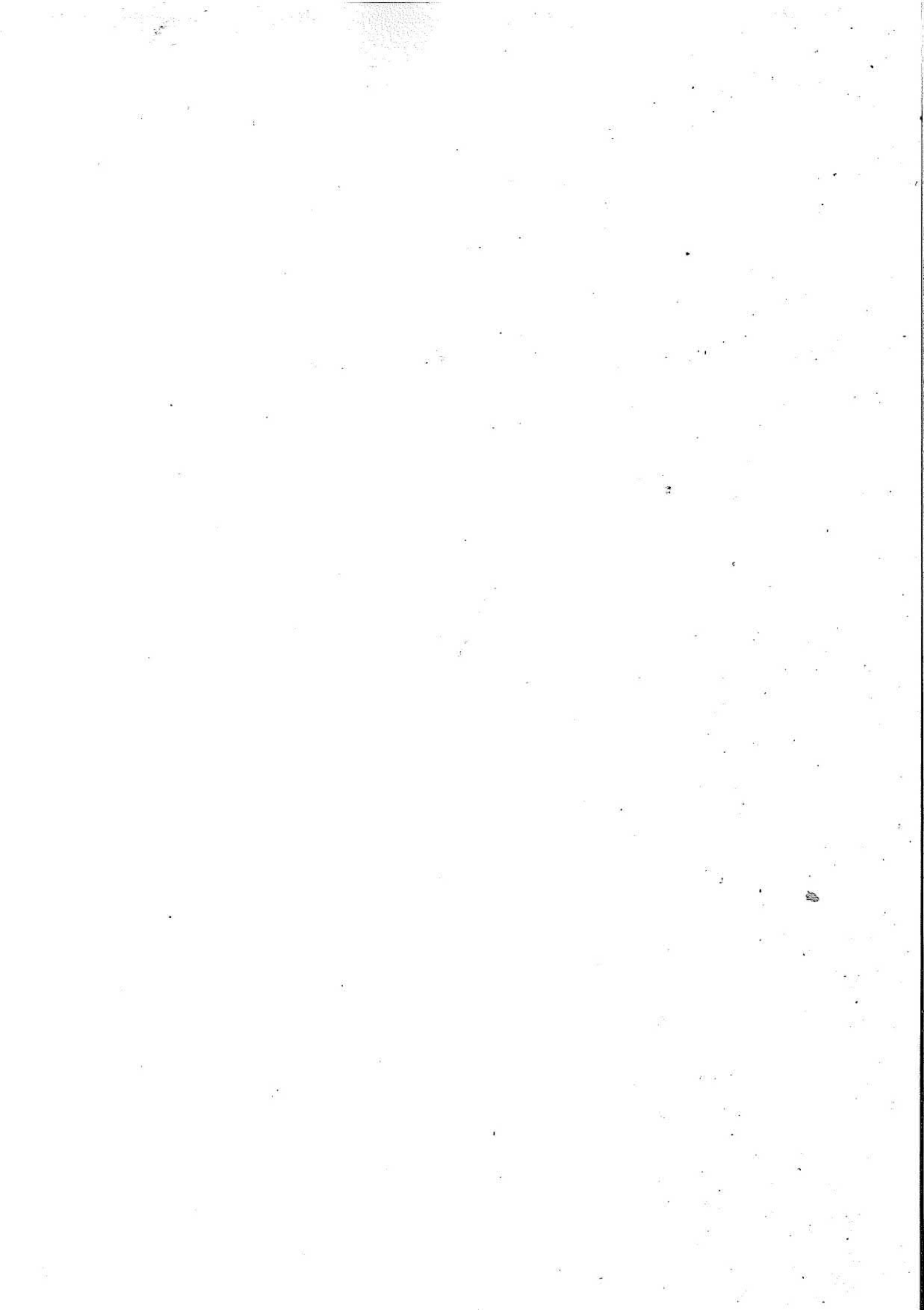
说明:

1. “所属学科专业”为《普通高等学校本科专业目录》中的学科门类下设的二级类名称、《普通高等学校高职高专教育指导性专业目录》中的专业类名称;
2. 课程层次为: 高起专, 高起本, 专升本;
3. 办学形式为: 函授, 业余, 脱产;
4. 课程类型为: 公共课, 基础课, 专业基础课, 专业课。

课程平台登录路径: <http://yc.njau.edu.cn:801/elcs/login/reLogin.jsp>

用户名: jpyzgxkc

密码: 123456



江苏省成人高等教育精品资源共享课程

《兽医寄生虫学》

相关证明材料

(含教师学历、职称、论文、教学科研成果等)

南京农业大学

二〇一六年十二月



目录

主讲教师、教学辅助人员基本信息	姓名	性别	出生年月	单位	职称	学科专业	在课程建设中承担的工作
	李祥瑞	男	1958.12	南京农业大学	教授	预防兽医学	课程建设与教学
	徐立新	男	1968.2	南京农业大学	讲师	预防兽医学	课程建设与教学
	严若峰	男	1976.8	南京农业大学	教授	预防兽医学	课程建设与教学
	宋小凯	男	1979.10	南京农业大学	副教授	预防兽医学	课程建设与教学
	陈 闻	女	1981.2	南京农业大学	实验师	预防兽医学	辅助教学
	仇亚伟	男	1981.2	南京农业大学	实验师	预防兽医学	辅助教学

Table 1

Table 1: Comparison of the proposed method and existing methods.

Method	Accuracy	Efficiency	Stability
Method A	0.85	High	High
Method B	0.78	Low	Low
Method C	0.82	Medium	Medium
Method D	0.75	Low	Low
Method E	0.80	Medium	Medium

The proposed method shows superior performance in terms of accuracy and efficiency compared to existing methods. It maintains high stability across different datasets and conditions.

化学系 化学人

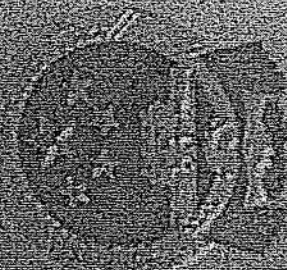
一九五一年一月一日

已通过博士学位的课程与
论文答辩，成绩合格。根据
《中华人民共和国学位条例》的
规定，授予 友 享 博士学位。

委员会主席
石心春

正式编号

友 享 博士学位



博士学位证书

博士后证书

李祥瑞 博士于一九九三年七月至一九九五年十一月

在中国农业科学院作物研究所农学

学科从事博士

后研究工作，并完成在 期间的科研任务。

特发此证

全国博士后管理委员会

主任

1000

一九九八年五月三十日

证 明

李祥瑞，男，1958年12月出生，南京农业大学动物医学院教师，1993年7月北京农业大学博士毕业，1999年1月获聘教授专业技术职务至今，并拟续聘至2022年12月。

特此证明



南京农业大学文件

校发[2005]156号

干部任免通知

各学院、各单位：

经校党委常委 2005 年 6 月 10 日会议研究决定，聘任：

张红生同志为外办主任、国际教育学院院长（兼）、港澳
办公室主任（兼）；

张兵同志为计财处处长；

刘营军同志为学生工作处处长；

李祥瑞同志为动物医学院院长；

周应恒同志为经济管理学院院长；

沈振国同志为生命科学学院院长（兼）；

吴益东同志为植物保护学院副院长（主持工作）。

二〇〇五年六月十七日

硕士研究生 毕业证书



研究生 徐立新 性别男 一九六八年二月二十一日生，于
二〇〇一年九月至二〇〇九年六月在 预防兽医学
专业学习，学制三年，修完硕士研究生培养计划规定的全部课程，成绩合格，
毕业论文答辩通过，准予毕业。

所在单位 南京农业大学

校院所长

郑永波

证书编号: 183071200902000067

二〇〇九年六月二十日

硕士学位证书



徐立新，男，1968年2月23日生，在南京农业大学
预防兽医学 学科(专业)已通过硕士学位的课程
考试和论文答辩，成绩合格。根据《中华人民共和国学位条例》的规
定，授予 农学 硕士学位。

南京农业大学

校 长

郑永波

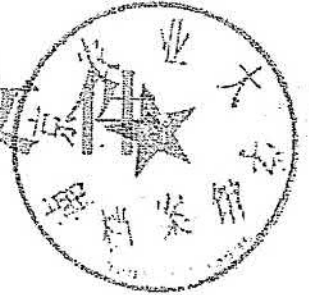
学位评定委员会主席

证书编号: 103071200902000067

二〇〇九年六月二十日

2004 X312 c
14 6 9

南京农业大学



校人字[2004]178号

关于丁艳锋等 100 位同志专业技术职务 聘任的通知

各学院、各单位：

我校 2004 年度专业技术职务评聘工作已告结束，经校高级（中级）专业技术职务评审委员会、校特别聘任委员会评审，经校职改领导小组审核，校长办公会议研究，同意聘任丁艳锋等 85 位同志相应的专业技术职务（除注明的以外，聘任时间从 2004 年 4 月 30 日开始计算）。另同意邢邯等 15 位同志同级转聘及初聘。现将名单公布如下。

一、正高级专业技术职务

（一）教授

丁艳锋 王绍华 郭旺珍 姜东 麻浩 高学文
李辉信 魏正贵 陈发棣 徐幸莲 王锋 江善祥

杨春龙 周 宏 王树进 陈东平 常向阳 陈利根
吴 群 李 放 王庆亚 赖 仞 何春霞
邵 涛（聘任时间自 2004 年 5 月 17 日开始计算）

（二）教育管理研究员

蹇兴东

二、副高级专业技术职务

（一）副教授

孙 敬 胡白石 王备新 刘向东 李恋卿 张亚丽
郭世伟 乔玉山 房伟民 高志红 姜 梅 韩兆玉
范红结 刘祖云 王舒曼 丁启朔 仲高艳 史立新
陆 慧 许晓明

（二）专职学生思想政治教育系列副教授

方 鹏

（三）教育管理副研究员

周 孜 张 鲲

（四）副研究馆员

毛莉菊

（五）高级实验师

王建新 周 钢

三、中级专业技术职务

（一）讲师

郑金伟 陈 宇 周振雷 徐立新 吴 芳 谷 政





姓名: 严若峰

性别: 男

出生年月: 1976.08

学科: 预防医学系

工作单位: 南京农业大学

编号: G-1361

经 南京农业大学高级专业

技术资格

评审委员会评审,

严若峰 同志已具备 教授

任职资格。



评审委员会 (公章)

2013 年 12 月 31 日

审批部门 (公章)

年 月 日

博士研究生 毕业证书



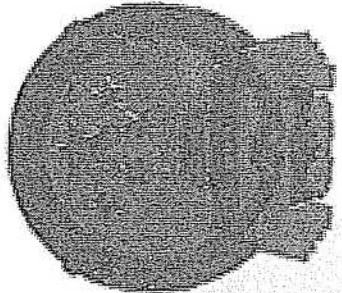
研究生 严若峰 性别男，一九七六年八月二十日生，于一九八〇年九月
至二〇〇四年八月在 预防兽医学 专业
学习，学制三年，修完博士研究生培养计划规定的全部课程，成绩合格，毕业
论文答辩通过，准予毕业。

培养单位： 北京农学院 校(院、所)长： 郑小波

证书编号：103071200401000058

二〇〇四年八月三十日

博士学位证书



严若峰 系安徽岳西

人，一九七六年八月

廿日生。在我校

预防兽医学 学科(专业)已通过
博士学位的课程考试和论文答辩，成
绩合格。根据《中华人民共和国学位
条例》的规定，授予 农学 博士
学位。



南京农业大学校长 邵小波
学位评定委员会主席

南京农业大学高级专业

技术资格

评审委员会评审

宋小凯同志已具备 副教授

任职资格。



姓名: 宋小凯
 性别: 男
 出生年月: 1979.10
 学科: 预防兽医学
 工作单位: 南京农业大学
 编号: G-1006

审批部门(公章)

年 月 日

博士研究生

毕业证书



研究生 宋小凯 性别 男，一九七九年十月八日生，于

二〇〇五年九月至二〇〇八年六月在 预防兽医学

专业学习，学制三年，修完博士研究生培养计划规定的全部课程，成绩合格，
毕业论文答辩通过，准予毕业。

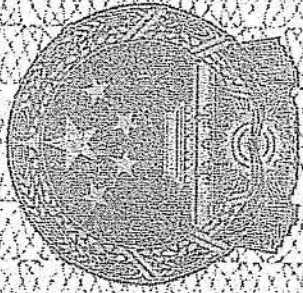
培养单位：南京农业大学

校(院、所)长：

郑小波

证书编号：103071200801000116

二〇〇八年六月十六日



博士学位证书

宋小凯，男，1979年10月8日生。在南京农业大学
 预防兽医学
 学科(专业)已通过博士学位的课程
 考试和论文答辩，成绩合格。根据《中华人民共和国学位条例》的规
 定，授予农学博士学位。

南京农业大学

校长

学位评定委员会主席



证书编号: 1030722008000116

二〇〇八年六月二十日

南京农业大学文件

校人发〔2015〕165号

南京农业大学关于公布2014年 教师及其他专业技术岗位分级聘用结果的通知

各学院、各单位：

根据国家有关文件及《南京农业大学关于开展2014年教师及其他专业技术岗位晋级聘用工作的通知》（校人发〔2014〕484号）精神，经个人申请，各级专家组评审，各单位岗位聘用工作小组、校岗位聘用工作小组和校岗位设置与聘用工作领导小组审核，并经2015年4月27日校长办公会议审定，同意聘用王秀娥等387位同志至相应的专业技术岗位等级（其他人员按学校有关规定原岗位等级聘用），聘期4年，时间自2015年1月1日至2018年12月

31日。

特此通知

附件：2014年度教师及其他专业技术岗位分级聘用名单



附件

2014 年度教师及其他专业技术岗位分级聘用名单

一、教授二级岗位

王秀娥 姜 东 张正光 姜 平 陈发棣 陈劲枫

二、教授三级岗位

王绍华 管荣展 戴廷波 李保平 高学文 董双林
董莎萌 柳李旺 陶建敏 陈 杰 姚 文 王丽平
姚火春 邵 涛 李辉信 余 玲 张瑞福 高彦征
黄启为 黄朝锋 王伟武 何 健 赵明文 杨春龙
彭增起 郁志芳 曾晓雄 陈坤杰 林乐芬 石晓平
冯淑怡

三、副教授一级岗位

江海东 高 英 张春玲 王广东 徐迎春 韩兆玉
李 强 王 静 李仕红 李娟玲 时均贤 胡忠伟
徐 萍 黄 芬 赵 力 徐梦洁 曾京京 武 锐
赵 军 林颂华 张 禾

四、副教授二级岗位

张文伟 周 琴 高聪芬 唐晓清 王三红 周振雷
潘翠玲 李玉峰 朱雪竹 张旭辉 任丽轩 李兆富
董长勋 黄丽琴 吴菊清 肖红梅 戴伟民 芮 琪

黎军胜	王昱泮	赵海珍	陈志刚	马开平	王 玲
李 建	李 骅	李 静	张 静	薛金林	蹇兴亮
白振田	朱毅华	谭 涛	张 颖	瞿忠琼	夏 敏
谢 勇	付坚强	李 燕	李 红	金锦珠	张春兰
徐冬青					

五、讲师一级岗位

王翠花	龙菊英	徐立新	崔春红	韩敏义	王明芳
李 林	李 晖	李 强	陈士进	於海明	顾 林
徐 进	黄桂林	程 明	赵青松	郭小清	韩喜秋
黄小丽	田舒黎	赵开堂	冯军政	纪燕玲	刘信宝

六、讲师二级岗位

王 娇	冯建英	李 凯	杨海水	赵文青	郭 娜
楚 璞	华修德	张美祥	王兴亮	胡 高	孙荆涛
叶文武	张清海	韩凝玉	贾海锋	金奇江	安玉艳
王彦杰	潘子豪	杨 平	白 娟	马 喆	陈兴祥
吴文达	汤 芳	陆春红	宋崇丽	蒋广震	于敏莉
张 林	李向飞	李延森	吴望军	申军士	余凯凡
李平华	万杰杰	顾 冕	刘树伟	凌 宁	韦 中
刘东阳	张 楠	唐 仲	刘志鹏	孙明明	何梅琳
魏 敏	魏良淑	朱晓莉	肖庆坤	任秀芳	国 静
张 帆	安红利	张 瑾	张懿彬	汪快兵	崔海燕
陈园园	姜 丽	王 玮	王 婷	杨润强	叶可萍
芮 昕	周 莉	丁 冬	王 凡	王永健	王全祥
王 念	毛敏芳	孔 倩	邓晓亭	卢 伟	田光兆

朱 跃	许 乐	孙 静	杨 勇	杨新莹	吴 丹
张大成	张云清	陆 静	陈 飞	陈 可	郑恩来
赵三琴	姜 姝	姜静静	顾宝兴	顾家冰	顾康静
章永年	葛艳艳	蒋文艳	熊燕华	戴存礼	李玉民
夏荣霞	徐 彦	王浩云	严斌剑	虞 祎	巩师恩
熊 航	季 璐	陈 哲	彭建超	沈苏燕	陈 叶
院玲玲	殷志华	杨秋兰	包 蕾	李 维	张 倩
王 薇	张 静	丁胜红	王 睿	张 宁	王小璐
杨灿君	张爱华	黎孔清	孟 凯	任 昂	师 亮
冉婷婷	黄 智	陈 凯	张紫刚	崔为体	孙政国
于景金	刘秦华				

七、教育管理岗位副高一级岗位

孙小伍 胡正平 施 珏 顾 南 曹志林

八、教育管理岗位副高二级岗位

由 杰 李 娟 俞建飞 姜凡桂 袁家明

九、教育管理岗位中级一级岗位

王诗平	尤树林	孔育红	吕春苗	孙锦明	李建雨
张 玮	周菊红	赵建业	施培菊	顾兴平	徐 云
徐 梅	章法洪	蒋 渊	滕秀梅	潘建华	鞠卫平

十、教育管理岗位中级二级岗位

宋和才	马吉锋	朱筱玉	刘婷婷	余 琛	张丽霞
陈 洁	邵存林	庞玉静	胡伟清	段 颖	贺 亮

夏德峰 郭军洋 郭翠霞 曹晶 崔滢 戴芳
徐衡 蒋正友

十一、教育管理岗位初级一级岗位

王玲 江海宁 许天颖 李伟锋 李爱玫 陈军
陈畅 邵祖琴 周激扬 赵建立 俞强

十二、其他专业技术岗位正高三级岗位

包平

十三、其他专业技术岗位副高一级岗位

黄明睿 胡琼英 夏爱红 唐惠燕 熊光骏 王祥珍
陈文喜 周晓莉

十四、其他专业技术岗位副高二级岗位

张守忠 陈雯 林国庆 吉翔 陆建红 秦新婷

十五、其他专业技术岗位中级一级岗位

贺平清 陈进 王全权 高天武 朱琳琳 朱新星
周广礼 高建清 韩梅 华玉明 冯秀珍 闫修荣
许向荣 孙环云 张婉怡

十六、其他专业技术岗位中级二级岗位

张小玉 李功兰 徐敏 杜郁梅 李玉霞 田云录
刘喜 王秋霞 沈秀萍 陈闻 周红 肖慎华
袁丽霞 王国祥 薛彦丹 王海萍 李立 丁青

李晓林 康中和 曹林凤 张勇 唐国萍

十七、其他专业技术岗位初级一级岗位

尹茜 邓绍林 吴金秀 丁正霞 王葳 李华
张婷 金巾 胡峰 蔡元康

南京农业大学文件

校人发（2014）253号

南京农业大学关于 2014 年管理岗位和 其他非教学科研岗位人员、院属系主任和 实验教学中心主任聘任的通知

各学院、各单位：

根据《关于做好 2014 年我校科级及以下管理岗位和其他非教学科研岗位人员聘任工作的通知》（校人发〔2014〕223 号）精神，经个人申请、聘任单位考核、校聘任工作领导小组审议及校长办公会议审定，决定聘任谭智赟等 620 位同志至科级及以下管理岗位和其他非教学科研岗位工作、聘任李刚华等 96 位同志担任系主任（或系副主任）、聘任胡白石等 20 位同志担任实验教学中心主任

任（或副主任），聘期至2017年6月30日止。接近退休年龄的人员，其聘期不超过国家规定的退休年龄。聘任职务中注明*人员，保留原科级岗位待遇并计算任职年限至退休。

请获聘人员做好工作交接手续。

特此通知

- 附件：1. 南京农业大学2014年管理岗位和其他非教学科研岗位聘任人员名单(科级及以下)
2. 南京农业大学院属系主任、系副主任聘任人员名单
3. 南京农业大学实验教学中心主任聘任人员名单



南京农业大学2014年管理岗位和其他非教学科研岗位聘任人员名单（科级及以下）

园艺学院		实验技术 I	梁剑茹	科研实验
		实验技术 II	陈岚	科研实验
		实验技术 III	张雯雯	科研实验
	办公室	主任	张金平	
		秘书 I	刘丹	
		秘书 II	陈新	
		秘书 III	周泳	
		管理员	何英群	
	学生工作办公室	辅导员 I	孙笑逸	
园艺园林实验教学中心	实验技术 I	张国富	实验教学	
	实验技术 II	陈洁、蔡斌华、王小文	实验教学	
	中药学实验教学中心	实验技术	陈漪	实验教学
	实验技术 I	马月花	科研实验	
	实验技术 II	谢智华、齐开杰	科研实验	
动物科技学院	办公室	主任	孟繁星	
		秘书 I	李青芳	
		秘书 II	李静	
		秘书 III	林桂娟	
		图书资料员	肖慎华	
		编辑	袁丽霞、陈雯	自收自支0.5
			胡晓玲	机动岗
	学生工作办公室	辅导员 I	刘素惠	
		辅导员 II	苗婧	
	动物科学实验教学中心	实验技术 II	向小娥、汪薇、刘秀红	实验教学
		实验技术 III	丁立人、周建国	实验教学
		实验技术 IV	樊懿萱	科研实验
	农业部牛冷冻精液质量监督检验测试中心（南京）	检测室主任	陆汉希	比照系级机构，自收自支1
		实验技术	黄文佳	
动物医学院	办公室	主任	杜菊	
		秘书 I	贾晓庆	
		秘书 II	朱健	
		秘书 III	段颖	
		编辑	黄明睿、吴开宝	自收自支0.5
	学生工作办公室	辅导员 I	盛馨	
		辅导员 II	曹猛	
	基础兽医学实验教学中心	实验技术 I	施玉萍	实验教学
		实验技术 II	张春兰	实验教学
		实验技术 III	刘仪	实验教学
	预防兽医学实验教学中心	实验技术 I	于勇、任建鸾	实验教学
		实验技术 II	陈闻、顾金燕	实验教学
		实验技术 III	仇亚伟	实验教学
	临床兽医学实验教学中心	实验技术 II	周红	实验教学



国家自然科学基金项目

现代农业科技专著大系

动物寄生虫病 彩色图谱

第二版

李祥瑞 主编

 中国农业出版社

第二版编写人员

主 编 李祥瑞

编 者 (按姓名笔画排序)

白 启 宁长申 刘 群 孙延鸣 严若峰

李祥瑞 宋小凯 张西臣 胡俊杰 格日勒图

徐立新 陶建平 薄新文

图书在版编目 (CIP) 数据

动物寄生虫病彩色图谱 / 李祥瑞主编. 2 版.
北京: 中国农业出版社, 2011. 10
ISBN 978-7-109-16153-5

I. ①动… II. ①李… III. ①动物疾病-寄生虫病
图谱 IV. ①S855.9-64

中国版本图书馆 CIP 数据核字 (2011) 第 205782 号

中国农业出版社出版
(北京市朝阳区农展馆北路 2 号)
(邮政编码 100125)
责任编辑 王玉英

北京通州皇家印刷厂印刷 新华书店北京发行所发行
2011 年 10 月第 2 版 2011 年 10 月第 2 版北京第 1 次印刷

开本: 787mm×1092mm 1/16 印张: 16.75

字数: 369 千字 印数: 1-3 000 册

定价: 208.00 元

(凡本版图书出现印刷、装订错误, 请向出版社发行部调换)



国家出版基金项目

现代农业科技专著大系

兽医

微生物学

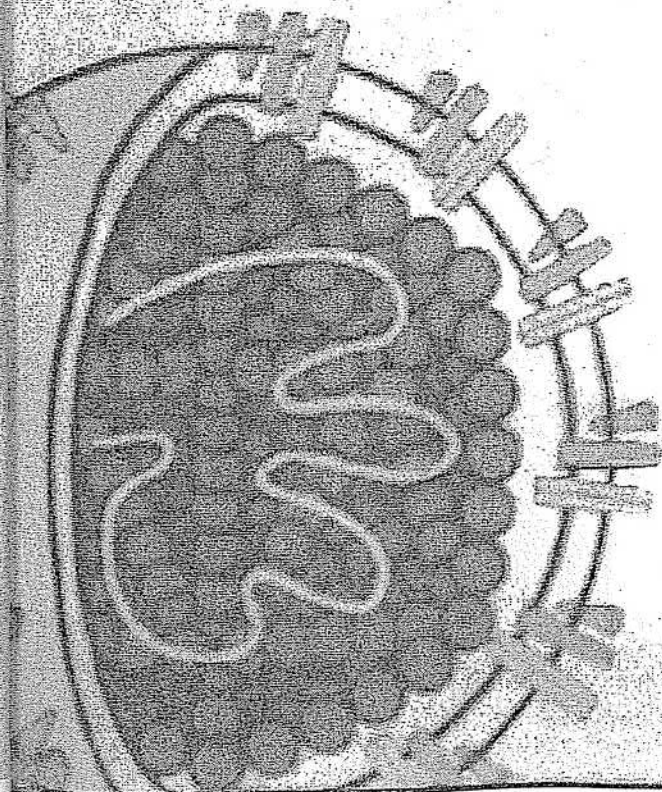
第二版

SHOUYI

WEISHENGWU XUE

中国农业科学院哈尔滨兽医研究所 组编

- 全面系统地介绍兽医微生物学理论和实验技术。
- 突出反映分子生物学实验技术、分析微生物的实验技术和最新免疫实验技术以及其它新的实验技术等。
- 重点叙述专业人员最需要了解的新技术和新方法等。



中国农业出版社

第二版编写人员

主编单位：中国农业科学院哈尔滨兽医研究所

主 编：孔宪刚

副主编：王笑梅

编审人员（按姓名笔画排序）：

于 力	马 建	马思奇	仇华吉	王云峰	王志亮	王秀荣
王春来	王景琳	王靖飞	丛明善	付朝阳	冯 力	冯 峰
卢彤岩	刘长明	刘恩国	刘胜旺	华育平	曲连东	祁小乐
初 秀	吴艳艳	张永强	李 成	李 爽	李 媛	李祥瑞
步志高	沈中元	沈国顺	谷守林	辛九庆	陆承平	陈化兰
周 婷	周建华	相文华	凌育樂	崔尚金	盖新娜	逯忠新
彭永刚	韩凌霞	雷连成	薛 飞			

第一版编写人员

主编单位：中国农业科学院哈尔滨兽医研究所

编审人员（按姓名笔画排序）：

于 力	于康霞	初 秀	白文彬	丛明善	朱尽围	刘滨东
宁希德	吴文芳	吴宝成	杨旭夫	李 成	谷守林	陈乃昌
陈章水	金 岳	周文举	相文华	荣骏弓	徐宜为	黄骏明

图书在版编目 (CIP) 数据

兽医微生物学/中国农业科学院哈尔滨兽医研究所
组编. —2版. —北京: 中国农业出版社, 2013. 7

(现代农业科技专著大系)

ISBN 978-7-109-17693-5

I. ①兽… II. ①中… III. ①兽医学—微生物学
IV. ①S852.6

中国版本图书馆 CIP 数据核字 (2013) 第 043359 号

中国农业出版社出版

(北京市朝阳区农展馆北路 2 号)

(邮政编码 100125)

策划编辑 黄向阳

北京中科印刷有限公司印刷 新华书店北京发行所发行
2013 年 12 月第 2 版 2013 年 12 月第 2 版北京第 1 次印刷

开本: 889mm×1194mm 1/16 印张: 63

字数: 1966 千字

定价: 280.00 元

(凡本版图书出现印刷、装订错误, 请向出版社发行部调换)



“十三五”国家重点图书
现代农业科技专著大系

兽医大辞典

SHOUYI DACIDIAN

第二版

汪明 主编

李祥瑞 副主编

中国农业出版社

图书在版编目 (CIP) 数据

兽医大辞典 / 汪明主编. — 2 版. — 北京: 中国农业出版社, 2013. 12

(现代农业科技专著大系)

ISBN 978-7-109-18609-5

I. ① 兽… II. ① 汪… III. ① 兽医学-词典 IV.
① S85-61

中国版本图书馆 CIP 数据核字 (2013) 第 270600 号

中国农业出版社出版

(北京市朝阳区农展馆北路 2 号)

(邮政编码 100125)

责任编辑 黄向阳

北京中科印刷有限公司印刷 新华书店北京发行所发行
2013 年 12 月第 2 版 2013 年 12 月第 2 版北京第 1 次印刷

开本: 787mm×1092mm 1/16 印张: 47.25

字数: 1585 千字

自然疫源性 疾病

唐家琪 主编



科学出版社
www.sciencep.com

《自然疫源性疾病》 编写委员会

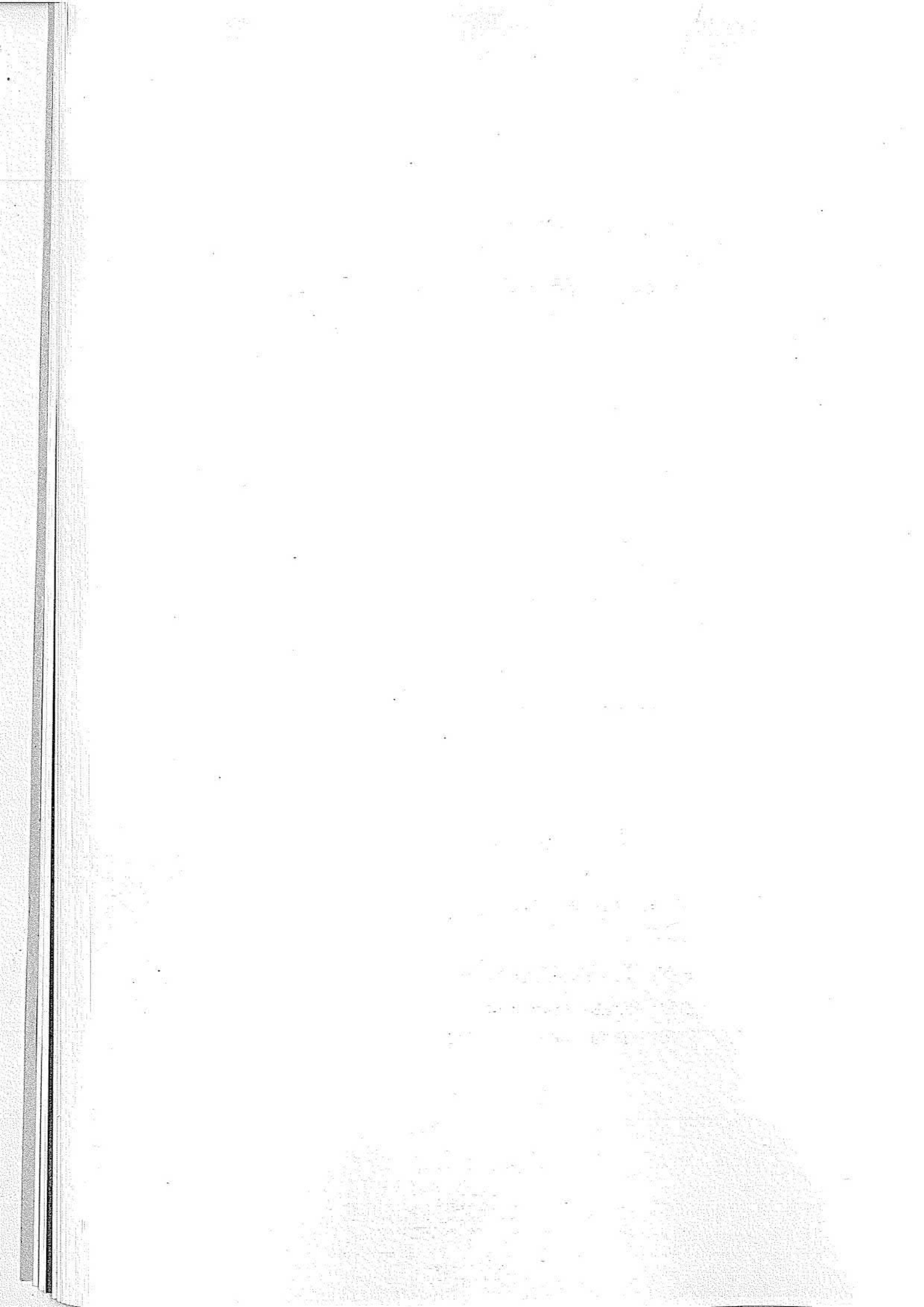
主 编 唐家琪

副主编 王长军 张金桐

编写者 (以姓氏笔画为序)

方 元	王长军	白 薇	庄汉澜
朱 进	李子华	李先富	李祥瑞
李德昌	张 云	张兆松	张泮河
张浩燕	张锦海	张耀娟	宋 阳
吴光华	陆承平	陆振勇	杨佩英
金立群	范明远	范宝昌	武 峰
尚德秋	战 威	俞树荣	徐克成
唐家琪	郭恒彬	章子豪	曹务春
焦新安	潘秀珍	操 敏	戴保民

主 审 方 元 吴光华



内 容 简 介

本书是一部全面系统论述自然疫源性疾病的专著。全书分为六篇,第一篇为总论,第二至六篇为各论,介绍了6类病原体所致的疾病95种,其中自然疫源性病毒病59种、立克次体病和衣原体病7种、螺旋体病3种、细菌病9种、寄生虫病17种。总论较系统地阐述了自然疫源学说的基本理论、自然疫源性疾病的流行病学特点及预防的原则与策略。各论内容基本上囊括了我国和世界各地已知(包括近年新发现和新出现)的主要自然疫源性疾病。每种疾病都从历史、病原学、流行病学、预防与控制、发病机制与病理学、临床表现与诊断、实验室诊断、治疗等项目予以详细阐述,尤其侧重病原学、流行病学、预防与控制、实验室诊断。内容广泛、翔实、新颖,汇集和归纳了国内外这一领域的研究成果和最新进展,融会了作者长期研究的成果和经验,较全面地反映了国内外自然疫源性疾病的研究现状。

本书可供预防医学、临床医学、兽医学和国境检疫工作者及相关研究人员参考阅读,也可用作大专院校医学、兽医学和生物学等相关专业的教学参考书。

敬告:本书的编者及出版者已努力使书中出现的疾病防治方案和药物使用方法等尽可能做到准确,并符合本书出版时国内普遍接受的标准。但随着医药学的发展,相关方案应适时作相应的调整。建议读者在借鉴本书内容时,结合最新进展慎重确定相关方案,尤其对使用新药或非常用药更应如此,编者及出版者拒绝对因参照本书内容而导致的事故与损失负责。

图书在版编目(CIP)数据

自然疫源性疾病/唐家琪主编. —北京:科学出版社,2005

ISBN 7-03-014242-X

I. 自… II. 唐… III. 自然疫源地-疾病-研究 IV. R521

中国版本图书馆CIP数据核字(2004)第097814号

责任编辑:莫培胜 乐俊河 / 责任校对:刘小梅
责任印制:钱玉芬 / 封面设计:耕者设计工作室

科学出版社 出版

北京东黄城根北街16号

邮政编码100717

<http://www.sciencep.com>

新蕾印刷厂 印刷

科学出版社发行 各地新华书店经销

2005年2月第 一 版 开本:889×1194 1/32

2005年2月第一次印刷 印张:15.4 插页:2

印数:1—2 000 字数:1 312 000

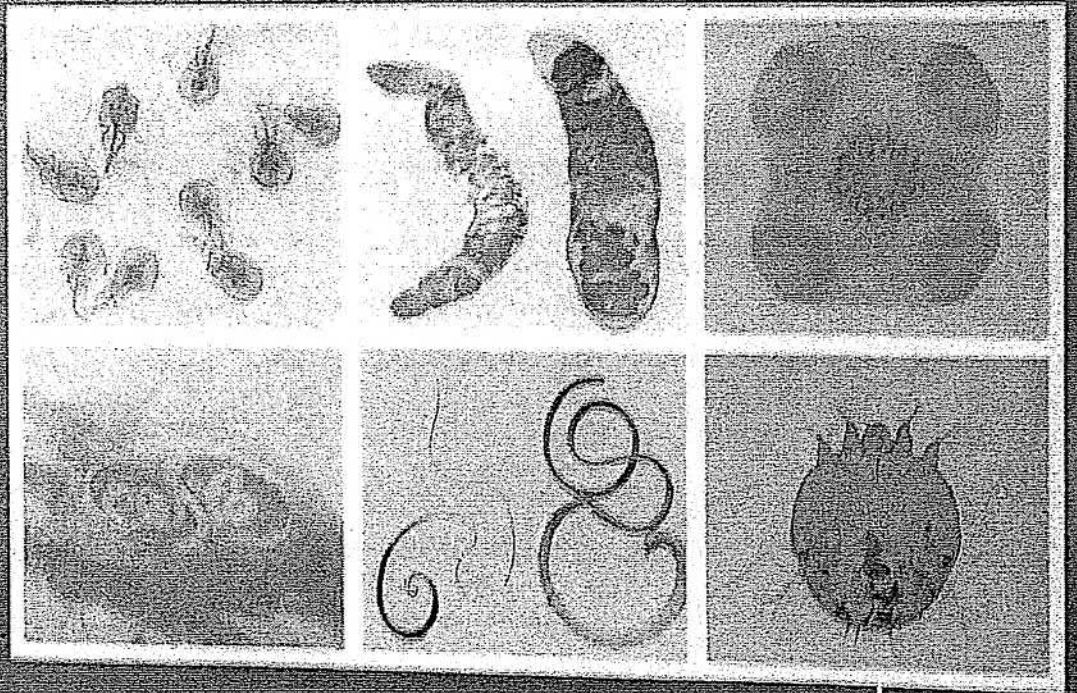
定价:170.00元

(如有印装质量问题,我社负责调换·新欣)

医学寄生虫图鉴

Yixue Jishengchong Tujian

主编 李朝品 高兴政



人民卫生出版社

编著者名单

CONTRIBUTORS

主 编 李朝品 高兴政

副主编 (以姓氏笔画为序)

王中全 王光西 王克霞 卢思奇 孙 新 孙恩涛 李祥瑞
沈浩贤 沈继龙 张兆松 张锡林 周本江 郑葵阳 赵亚娥
赵金红 黄 兵 黄 勇 崔 昱 崔 晶 程彦斌 湛孝东

主 审 吴中兴 常正山

《医学寄生虫图鉴》编辑委员会名录 (以姓氏笔画为序)

王少圣 王中全 王光西 王克霞 王慧勇 方 强 卢思奇
叶 彬 包怀恩 朱玉霞 刘忠湘 刘宜升 汤自豪 孙 新
孙恩涛 李祥瑞 李朝品 杨庆贵 吴增强 汪天平 沈浩贤
沈继龙 张 浩 张兆松 张锡林 陈盛霞 罗恩杰 周本江
郑学礼 郑葵阳 赵 亚 赵亚娥 赵金红 胡守锋 贺 骥
袁 俐 夏超明 徐大刚 高兴政 郭 家 郭增柱 唐小牛
黄 兵 黄 勇 崔 昱 崔 晶 程彦斌 湛孝东 蔡 茹

《医学寄生虫图鉴》编著者名单 (以姓氏笔画为序)

- | | | | |
|-----|---------------------|-----|-----------------|
| 马锐 | 宁夏医科大学 | 牟荣 | 贵州医学院 |
| 马雅军 | 第二军医大学 | 李小宁 | 皖南医学院 |
| 王健 | 安徽理工大学医学院 | 李生吉 | 安徽中医药高等专科学校 |
| 王少圣 | 皖南医学院 | 李祥瑞 | 南京农业大学 |
| 王中全 | 郑州大学医学院 | 李朝品 | 皖南医学院 |
| 王立英 | 中国疾病预防控制中心寄生虫病预防控制所 | | 安徽理工大学医学院 |
| 王光西 | 泸州医学院 | 杨庆贵 | 江苏出入境检验检疫局 |
| 王先寅 | 皖南医学院 | 杨照青 | 昆明医学院 |
| 王克霞 | 安徽理工大学医学院 | 吴增强 | 天津医科大学 |
| 王继春 | 中国医科大学 | 谷生丽 | 皖南医学院 |
| 王慧勇 | 淮北职业技术学院医学系 | 汪天平 | 安徽省寄生虫病防治研究所 |
| 方强 | 蚌埠医学院 | 沈静 | 安徽理工大学医学院 |
| 卢思奇 | 首都医科大学 | 沈浩贤 | 广州医学院 |
| 叶彬 | 重庆医科大学 | 沈继龙 | 安徽医科大学 |
| 田晔 | 安徽理工大学医学院 | 张忠 | 泰山医学院 |
| 付琳琳 | 徐州医学院 | 张威 | 齐齐哈尔医学院 |
| 包怀恩 | 贵州医学院 | 张超 | 皖南医学院 |
| 朱玉霞 | 安徽理工大学医学院 | 张西臣 | 吉林大学畜牧兽医学院 |
| 伍卫平 | 中国疾病预防控制中心寄生虫病预防控制所 | 张兆松 | 南京医科大学 |
| 向征 | 昆明医学院 | 张红卫 | 河南省疾病预防控制中心 |
| 刘浏 | 皖南医学院 | 张莺莺 | 皖南医学院 |
| 刘婷 | 皖南医学院 | 张锡林 | 第三军医大学 |
| 刘小燕 | 安徽理工大学医学院 | 陆维 | 皖南医学院 |
| 刘文权 | 温州医学院 | 陈光 | 佳木斯大学基础医学院 |
| 刘文艳 | 皖南医学院 | 陈文魁 | 皖南医学院 |
| 刘红丽 | 山西医科大学 | 陈兴智 | 蚌埠医学院 |
| 刘志刚 | 深圳大学生命科学院 | 陈盛霞 | 江苏大学基础医学与医学技术学院 |
| 刘忠湘 | 第四军医大学 | 武卫华 | 重庆医科大学 |
| 刘宜升 | 徐州医学院 | 罗庆礼 | 安徽医科大学 |
| 刘继鑫 | 齐齐哈尔医学院 | 罗恩杰 | 中国医科大学 |
| 江佳佳 | 安徽理工大学医学院 | 金立群 | 汕头大学医学院 |
| 汤自豪 | 九江医学院 | 周书林 | 皖南医学院 |
| 安春丽 | 中国医科大学 | 周本江 | 昆明医学院 |
| 许礼发 | 安徽理工大学医学院 | 郑学礼 | 南方医科大学 |
| 孙新 | 蚌埠医学院 | 郑葵阳 | 徐州医学院 |
| 孙恩涛 | 皖南医学院 | 赵亚 | 第四军医大学 |

赵金红 皖南医学院
 胡守隆 蚌埠医学院
 胡欢欢 中国疾病预防控制中心寄生虫病预防控制所
 姜 鹏 蚌埠医学院
 姜玉新 皖南医学院
 官鹏涛 吉林大学兽医学部
 贺 骥 厦门出入境检验检疫局
 秦元华 大连医科大学
 秦志辉 安徽理工大学医学院
 袁 俐 百河子大学医学院
 夏 惠 蚌埠医学院
 夏超明 苏州大学医学院
 顾有方 安徽科技学院
 徐大刚 上海交通大学医学院
 殷国荣 山西医科大学
 奚旭霞 芜湖市第一人民医院
 高兴政 北京中医药大学
 高锡强 皖南医学院
 郭 家 齐齐哈尔医学院

魏增旺 北京热带医学研究所
 滕小平 皖南医学院
 潘 春 皖南医学院
 陶 蔚 南京中医药大学
 黄 兵 上海兽医研究所
 黄 勇 山东省寄生虫病防治研究所
 黄永杰 安徽师范大学
 崔 昱 大连医科大学
 崔 洁 蚌埠医学院
 崔 晶 郑州大学医学院
 梁国雄 温州医学院
 程彦斌 西安交通大学医学院
 程孝东 皖南医学院
 蔡 菲 安徽理工大学医学院
 黄西萌 河南省疾病预防控制中心
 缪 峰 山东省寄生虫病防治研究所
 楼治国 安徽省寄生虫病防治研究所
 戴晓冬 大连医科大学

姓名: 李祥瑞

单位代码: 21001412

单位名称: 南京农业大学

主持项目列表:

批准号	负责人	申请单位	项目名称
30371078	李祥瑞	南京农业大学	捻转血矛线虫半乳糖结合凝集素在免疫和疾病发生中的作用及机理研究
30571393	李祥瑞	南京农业大学	捻转血矛线虫半胱氨酸蛋白酶新基因Hc58生物学特性研究
30771617	李祥瑞	南京农业大学	堆型艾美耳球虫免疫功能基因组研究
31172308	李祥瑞	南京农业大学	捻转血矛线虫重组galectin抑制山羊外周血淋巴细胞细胞因子转录的通路研究
31372428	李祥瑞	南京农业大学	鸡艾美耳球虫侵入部位特异性关键分子研究

关闭



全局数据统计

捻转血矛线虫重组galectin抑制山羊外周血淋巴细胞因子转录的通路研究

基本信息

批准号 31172308

项目名称 捻转血矛线虫重组galectin抑制山羊外周血淋巴细胞因子转录的通路研究

项目类别 面上项目

申请代码 C1804

项目负责人 李祥瑞

负责人职称 教授

依托单位 南京农业大学

研究期限 2012-01-01 到 2015-12-31

资助经费 62 (万元)

项目摘要

中文摘要 捻转血矛线虫是重要消化道寄生线虫，也是寄生线虫的模式，对反刍动物危害极大。已经证明，该虫体的galectin是重要的免疫抑制分子，体外试验可以抑制山羊PBMCs有丝分裂原诱导的多种细胞因子mRNA的转录水平。本研究拟将捻转血矛线虫重组galectin Hco-gal-卵和Hco-gal-m以及有丝分裂原Con A或LPS与山羊外周血淋巴细胞共同培养，鉴定淋巴细胞的galectin结合分子，观察细胞因子转录信号传导通路、调控通路以及有丝分裂原信号通路中多种关键分子的变化，并用RNA技术和蛋白质组学技术加以验证，研究galectin抑制有丝分裂原诱导的细胞因子转录的信号传导通路，对于阐明寄生性线虫galectin的生物学功能以及虫体所引起的免疫抑制机制具有重要意义，对于虫体的免疫防控以及促进我国养殖业的发展具有重要意义。

中文主题词 捻转血矛线虫；半乳糖结合凝集素；受体；信号通路；山羊

英文主题词 Haemonchus contortus; galectin; receptor; signal pathway; goat

结题项目:

结题项目	[161768]
成果类型:	
期刊论文	[1920273]
会议论文	[490577]
著作	[34309]
奖励	[41160]
专利	[56114]

结题时间:

2006	[7063]
2007	[5635]
2008	[5449]
2009	[10470]
2010	[11502]
2011	[15088]
2012	[19675]
2013	[23592]
2014	[16403]
2015	[32592]

项目资助 | [统计报告](#) | [优秀成果选编](#) | [年度报告](#)

当前位置: [首页](#) >> [基金要闻](#) >> [通知公告](#)

2016年度国家自然科学基金委员会与巴基斯坦科学基金会合作研究项目批准通知

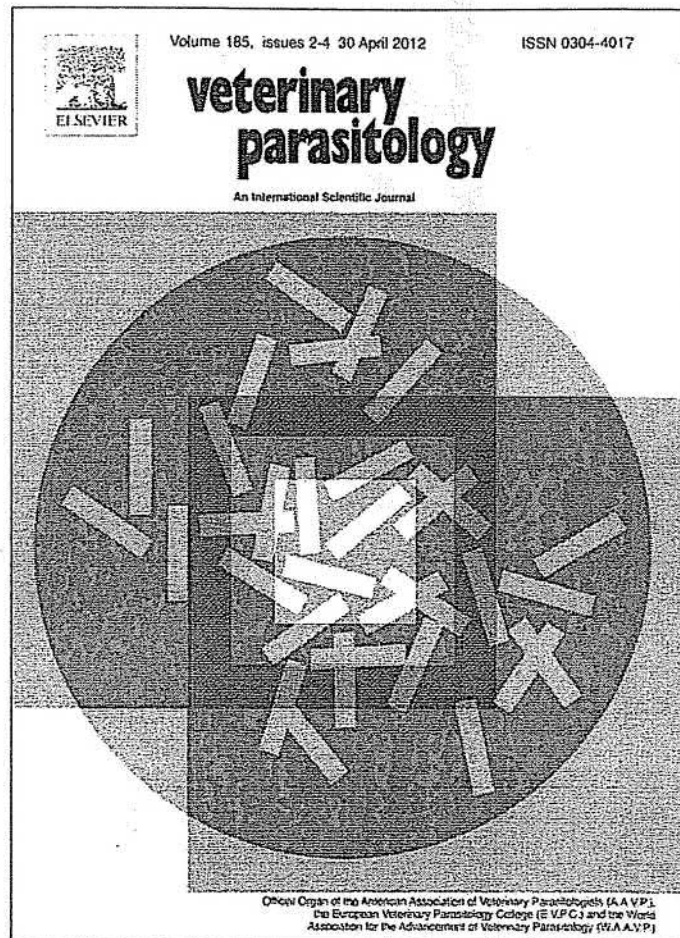
日期 2016-10-17 来源: 国际合作局 作者: 赵珂 【大】 【中】 【小】 【打印】 【关闭】

根据国家自然科学基金委员会 (NSFC) 与巴基斯坦科学基金会 (PSF) 签署的谅解备忘录和之后达成的合作共识, 2016年双方将在农业与生物科技 (Agriculture & Biotechnology)、地球科学 (Earth Sciences)、工程与材料科学 (Engineering & Material Sciences) 3个领域共同资助合作研究项目, 支持两国科学家开展实质性的创新研究与合作。经过公开征集, 双方各自组织评审并协商, 确定以下14个项目获得批准, 项目执行期限为2016年11月1日至2019年10月31日。

农业与生物科技领域 (3项)

序号	科学部编号	项目名称	中方申请人 中方单位名称	巴方申请人 巴方单位名称
1	3161101267	适宜我国和巴基斯坦杂交小麦品种创制及其水分高效利用研究	赵昌平 北京市农林科学院	Muhammad Arif University of Agriculture Peshawar
2	3161101242	鸡球虫树突状细胞刺激性抗原的确定及其应用	李祥瑞 南京农业大学	Muhammad Ali Shab PMAS Arid Agriculture University, Rawalpindi

Provided for non-commercial research and education use.
Not for reproduction, distribution or commercial use.

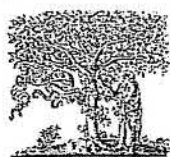


This article appeared in a journal published by Elsevier. The attached copy is furnished to the author for internal non-commercial research and education use, including for instruction at the authors institution and sharing with colleagues.

Other uses, including reproduction and distribution, or selling or licensing copies, or posting to personal, institutional or third party websites are prohibited.

In most cases authors are permitted to post their version of the article (e.g. in Word or Tex form) to their personal website or institutional repository. Authors requiring further information regarding Elsevier's archiving and manuscript policies are encouraged to visit:

<http://www.elsevier.com/copyright>



ELSEVIER

Veterinary Parasitology

journal homepage: www.elsevier.com/locate/vetpar

Detection of *Toxoplasma gondii* in free-range chickens in China based on circulating antigens and antibodies

GuangWei Zhao, Bo Shen, Qing Xie, Li Xin Xu, Ruo Feng Yan, Xiao Kai Song, I.A. Hassan, Xiang Rui Li*

College of Veterinary Medicine, Nanjing Agricultural University, Nanjing, Jiangsu 210095, PR China

ARTICLE INFO

Article history:

Received 1 June 2011

Received in revised form 21 October 2011

Accepted 24 October 2011

Keywords:

Toxoplasma gondii

Prevalence

Chicken

China

ABSTRACT

Toxoplasma gondii is widely distributed in humans and other animals including domestic poultry throughout the world, but the data on prevalence of *T. gondii* in free-ranged (FR) chickens in People's Republic of China (PRC) are limited. In the present study, the seroprevalence of *T. gondii* infection in FR chickens was investigated in 13 provinces/municipalities of China during the period from January to June 2010. A total of 1173 serum samples were collected and assayed for *T. gondii* circulating antigens (TCA) and antibodies (TCAb) using enzyme linked immunosorbent assay (ELISA) technique. Out of this number, 199 samples were TCA positive (16.97%), 226 samples were TCAb positive (19.27%), 69 samples were positive for both TCA and TCAb (5.88%), and the total seropositive rate was found in 356 of 1173 (30.36%). The results of the present survey indicated that infection with *T. gondii* in FR chickens is widely spread in China.

© 2011 Elsevier B.V. All rights reserved.

1. Introduction

Infections by *Toxoplasma gondii* are widely prevalent in animals and humans throughout the world. It is estimated that around 25% of the world human population is carrying the parasite (Petersen, 2007). A recent paper reviewed worldwide reports of clinical toxoplasmosis in experimentally and naturally infected chickens concluded that clinical toxoplasmosis is rare in chickens (Dubey, 2009). However, free-range (FR) chickens are considered as one of the most important hosts in the epidemiology of *T. gondii* infection because they are an efficient source of infection for both cats that excrete the environmentally resistant oocysts and humans who may become infected with this parasite after eating undercooked infected chicken meat. So, FR chickens are considered an important indicator of soil contamination with the environmentally resistant oocysts of *T. gondii* (Ruiz and Frenkel, 1980).

Sero-epidemiological surveys about the *T. gondii* infection of chickens have been conducted in southern and northeast China (Yan et al., 2009; Zhu et al., 2008) recently. However, only four provinces (Hainan province, Hunan province, Guangdong province and Guangxi Zhuang Nationality autonomous region) in southern China and two provinces (Liaoning province and Jilin province) in northeast China were investigated in the previously surveys. Furthermore, the surveys' for *T. gondii* infection were conducted only according to their antibodies while antigens were not considered. So, in this research, we reported the *T. gondii* infection situation of chickens in 13 provinces/municipality of China based on *T. gondii* circulating antigens (TCA) and antibodies (TCAb).

2. Materials and methods

2.1. Free-range chickens and sampling locations

Blood samples were collected by venipuncture from 1173 FR chickens of 13 provinces/municipalities in China from January to June in 2010. The number of serum

* Corresponding author. Tel.: +86 25 84399000; fax: +86 25 84399000.
E-mail address: Lixiangrui@njau.edu.cn (X.R. Li).

Table 1
Seroprevalence of *Toxoplasma gondii* in FR chickens of PRC.

Provinces/municipality [location on map (Fig. 1)]	Age	No. tested	TCA positive	TCAb positive	TCA and TCAb positive	Positive ratio ^a
Xinjiang Uygur autonomous region (XJ)	180 days	67	8.96% ^a (6/67)	10.45% ^a (7/67)	2.99% ^a (2/67)	16.42% ^a (11/67)
Neimenggu autonomous region (NMG)	180 days	61	16.39% ^{a,c} (10/61)	14.75% ^a (7/61)	3.28% ^a (2/61)	27.87% ^a (17/61)
Liaoning province (LN)	90 days	50	18% ^{a,c} (9/50)	8% ^a (4/50)	6% ^a (3/50)	20% ^a (10/50)
Shandong province (SD)	180 days	71	32.39% ^c (23/71)	12.68% ^a (9/71)	2.82% ^a (2/71)	42.25% ^{b,d} (30/71)
Henan province (HN)	180 days	135	8.89% ^a (12/135)	12.59% ^a (17/135)	1.48% ^b (2/135)	20.00% ^a (27/135)
Jiangsu province (JS)	180 days	165	16.36% ^{a,c} (27/165)	35.15% ^b (58/165)	4.24% ^a (7/165)	47.27% ^d (78/165)
Anhui province (AH)	90 days	60	6.67% ^a (4/60)	0% ^c (0/60)	0% ^b (0/60)	6.67% ^c (4/60)
Sichuan province (SC)	90 days	93	21.51% ^c (20/93)	11.83% ^a (11/93)	7.53% ^c (7/93)	25.81% ^{a,e} (24/93)
Chongqing municipality (CG)	180 days	84	25% ^c (21/84)	29.76% ^b (25/84)	19.05% ^d (16/84)	35.71% ^{b,e} (30/84)
Jiangxi province (JX)	90 days	111	24.32% ^c (27/111)	22.52% ^b (25/111)	7.21% ^c (8/111)	39.64% ^{b,d} (44/111)
Fujian province (FJ)	180 days	64	0% ^d (0/64)	15.63% ^{a,b} (10/64)	0% ^b (0/64)	15.63% ^{a,c} (10/64)
Guangxi Zhuang Nationality autonomous region (GX)	90 days	140	22.86% ^c (32/140)	27.86% ^b (39/140)	12.14% ^{c,d} (17/140)	38.57% ^{b,d,e} (54/140)
Guangdong province (GD)	90 days	72	11.11% ^a (8/72)	19.44% ^{a,b} (14/72)	4.17% ^a (3/72)	26.39% ^{a,e} (19/72)
Total	–	1173	16.97% (199/1173)	19.27% (226/1173)	5.88% (69/1173)	30.35% (356/1173)

Values bearing a different superscript letter (a, b, c, d, e) within a column differ significantly from one another ($P < 0.05$).

^a Positive ratio (%) = [(numbers positive by TCA + numbers positive by TCAb) – (numbers positive by both TCA & TCAb)] / numbers of total samples.

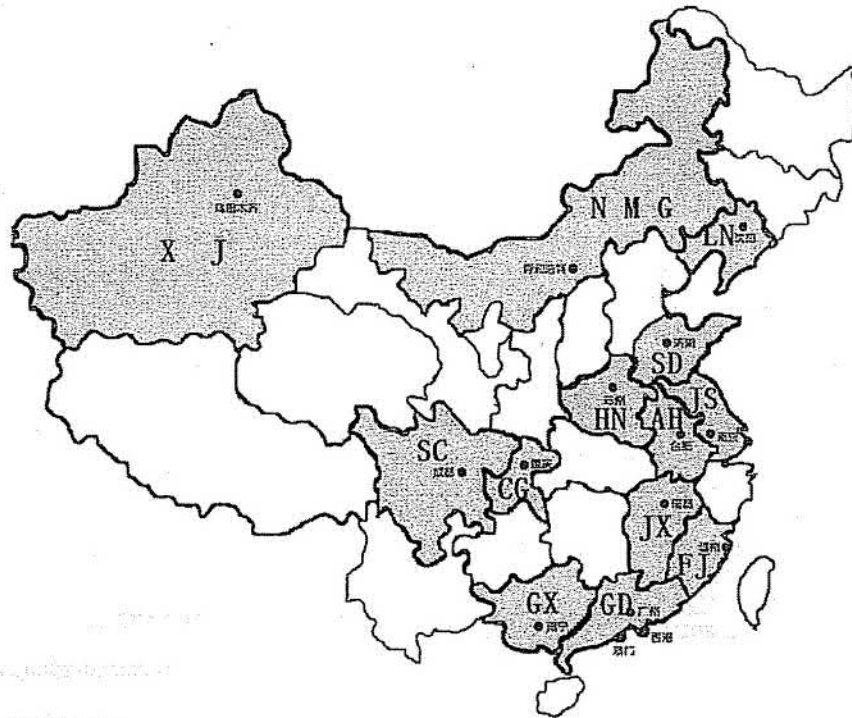


Fig. 1. The provinces/municipalities in Mainland China where chickens have been surveyed for *T. gondii*. Shaded areas are the sampling locations for the present survey. XJ, Xinjiang Uygur autonomous region; NMG, Neimenggu autonomous region; LN, Liaoning province; SD, Shandong province; HN, Henan province; AH, Anhui province; JS, Jiangsu province; SC, Sichuan province; CG, Chongqing municipality; JX, Jiangxi province; FJ, Fujian province; GX, Guangxi Zhuang Nationality autonomous region; GD, Guangdong province.

samples from each province was shown in Table 1. The chickens of each flock were randomly selected, and one blood sample was collected from each chicken. The samples were collected according to the rate of 1:100 in the flock. From each province or municipality, six flocks with the size 1000–3500 were investigated. The thirteen provinces/municipalities selected for the study covered Eastern China (Shandong province, Jiangsu province, Anhui province and Fujian province), Southern China (Guangdong province, Guangxi Zhuang Nationality autonomous region), Central China (Henan province, Jiangxi province), Northern China (Neimenggu autonomous region), northwest (Xinjiang Uygur autonomous region), northeast (Liaoning province) and southwest (Sichuan province, Chongqing municipality) of China. The location of the flocks is shown in Fig. 1.

Data regarding these chickens (species, age, and location) were also recorded. All these FR chickens were raised on ground, allowed to roam freely without fencing and only housed at night with the maximum density of 1 chicken/m².

2.2. Sera preparation

Sera were obtained by centrifugation of clotted blood and kept at 4°C until being dispatched to the laboratory with cold packs by air. After that, all the sera were stored at –20°C before use.

2.3. Serological examination

The circulating antigens and antibodies were determined with the “Chicken toxoplasma circulating antigen (TCA) ELISA Kit” (DRE73521, R&B Scientific, USA) and “Chicken toxoplasma circulating antibody (TCAb) ELISA Kit” (DRE73549, R&B Scientific, USA), respectively, according to manufacturer’s instructions. In brief, 50 µL of diluted chicken sera (1:5) were added to each well (pre-coated with antigen or an antibody specific to TCA) in triplicate and incubated at 37°C for 1 h. The wells were washed five times with washing solution (PBS containing 0.05%, v/v Tween-20) and peroxidase-conjugated rabbit anti-chicken antibody (IgY-HRP) or HRP-conjugated rat anti-TCA specific antibody was added to each well afterwards. The tetramethylbenzidine (TMB)-peroxidase substrate system was used for the colorimetric reaction. After stopped by 50 µL 2 M sulphuric acid (H₂SO₄), plates were read at an optical density of 450 nm in the Model 550 microplate ELISA reader (Bio-Rad). Standard positive and negative controls were included on each plate. When positive control serum reached OD > 1 and negative control serum should not exceed OD = 0.15. The cut-off point of OD value of a positive sample was set to be the least >OD value of negative control (+0.15).

2.4. Determination for the positive ratio

The positive ratio from a given locality was calculated using the following formula: positive ratio (%) = [(numbers positive by TCA + numbers positive by TCAb) – (numbers positive by both TCA and TCAb)]/numbers of total samples.

The overall positive ratio was taken from all the positive samples of all locations using the same formula (Table 1).

2.5. Statistical analysis

Statistical analyses of *T. gondii* prevalence in FR chickens from different administrative regions and age groups were performed by χ^2 -test with excel (Microsoft® Excel 2003). The differences were considered statistically significant if $p < 0.05$. Correlations between TCA and TCAb were tested with Pearson’s rank correlation coefficient.

3. Results

3.1. Positive ratios for TCA and TCAb and the overall ratios for the thirteen provinces/municipalities

A total of 1173 FR chicken serum samples from 13 provinces/municipalities were tested for *T. gondii* circulating antigens and antibodies, respectively. 199 (16.97%) were positive for TCA, 226 (19.27%) were positive for TCAb, 69 (5.88%) were positive for both TCA and TCAb, and the total seropositive rate was found in 356 (30.35%) out of 1173 samples (Table 1). The total seropositive rates of the 13 provinces/municipalities ranged from 6.67% to 47.27%.

Detecting TCA, the positive rates of the 13 provinces/municipalities ranged from 0% to 32.39% (Table 1). Shandong province (SD) was the highest location ($p < 0.01$) compared with the other 12 provinces/municipalities. Seven provinces/municipalities including Neimenggu autonomous region (NMG), Liaoning province (LN), Jiangsu province (JS), Sichuan province (SC), Chongqing municipality (CG), Jiangxi province (JX) and Guangxi Zhuang Nationality autonomous region (GX) had relatively high positive rates ranged from 16.36% to 24.32%, but with no significant differences among them ($p > 0.05$). However, no samples out of 64 tested were found positive (0%) in Fujian province (FJ) and it was the lowest ($p < 0.01$) province in this study.

Detecting TCAb, the positive rates of the 13 provinces/municipalities ranged from 0% to 35.15% (Table 1). Jiangsu province (JS) was significantly higher than the other 12 provinces/municipalities except Chongqing municipality (CG) ($p > 0.05$, $\chi^2 = 3.248$) and Guangxi Zhuang Nationality autonomous region (GX) ($p > 0.05$, $\chi^2 = 1.231$). The TCAb positive rates in Xinjiang Uygur autonomous region (XJ), Neimenggu autonomous region (NMG), Liaoning province (LN), Shandong province (SD), Henan province (HN), Sichuan province (SC) and Fujian province (FJ) ranged from 8.0% to 15.63%, and differences among these regions were not statistically significant ($p > 0.05$). However, no samples out of 60 tested were found positive (0%) in Anhui province (AH) and it was the lowest ($p < 0.01$) province in this study.

The overall positive ratios of Jiangsu province (JS) and Shandong province (SD), Chongqing municipality (CG), Jiangxi province (JX) and Guangxi Zhuang Nationality autonomous region (GX) were highly significant ($p < 0.01$) than the other provinces/municipalities while Anhui province (AH) and Fujian province (FJ) both of them had the low positive ratios ($p < 0.01$) compared to

Table 2
Seroprevalence of *Toxoplasma gondii* in FR chickens of seven large regions of China.

Provinces/municipality (location on map)	No. tested	TCA positive	TCAb positive	TCA and TCAb positive	Positive ratio [†]
Eastern China	360	15.0% ^a (54/360)	21.39% ^{cd} (77/360)	2.5% ^a (9/360)	33.89% ^a (122/360)
Southern China	212	18.87% ^a (40/212)	25.0% ^{ad} (53/212)	9.43% ^b (20/212)	34.43% ^a (73/212)
Central China	246	15.85% ^a (39/246)	17.07% ^{bc} (42/246)	4.07% ^a (10/246)	28.86% ^a (71/246)
Northern China	61	16.39% ^a (10/61)	11.48% ^b (7/61)	3.28% ^a (2/61)	24.59% ^{ab} (15/61)
Northwest of China	67	8.96% ^a (6/67)	10.45% ^b (7/67)	2.99% ^a (2/67)	16.42% ^b (11/67)
Northeast of China	84	25.0% ^b (21/84)	29.76% ^{ad} (25/84)	19.05% ^c (16/84)	35.71% ^a (30/84)
Southwest of China	177	23.16% ^b (41/177)	20.34% ^{cd} (36/177)	12.99% ^{bc} (23/177)	30.51% ^a (54/177)

Values bearing a different superscript letter (a, b, c, d) within a column differ significantly from one another ($P < 0.05$).

[†] Positive ratio (%) = [(numbers positive by TCA + numbers positive by TCAb) - (numbers positive by both TCA & TCAb)] / numbers of total samples.

other provinces/municipalities. There were no significant differences ($p > 0.01$) among Xinjiang Uygur autonomous region (XJ), Neimenggu autonomous region (NMG), Liaoning province (LN), Henan province (HN), Sichuan province (SC) and Guangdong province (GD).

No significant correlation was found between TCA and TCAb in the 13 provinces/municipalities ($r = 0.463$, $p > 0.05$).

3.2. Positive ratios for TCA and TCAb and the overall ratios for the seven large regions of China

TCA positive rates for the seven regions were ranged from 8.96% to 25.0% as shown in Table 2. Northeast of China was significantly higher than both Eastern China ($p < 0.05$, $\chi^2 = 4.853$) and northwest of China ($p < 0.05$, $\chi^2 = 6.534$). Similarly, southwest of China was also significantly higher than both Eastern China ($p < 0.05$, $\chi^2 = 5.431$) and northwest of China ($p < 0.05$, $\chi^2 = 6.309$).

TCAb positive rates for the seven regions were ranged from 10.45% to 29.76% as shown in Table 2. Northeast of China was significantly higher than Central China ($p < 0.05$, $\chi^2 = 4.352$), Northern China ($p < 0.05$, $\chi^2 = 5.053$) and northwest of China ($p < 0.05$, $\chi^2 = 6.387$). Meanwhile, southern China was also highly significant compared to Central China ($p < 0.05$, $\chi^2 = 6.231$), Northern China ($p < 0.01$, $\chi^2 = 6.871$) and northwest of China ($p < 0.01$, $\chi^2 = 8.325$). The positive ratios of northern China and northwest of China were relatively lower than those of other regions in the present study with 11.48% and 10.45%, respectively.

The overall positive ratios in each region ranged from 16.42% to 34.43% (Table 2). Northwest of China was statistically the lowest region compared to the other 6 regions.

However, among the remaining 6 regions of Eastern China, Southern China, Central China, Northern China, northeast of China and southwest of China, the levels were not significantly different.

A significant correlation was detected between TCA and TCAb in the seven large regions of China ($r = 0.876$, $p < 0.01$).

3.3. TCA, TCAb and the overall positive ratios to *T. gondii* of FR chickens affected by age

The TCA positive rates for the 180 days old and 90 days old chickens were 15.3% and 19.01%, respectively, while for TCAb they were 20.56% and 17.68%, respectively (Table 3). And for the overall positive rate it was 31.38% and 29.47%, for both groups respectively. The TCA positive rate of 180 days old FR chickens was a little lower than that of 90 days old FR chickens, while TCAb and overall positive rates were slightly higher. There were no statistically significant differences between the two groups with TCA ($p > 0.05$, $\chi^2 = 2.835$), TCAb ($p > 0.05$, $\chi^2 = 1.543$) and overall positive rate ($p > 0.05$, $\chi^2 = 1.179$).

There was no significant correlation between TCA and TCAb in the two age groups ($r = 0.402$, $p > 0.05$).

4. Discussion

Many surveys detecting *T. gondii* infection in FR chickens have been conducted in a number of countries and the prevalence rates in most of these studies ranged between 36.3% and 85.7% (Dubey et al., 2003, 2004, 2005b,c, 2006a,b,c, 2007, 2008; Lindstrom et al., 2008). However, in the present study, the 13 surveyed

Table 3
Toxoplasma gondii infection in chickens of China determined by ELISA test affected by age.

Age	No. examined	No. TCA positive	TCA prevalence	No. TCAb positive	TCAb prevalence	No. TCA and TCAb positive	TCA and TCAb prevalence	Total prevalence
180 days	647	99	15.3%	133	20.56%	31	4.79%	31.38%
90 days	526	100	19.01%	93	17.68%	38	7.22%	29.47%

provinces/municipalities showed that the total seroprevalence of *T. gondii* in FR chickens was 30.35% which is significantly lower than some reports in other countries including Nicaragua (Dubey et al., 2006c), Uganda (Lindstrom et al., 2008), Chile (Dubey et al., 2006a), Israel (Dubey et al., 2004) and Colombia (Dubey et al., 2005b). Although the average seroprevalence was lower, some provinces/municipalities such as Jiangsu province (47.27%) and Shandong province (42.25%) still existed a high infection rate. In addition, comparing the findings of the current investigation with those previously conducted in China, the prevalence rate of total TCAB (29.76%) in northeast China was also lower but without significance ($p > 0.05$, $\chi^2 = 0.559$) compared with previous reports (34.7%) (Zhu et al., 2008). Meanwhile, the rate of total TCAB (25.0%) in southern China was significantly higher ($p < 0.05$, $\chi^2 = 6.212$) compared with the other report (11.4%) (Yan et al., 2009). In the previous study of northeast China (Zhu et al., 2008), the FR chickens were purchased without any consideration on sex and age from 3 villages and enzyme-linked immunosorbent assay (ELISA) method was used to detect the anti-*T. gondii* IgG in chickens, while in the study of southern China (Yan et al., 2009), serum samples were collected from two slaughterhouses in Guangzhou City from approximately six-month old FR chickens and tested for *T. gondii* antibodies with the modified agglutination test (MAT). All the chickens in these studies were raised on ground and had free access to feed and water. The breeds in this study were local chicken for egg or meat, but were not detailed in the previous studies. The infection rate in this study was significantly higher than previous study in southern China while northeast China was not which indicated that ELISA method was more sensitive than MAT. So, the variation in seroprevalence rates of China might mainly depend on the sensitivity of the serological methods used and also the age at which the samples were collected. These results indicated that *T. gondii* infection was spread widely in China and in accordance with previous study that the average rate always above 30% (Dubey, 2009).

Worldwide seroepidemiology studies of *T. gondii* infection in free-range chickens were performed with techniques like MAT (Modified agglutination test) method (Dubey et al., 2005a, 2008; Dubey and Jones, 2008). However, the MAT titer that should be considered specific for the diagnosis of toxoplasmosis in poultry has not been determined (Dubey, 2009) because *T. gondii* could be isolated from chickens with a MAT titer of only 1:5 occasionally. Similar studies in pigs (Garcia et al., 2008; Hill et al., 2006) had shown that ELISA method has a higher sensitivity rate and it could perform better than the MAT method for detecting serum antibodies for *Toxoplasma*. So, in this research, we used ELISA method to detect the infection with *Toxoplasma*.

As reported previously *T. gondii* circulating antigen (TCA) was considered to be a direct evidence that an infection was present and could be easily detected during the acute phase (Wang et al., 2011b). But, in this phase, the antibodies may not produce. Therefore, if detection only relies on circulating antibodies some positive samples might be neglected. So, in the present study, serological detection

assays using both TCA and TCAB were performed by ELISA technique.

Geographically, there are seven large regions in China, including Eastern China, Southern China, Central China, Northern China, northwest, northeast and southwest of China based on the different natural climates. In the seven regions, the overall positive rate of northwest China was lower than that of the other six regions. The reason behind that might be the arid and rainless climate there, and the drying under low humidity and high temperature were deleterious for the oocysts (Dubey, 2009). So possibly that is the main reason for the lower infection rate to *T. gondii* of FR chickens in the northwest of China. Northeast of China had relatively higher overall positive rate than the other regions in this study and this might be associated with the lower temperature in the summer (an average temperature of -5°C in the north and 5°C in the south) which could keep the oocysts of *T. gondii* alive after shedded by infected cats and likely to infect the FR chickens.

Considering the age, the present survey showed that TCAB rates were higher in older group (180 days) in contrast to TCA rates which were higher in younger (90 days), although the differences were not statistically significant ($p > 0.05$). Meanwhile, the overall seroprevalence showed that the infection was much more spread in older chickens than the younger ones (Table 3). These findings were similar to those of some previous investigations in goats and sheep (Wang et al., 2011a). The reasons behind this might be that the older animals had more opportunities to get infected than the younger ones. In addition, for generally TCAB once produced may persist for a long time while TCA is short, so it is much likely to detect antibodies in older chickens than in the younger ones and accordingly the infection status can be defined as dormant in olders and active in the younger. In this research, only two age groups were investigated. The relationship between the age and the infection needs further researched.

Felids, in particular the cat, are the only known animals that can excrete environmentally resistant oocysts, playing an important role in the epidemiology of toxoplasmosis (Dubey, 2009). The distribution of *T. gondii* in chicken might be related to the cats that disseminated the oocysts in the soil. On the other hand, cats could be infected from eating chicken meat, wild birds and rodents infected with *T. gondii*. However, investigations on these hypotheses still need to be conducted.

Some studies have shown that consuming undercooked infected chicken is an important source of *T. gondii* infection for humans (Boyer et al., 2005). Therefore, *T. gondii* infection in chickens is epidemiologically significant. People in some places of China have the habit of eating under-cooked chicken 'kabob', so people there should be aware of the risk of encountering *T. gondii* infection.

In conclusion, the results of the present survey and other surveys indicated that infection with *T. gondii* in free-ranged chickens is widely spread in China, and since it is a zoonotic health problem, public health care organizations including human and animal departments beside the hygiene policy makers should raise the concerns and collaborate together to confine this issue.

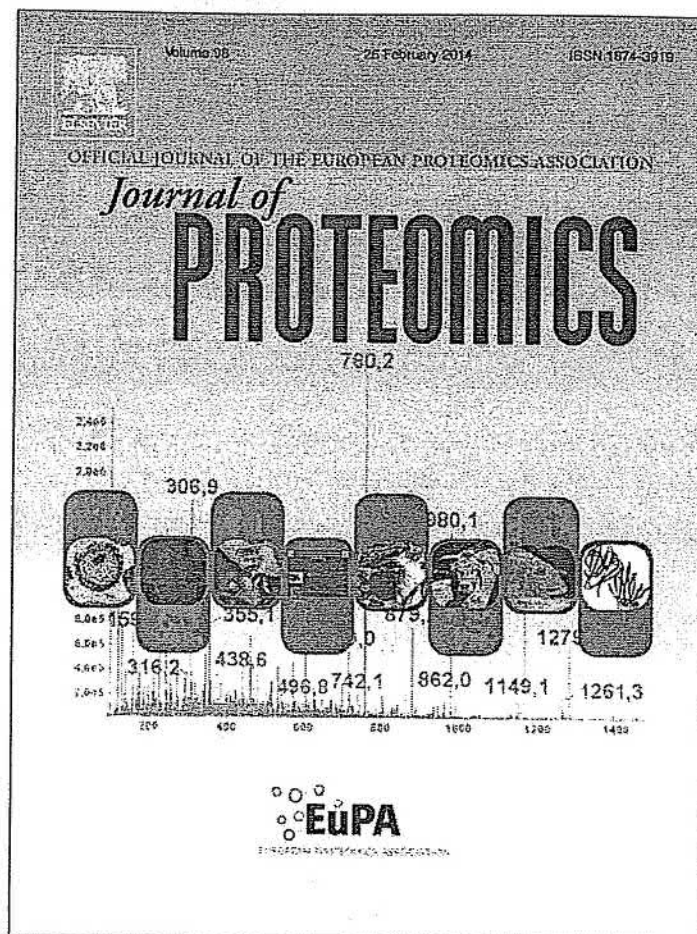
Acknowledgements

This work was supported by the Special Fund for Public Welfare Industry of Ministry of Agriculture of China (200903036-04). The authors are grateful to those staff in the thirteen surveyed provinces/municipalities who assisted in the collection of free-ranged chicken blood samples.

References

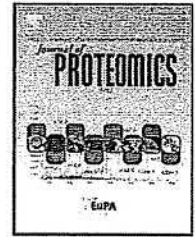
- Boyer, K.M., Holfels, E., Roizen, N., Swisher, C., Mack, D., Remington, J., Withers, S., Meier, P., McLeod, R., 2005. Risk factors for *Toxoplasma gondii* infection in mothers of infants with congenital toxoplasmosis: implications for prenatal management and screening. *Am. J. Obstet. Gynecol.* 192, 564–571.
- Dubey, J.P., 2009. *Toxoplasma gondii* infections in chickens (*Gallus domesticus*): prevalence, clinical disease, diagnosis and public health significance. *Zoonoses Public Health* 57, 60–73.
- Dubey, J.P., Edelhofer, R., Marcet, P., Vianna, M.C., Kwok, O.C., Lehmann, T., 2005a. Genetic and biologic characteristics of *Toxoplasma gondii* infections in free-range chickens from Austria. *Vet. Parasitol.* 133, 299–306.
- Dubey, J.P., Gomez-Marin, J.E., Bedoya, A., Lora, F., Vianna, M.C., Hill, D., Kwok, O.C., Shen, S.K., Marcet, P.L., Lehmann, T., 2005b. Genetic and biologic characteristics of *Toxoplasma gondii* isolates in free-range chickens from Colombia, South America. *Vet. Parasitol.* 134, 67–72.
- Dubey, J.P., Graham, D.H., Dahl, E., Hilali, M., El-Ghaysh, A., Sreekumar, C., Kwok, O.C., Shen, S.K., Lehmann, T., 2003. Isolation and molecular characterization of *Toxoplasma gondii* from chickens and ducks from Egypt. *Vet. Parasitol.* 114, 89–95.
- Dubey, J.P., Huong, L.T., Lawson, B.W., Subekti, D.T., Tassi, P., Cabaj, W., Sundar, N., Velmurugan, G.V., Kwok, O.C., Su, C., 2008. Seroprevalence and isolation of *Toxoplasma gondii* from free-range chickens in Ghana, Indonesia, Italy, Poland, and Vietnam. *J. Parasitol.* 94, 68–71.
- Dubey, J.P., Jones, J.L., 2008. *Toxoplasma gondii* infection in humans and animals in the United States. *Int. J. Parasitol.* 38, 1257–1278.
- Dubey, J.P., Patitucci, A.N., Su, C., Sundar, N., Kwok, O.C., Shen, S.K., 2006a. Characterization of *Toxoplasma gondii* isolates in free-range chickens from Chile, South America. *Vet. Parasitol.* 140, 76–82.
- Dubey, J.P., Salant, H., Sreekumar, C., Dahl, E., Vianna, M.C., Shen, S.K., Kwok, O.C., Spira, D., Hamburger, J., Lehmann, T.V., 2004. High prevalence of *Toxoplasma gondii* in a commercial flock of chickens in Israel, and public health implications of free-range farming. *Vet. Parasitol.* 121, 317–322.
- Dubey, J.P., Su, C., Oliveira, J., Morales, J.A., Bolanos, R.V., Sundar, N., Kwok, O.C., Shen, S.K., 2006b. Biologic and genetic characteristics of *Toxoplasma gondii* isolates in free-range chickens from Costa Rica, Central America. *Vet. Parasitol.* 139, 29–36.
- Dubey, J.P., Sundar, N., Gennari, S.M., Minervino, A.H., Farias, N.A., Ruas, J.L., dos Santos, T.R., Cavalcante, G.T., Kwok, O.C., Su, C., 2007. Biologic and genetic comparison of *Toxoplasma gondii* isolates in free-range chickens from the northern Para state and the southern state Rio Grande do Sul, Brazil revealed highly diverse and distinct parasite populations. *Vet. Parasitol.* 143, 182–188.
- Dubey, J.P., Sundar, N., Pineda, N., Kyvsgaard, N.C., Luna, L.A., Rimbaud, E., Oliveira, J.B., Kwok, O.C., Qi, Y., Su, C., 2006c. Biologic and genetic characteristics of *Toxoplasma gondii* isolates in free-range chickens from Nicaragua, Central America. *Vet. Parasitol.* 142, 47–53.
- Dubey, J.P., Fair, P.A., Bossart, G.D., Hill, D., Fayer, R., Sreekumar, C., Kwok, O.C., Thulliez, P., 2005c. A comparison of several serologic tests to detect antibodies to *Toxoplasma gondii* in naturally exposed bottlenose dolphins (*Tursiops truncatus*). *J. Parasitol.* 91, 1074–1081.
- Garcia, J.L., Gennari, S.M., Navarro, I.T., Machado, R.Z., Headley, S.A., Vidotto, O., da Silva Guimaraes Junior, J., Bugni, F.M., Igarashi, M., 2008. Evaluation of IFA, MAT, ELISAs and immunoblotting for the detection of anti-*Toxoplasma gondii* antibodies in paired serum and aqueous humour samples from experimentally infected pigs. *Res. Vet. Sci.* 84, 237–242.
- Hill, D.E., Chirukandoth, S., Dubey, J.P., Lunney, J.K., Gamble, H.R., 2006. Comparison of detection methods for *Toxoplasma gondii* in naturally and experimentally infected swine. *Vet. Parasitol.* 141, 9–17.
- Lindstrom, I., Sundar, N., Lindh, J., Kironde, F., Kabasa, J.D., Kwok, O.C., Dubey, J.P., Smith, J.E., 2008. Isolation and genotyping of *Toxoplasma gondii* from Ugandan chickens reveals frequent multiple infections. *Parasitology* 135, 39–45.
- Petersen, E., 2007. Toxoplasmosis. *Semin. Fetal Neonatal Med.* 12, 214–223.
- Ruiz, A., Frenkel, J.K., 1980. Intermediate and transport hosts of *Toxoplasma gondii* in Costa Rica. *Am. J. Trop. Med. Hyg.* 29, 1161–1166.
- Wang, C.R., Qiu, J.H., Gao, J.F., Liu, L.M., Wang, C., Liu, Q., Yan, C., Zhu, X.Q., 2011a. Seroprevalence of *Toxoplasma gondii* infection in sheep and goats in northeastern China. *Small Ruminant Res.* 97, 130–133.
- Wang, Y.H., Li, X.R., Wang, G.X., Yin, H., Cai, X.P., Fu, B.Q., Zhang, D.L., 2011b. Development of an immunochromatographic strip for the rapid detection of *Toxoplasma gondii* circulating antigens. *Parasitol. Int.* 60, 105–107.
- Yan, C., Yue, C.L., Yuan, Z.G., He, Y., Yin, C.C., Lin, R.Q., Dubey, J.P., Zhu, X.Q., 2009. *Toxoplasma gondii* infection in domestic ducks, free-range and caged chickens in southern China. *Vet. Parasitol.* 165, 337–340.
- Zhu, J., Yin, J., Xiao, Y., Jiang, N., Ankariev, J., Lindh, J., Chen, Q., 2008. A seroepidemiological survey of *Toxoplasma gondii* infection in free-range and caged chickens in northeast China. *Vet. Parasitol.* 158, 360–363.

Provided for non-commercial research and education use.
Not for reproduction, distribution or commercial use.



Available online at www.sciencedirect.com

ScienceDirect

www.elsevier.com/locate/jprot

Transcriptional and proteomic analysis reveal recombinant galectins of *Haemonchus contortus* down-regulated functions of goat PBMC and modulation of several signaling cascades *in vitro*



Wang Wang, Cheng Yuan, Shuai Wang, XiaoKai Song, LiXin Xu, RuoFeng Yan, I.A. Hasson, XiangRui Li*

College of Veterinary Medicine, Nanjing Agricultural University, Nanjing 210095, PR China

ARTICLE INFO

Article history:

Received 12 June 2013

Accepted 20 December 2013

Available online 5 January 2014

Keywords:

Galectins

Haemonchus contortus

PBMC

Signal pathway

ABSTRACT

In this study, a combined proteomic and transcriptomic analysis was performed to understand the mechanisms underlying the immunomodulation induced by recombinant galectins of *Haemonchus contortus* (rHco-gal-m/f) on goat peripheral blood mononuclear cells (PBMC). We demonstrated that rHco-gal-m/f could be distinguished by antisera from goats experimentally infected with *H. contortus* and bound to the surface of goat PBMC. Following rHco-gal-m/f exposure, 16 differentially expressed proteins were identified, which function in biological processes such as stimulus response, biological regulation and localization. According to Gene Ontology Annotation, 15 proteins (93.8%) had binding activity and 9 proteins (56.3%) had catalytic activity. A series of transcriptomic analyses were performed subsequently to assess the expression change of certain pathway members. The integrated results of proteomic and transcriptomic analysis suggested that the activation of VEGF pathway, free radical producing pathway, NF- κ B pathway and ubiquitin–proteasome pathway was inhibited following exposure to rHco-gal-m/f, while the TLR pathway and CASPASE pathway were activated. Cytokine production and T cell differentiation were also influenced. Cell migration assays and ELISA were performed and the results were in accordance with the change of the proteins and genes. The protein and gene profiles determined here identified several mechanisms underlying the rHco-gal-m/f-induced immunomodulation of goat PBMC.

Biological significance

This research provided insight into the interactive relationship between parasitic nematode galectins and host PBMC. It also shed new lights on the understanding of molecular mechanisms of helminthic immune evasion.

© 2014 Elsevier B.V. All rights reserved.

1. Introduction

Galectins are a family of S-type lectins, found in vertebrates and invertebrates, that are characterized by two features: a

specific affinity for β -galactoside and a conserved specific sequence motif called the carbohydrate recognition domain (CRD) [1]. Although galectins lack a typical secretion signal peptide and have features of cytosolic and nuclear proteins,

* Corresponding author at: College of Veterinary Medicine, Nanjing Agricultural University, Nanjing 210095, Jiangsu, PR China. Tel./fax: +86 25 84399000.

E-mail address: lixiangrui@njau.edu.cn (X. Li).

they can be secreted into the extracellular space by non-classical (non-Endoplasmic Reticulum-Golgi body) pathways [2]. To date, 15 mammalian galectins (galectin-1 to 15) have been cloned and functionally characterized, revealing various roles in apoptosis, chemoattraction, cell adhesion, cell proliferation, cytokine secretion and immune responses [3]. Growing evidence from recent studies indicates that host galectins can function as pattern recognition receptors (PRRs) that crosslink glycans on the surfaces of viruses [4], bacteria [5] and helminths [6], which, like many other receptor-ligand systems, can trigger a cascade of transmembrane signaling events in different biological processes such as cell-cell interaction, cell-pathogen interaction as well as activation and homeostasis of immune cells [3].

Parasitic nematodes infections induce serious diseases in humans and animals [7]. Galectin-like proteins have also been identified in parasitic nematodes, cestodes and protozoa, such as *Onchocerca volvulus*, *Teladorsagia circumcincta*, *Caenorhabditis elegans*, *Haemonchus contortus*, *Trichostrongylus colubriformis*, *Taenia serialis* and *Fasciola hepatica* [3]. It was reported that galectins of *T. colubriformis* could be recognized by sera from sheep artificially infected with the nematode [8]. Turner et al. [9,10] reported that galectins extracted from infective larvae (L3 stage) of *H. contortus* exhibited a specific chemokinetic activity to attract eosinophils. Recently, it was demonstrated that a recombinant galectin of *Toxascaris leonina* could enhance the production of TGF- β and IL-10 in mice spleen lymphocytes and suppress intestinal inflammation [11]. Proteomic analysis of excretory/secretory (ES) proteins indicated galectins were expressed numerously in *H. contortus*, *Ostertagia ostertagi* and *T. circumcincta* [12]. ES proteins, produced during the invasion and development of parasites, could help them to penetrate the defensive barriers and avoid the immune attack of the host [12], so the parasitic galectins might play an important role in the parasite survival and immune evasion.

In our previous research, we reported that two isoforms of galectins, Hco-gal-m (Acc. No. AY253330) and Hco-gal-f (Acc. No. AY253331), derived, respectively, from male (m) and female (f) *H. contortus*, varied by one amino acid in the C-terminal CRD [13]. Both galectins could hemagglutinate human, dog, rabbit, chicken and mouse erythrocytes, but not the erythrocytes of goat, one natural host of *H. contortus* [14]. They also had the ability to inhibit the mRNA transcription of goat cytokines [15] and induce apoptosis of goat PBMC in a dose-dependent manner [16]. Vaccination of goats with rHco-gal-m/f significantly reduced the fecal egg output, as well as worm burdens, and increased levels of IgG in the vaccinated groups compared to the negative controls post challenge with *H. contortus* [17].

All these findings suggested that galectins of parasitic origin actively participated in the interactions between mammalian hosts and infective pathogens and might contribute to parasitic invasion or modulation of the host immune response [18]. However, the mechanisms underlying the immune modulation and evasion induced by parasitic galectins remain unclear.

The aim of this research was to study changes in the expression of genes and proteins in host immune cells (goat PBMC) following exposure to parasitic galectins (rHco-gal-m/f). To achieve this, a proteomic study was conducted to identify potential protein regulators that underlie the rHco-gal-m/f induced immunomodulation by comparing the changes in the proteome of goat PBMC. Simultaneously, real-time PCR analysis

was performed to analyze the effects of rHco-gal-m/f on some related signaling cascades. The integrated results are of fundamental importance for further studies of the mechanisms by which parasitic galectins contribute to parasite immune evasion or modulation of the host immune response, and provide a new insight into the pathways involved in host-parasite interactions.

2. Materials and methods

2.1. Ethics statement

The experiment was conducted following the guidelines of the Animal Ethics Committee, Nanjing Agricultural University, China. All experimental protocols were approved by the Science and Technology Agency of Jiangsu Province. The approval ID is SYXK (SU) 2010-0005.

2.2. Parasites and animals

H. contortus strain (designated Nanjing 2005) was originally obtained from Nanjing (Jiangsu Province, China) and maintained by serial passage in 3–6-month-old, helminth-free goats [19]. Third stage larvae (L3) used for challenge were cultured from the feces of the monospecifically infected goats at 26 °C and stored in water at a concentration of 2500 larvae/ml at 4 °C.

Local crossbred male goats (3–6-month-old) from the teaching and research flock at Nanjing Agricultural University were housed indoors in pens containing six goats per pen. The male goats were fed hay and whole shelled corn and provided with water *ad libitum*. All goats were dewormed twice at 2 week intervals with levamisole (8 mg/kg bodyweight) orally at the time of housing to remove naturally acquired strongylid infection. After 2 weeks, a fecal sample from each goat was examined by microscope for helminth eggs, according to standard parasitological techniques. Goats exhibiting no eggs were used in the subsequent study and daily health observations were performed throughout the experiment.

SD rats (body weight ~150 g) were purchased from Experimental Animal Center of Jiangsu, PR China (Qualified Certificate: SCXK 2008-0004) and were raised in a sterilized room and fed sterilized food and water.

2.3. Preparation of rHco-gal-m/f

The rHco-gal-m and rHco-gal-f were expressed and purified as previously described [17]. In brief, galectin cDNAs of male (m) and female (f) adult *H. contortus* worms were cloned into the pBV220 prokaryotic expression vector, respectively. *Escherichia coli* DH5 α cells containing Hco-gal-m or Hco-gal-f expression plasmid were cultured in Luria-Bertini medium with ampicillin (100 μ g/ml) and induced at 42 °C to express the recombinant proteins. The purified recombinant proteins were dissolved in PBS (pH 8.0) containing 0.1 mM DTT (PBS/DTT). The purity of the protein preparation was determined by SDS-PAGE. Protein concentrations were determined by Bradford method. LPS was depleted from the recombinant galectins using Detoxi-Gel Affinity Pak prepacked columns (Pierce, USA). Endotoxin levels of the purified samples (<50 ng per 1 mg of the recombinant proteins) were measured using a LAL gel clot assay (Cape Cod,

USA). Then, equal amounts of rHco-gal-m and rHco-gal-f were mixed and named as rHco-gal-m/f for further application.

2.4. Generation of polyclonal antibodies

The goat antisera used in western blot analyses were collected from five goats experimentally infected with *H. contortus*. The goats were raised in helminth-free conditions and then orally challenged with 5000 infective L3. One month later, the goat antisera were collected and stored at -70°C until use.

To generate polyclonal antibodies against rHco-gal-m/f, 0.3 mg of purified rHco-gal-m/f was mixed with Freund's complete adjuvant (1:1) and injected into SD rats subcutaneously in multiple places, following the method described by Han et al. [20]. After the first injection, rats were then boosted four times at 2-week intervals with the same dose. The sera containing specific anti-rHco-gal-m/f antibodies were harvested 10 days following the last injection and the specific reactivity with rHco-gal-m/f was checked by western blot (Supplementary data, Fig. S1).

2.5. Western blot analysis

Purified rHco-gal-m and rHco-gal-f (20 μg) were resolved on 10% SDS-PAGE and transferred to Hybond-C extra nitrocellulose membranes (Amersham Biosciences, UK). Non-specific binding sites were blocked by immersing the membranes in 5% skim milk in Tris-buffered saline (TBS) for 1 h at room temperature. The membranes were then washed 5 times (5 min each) in TBS containing 0.1% Tween-20 (TBST). Subsequently, the membranes were incubated with the primary antibodies (antiserum from goats experimentally infected with *H. contortus*) for 1 h at 37°C (dilutions 1:100 in TBST). After being washed 5 times in TBST, the membranes were then incubated with HRP-conjugated rabbit anti-goat IgG (Sigma, USA) for 1 h at 37°C (diluted 1:2000 in TBST). Finally, the immunoreaction was visualized using freshly prepared diaminobenzidine (DAB, Sigma) as a chromogenic substrate after 5 min.

2.6. Isolation and treatments of PBMC

Heparinised blood was collected by venipuncture from six dewormed healthy goats. PBMC were separated with the standard Ficoll-Hypaque (GE Healthcare, USA) gradient centrifugation method [21] and washed twice in $\text{Ca}^{2+}/\text{Mg}^{2+}$ -free PBS pH 7.4. Cell viability assessed by means of the trypan blue exclusion test was consistently $>95\%$. The PBMC were resuspended to a final density of 1×10^6 cells/ml in DMEM (GIBCO, USA) containing 10% heat inactivated fetal calf serum (FCS), 100 U/ml penicillin and 100 mg/ml streptomycin (Invitrogen, USA). PBMC were treated with rHco-gal-m/f (20 $\mu\text{g}/\text{ml}$) or equal volume of vehicle control buffer (PBS/DTT) for 24 h at 37°C in a humidified environment containing 5% CO_2 . After different treatments, the PBMC were harvested for proteomic study and real-time PCR analysis.

2.7. Binding of rHco-gal-m/f to PBMC

Freshly isolated PBMC as described above (Section 2.6.) were seeded into 24-well plates and cultured on glass coverslips

with rHco-gal-m/f (5 $\mu\text{g}/\text{ml}$). The non-treated cells were set as control. After incubation at 37°C for 1 h, the coverslips were washed with 0.1 M PBS and fixed in 4% paraformaldehyde for 30 min at room temperature. The cells were then incubated with PBS containing 5% normal goat serum for 30 min at room temperature to block non-specific binding before the addition of rat anti-rHco-gal-m/f polyclonal antibodies (diluted 1:100 in PBS containing 5% normal goat serum), which was incubated overnight at 4°C . Primary antibodies were detected by Cy3 goat anti-rat IgG (ab6953, Abcam) diluted 1:400 with the same blocking solution and incubated at 37°C for 1 h. Cells were counterstained with DAPI and DiO (Beyotime Institute of Biotechnology, China). Thus, rHco-gal-m/f, nucleus and cell membrane appeared to be red, blue and green, respectively. The cells were visualized with a confocal laser scanning microscopy (LSM 710; Carl Zeiss, Germany) with a 100 \times oil immersion objective. Red, green and blue color channels, corresponding to Cy3, DiO and DAPI, respectively, were selected to acquire image. The fluorescence settings used for rHco-gal-m/f-treated cells were the same to that used for control cells. An unstained control was conducted to detect auto-fluorescence or background staining of the cells and the protein. Image acquisition and synergistic combination were performed automatically using ZEN software (Carl Zeiss, Germany). Three independent samples were investigated.

2.8. 2-DE

Control and treated PBMC were resuspended by pipetting repeatedly and collected by centrifuge at 400 $\times g$ for 10 min. Subsequently the cells were washed 3 times with ice-cold PBS. After centrifugation for 10 min at 2500 $\times g$, the supernatants were discarded, and cell pellets were dissolved in lysis buffer (7 M urea, 2 M thiourea, 4% CHAPS, 40 mM DTT, 0.2% Bio-Lyte 3–10 ampholytes) containing protease inhibitor (Sigma-Aldrich). The cells were homogenized by ultrasonication (10 strokes, low amplitude) on ice. The lysed cells were centrifuged at 15,000 $\times g$ for 30 min at 4°C , and the supernatants containing the solubilized proteins were used directly or stored at -80°C .

A 100 μg protein sample was applied for isoelectric focusing (IEF) using the Immobiline DryStrip (18 cm, pH 3–10, GE healthcare). The strips were placed into the Ettan IPGphor Isoelectric Focusing System (GE Amersham) and were rehydrated at 30 V for 12 h. The proteins were separated based on their pI according to the following protocol: 500 V for 1 h, 1000 V for 1 h, 8000 V for 8 h and 500 V for 4 h. After IEF, the IPG strips were equilibrated in equilibration buffer I (6 M urea, 2% W/V SDS, 375 mM Tris-HCl pH 8.8, 20% V/V glycerol, 2% W/V DTT) for 15 min, followed by further treatment in equilibration buffer II (6 M urea, 2% W/V SDS, 375 mM Tris-HCl pH 8.8, 20% V/V glycerol, 2.5% W/V iodoacetamide) for another 15 min. The IPG strips were then directly applied onto 12.5% SDS-PAGE gels for electrophoresis using a Hoefer SE 600 Series Vertical Electrophoresis Systems (GE Amersham) with an initial constant current of 15 mA/gel for 30 min, followed by 30 mA/gel until the tracking dye reached the bottoms of the gels. For the paired (control and rHco-gal-m/f-treated) protein samples, triplicate electrophoreses were performed to ensure reproducibility. The gels were then stained using Silver Stain Plus Kit (Bio-Rad, USA) according to the manufacturer's instructions.

2.9. Image analysis

The stained 2-DE gels were visualized at 150 dots/in (dpi) using Typhoon 9200 laser scanner (GE Healthcare, USA) and analyzed using ImageMaster™ 2D Platinum 5.0 software (GE Healthcare, USA). Comparisons were made between gel images of protein profiles obtained from the rHco-gal-m/f-treated group and control group. The individual protein spot value was normalized as follows: the volume of each spot in a member gel was divided by the total volume of the valid spots in the gel, and normalized spot volumes were expressed in volume percentage (vol.%). The overlapping measures ratio was chosen to find protein expression changes according to the manual of Image Master 2D Platinum software (version 5.0). Spots with volume alteration greater than 50% (fold change ≥ 1.5) at 95% confidence interval (Student's *t* test; $p < 0.05$) were considered to be statistically significant.

2.10. Gel excision, tryptic digestion, and desalting

The differentially expressed protein spots were excised manually from the gels and placed into a 96-well microtiter plate. Briefly, gel pieces were destained with a solution of 30 mM potassium ferricyanide and 100 mM sodium thiosulfate (1:1 v/v) for 20 min at room temperature. Then the gel pieces were washed with Milli-Q water until the gels were destained. The spots were incubated in 0.2 M NH_4HCO_3 for 20 min and then lyophilized. Each spot was digested overnight in 12.5 ng/ μl trypsin in 25 mM NH_4HCO_3 . The peptides were extracted three times with 60% acetonitrile (ACN)/0.1% trifluoroacetic acid (TFA). The extracts were pooled and dried completely by a vacuum centrifuge.

2.11. MALDI-TOF MS/MS, database search and bioinformatic analysis

MS and MS/MS analyses were performed at Shanghai Applied Protein Technology Co. Ltd. MS and MS/MS data for protein identification were obtained by using a MALDI-TOF-TOF instrument (4800 proteomics analyzer; Applied Biosystems). Instrument parameters were set using the 4000 Series Explorer software (Applied Biosystems). The MS spectra were recorded in reflector mode in a mass range from 800 to 4000 with a focus mass of 2000. MS was used a CalMix5 standard to calibrate the instrument (ABI 4700 Calibration Mixture). For one main MS spectrum 25 subspectra with 125 shots per subspectrum were accumulated using a random search pattern. For MS calibration, autolysis peaks of trypsin ($[\text{M} + \text{H}]^+ 842.5100$ and 2211.1046) were used as internal calibrates, and up to 10 of the most intense ion signals were selected as precursors for MS/MS acquisition, excluding the trypsin autolysis peaks and the matrix ion signals. In MS/MS positive ion mode, one main MS spectrum 50 subspectra with 50 shots per subspectrum were accumulated using a random search pattern. Collision energy was 2 kV, collision gas was air, and default calibration was set by using the Glu1-Fibrino-peptide B ($[\text{M} + \text{H}]^+ 1,570.6696$) spotted onto Cal 7 positions of the MALDI target.

Combined peptide mass fingerprinting (PMF) and MS/MS queries were performed by using the MASCOT search engine 2.2 (Matrix Science, Ltd.) embedded into GPS-Explorer Software 3.6 (Applied Biosystems) on the Mammalia (1042,413

sequences) subset of the sequences in the National Center for Biotechnology non-redundant (NCBI nr) database (updated on Feb. 10, 2012) with the following parameter settings: 100 ppm mass accuracy, trypsin cleavage one missed cleavage allowed, carbamidomethylation set as fixed modification, oxidation of methionine was allowed as variable modification, MS/MS fragment tolerance was set to 0.4 Da. A MASCOT confidence interval of 95% was used for further manual validation.

Gene ontology (GO) annotations for identified proteins based on BLAST results were performed using Blast2GO (www.blast2go.de) [22]. The identified protein sequences were searched against UniProtKB databases to find homologue sequences, from which the functional annotation can be transferred to the studied sequences. In this work, the top blast hits with similarity over 30% and E-value less than $1e^{-10}$ for each query sequence were retained, following which the GO terms associated to the blast hits were retrieved and annotated. The Blast2GO software was used to complement multiple identified proteins within the Kyoto Encyclopedia of Genes and Genomes (KEGG) metabolic pathway database (<http://www.genome.ad.jp/kegg/pathway.html>).

2.12. RNA extraction and preparation of cDNA

Total RNA was isolated from rHco-gal-m/f-treated and control PBMC, which were isolated at the same time and from the same animals used in the proteomic analysis. For each RNA preparation, 5×10^6 cells were collected, then added into the buffer RLT (QIAGEN, Germany) and immediately homogenized by vortex. Total RNA was extracted using RNeasy Mini Kit (QIAGEN, Germany) according to the manufacturer's instructions. To determine quantity and ensure integrity of extracted RNA, spectrophotometry was performed, using Biophotometer (Eppendorf, Germany). The $\text{OD}_{260}/\text{OD}_{280}$ absorption ratio of all samples was between 1.8 and 2.0.

Residual genomic DNA was removed by treatment with RNase-free DNase I (TaKaRa, Japan) according to the manufacturer's instructions. For each reaction, 10 μg RNA was treated with 10 U DNase I at 37 °C for 40 min followed by inactivation of the enzyme with 2.5 μl of 0.5 M EDTA at 80 °C for 3 min. Following digestion, RNA was precipitated by the addition of 10 μl of 3 M sodium acetate and 250 μl of cold ethanol, and incubation on ice for 10 min. RNA precipitate was harvested by centrifugation (12,000 $\times g$, 15 min, 4 °C), washed with 70% ethanol and re-suspended in 20 μl of RNase free water (TaKaRa, Japan). RNA quality was checked by agarose gel electrophoresis.

cDNA was prepared in a 20 μl reaction volume using 2 μg of DNA-free total RNA per reaction. ThermoScript RT and Oligo(dT)20 primers (Invitrogen, USA) were used to synthesize cDNA, according to the manufacturer's specifications. At the completion of the reaction, cDNA was diluted 1/5 in water and stored at -80 °C until use.

2.13. Real-time PCR analysis of differentially expressed proteins

Real-time PCR was conducted on the ABI 7500 Real-Time PCR System (Applied Biosystems, USA), using standard procedure (Stage 1: Initial denaturation, 95 °C for 30 s, 1 cycle; Stage 2: Amplification, 95 °C for 5 s, 60 °C for 60 s, 40 cycles; Melt Curve Stage: 60 °C–95 °C, ramp rate 1%). Each reaction was

performed in a total volume of 20 μ l containing 1 \times SYBR[®] Premix Ex Taq (TaKaRa, Japan), 500 nM of each primer and a constant amount of cDNA (corresponding to 20 ng of reverse transcribed RNA for each sample). To ensure cDNA samples were not contaminated with genomic DNA, reactions were set up using 20 ng of non-reverse transcribed RNA in place of cDNA. Failure to generate a detectable signal signified the sample as DNA free. Negative (no template) controls were included in each PCR run. Melt curves were generated to ensure a single amplicon had been produced. Primers specific for target goat genes were designed with Beacon Designer 7.0 software (Premier Biosoft International, USA) according to manufacturer's guidelines and the efficiency of each primer set was verified by running standard curves in triplicates using serial dilutions of the cDNA (Supplementary data, Table S1).

The data processing was performed by the method of Kubista et al. [23]. Target gene expression was normalized to GAPDH, using the 7500 software version 2.0.6 (Applied Biosystems, USA). The stability of GAPDH was analyzed as previously described [24], using the cDNA samples derived from control and rHco-gal-m/f-treated PBMC (Supplementary data, Table S2). The PBS/DTT treated PBMC were selected as the reference sample and the relative mRNA expression levels of target genes in rHco-gal-m/f treated PBMC were calculated using the $2^{-\Delta\Delta Ct}$ method [25]. Each experiment was tested in triplicate.

2.14. Transcriptional analysis of key genes related to signal pathways

To detect gene expression changes of candidate signaling pathways, RNA isolation and real-time PCR were performed as described above (Section 2.12.). The expression profile of the fifty-three selected genes associated with the vascular endothelial growth factor (VEGF) pathway, free radical producing pathway, toll-like receptor (TLR) pathway, T cell development pathway, apoptosis pathway, as well as cytokine-cytokine receptor signal pathway were determined in response to rHco-gal-m/f stimulus. Each experiment was tested in triplicate. The primers for PCR are listed in Supplementary data, Table S3.

2.15. Detection of the cytokine levels by ELISA

The freshly isolated PBMC were resuspended to a final density of 5×10^6 in complete medium (RPMI 1640 supplemented with 100 U/ml penicillin, 100 μ g/ml streptomycin, 2 mM L-glutamine, 10% FCS). In the test groups, cells were treated with ConA (10 μ g/ml) or rHco-gal-m/f (20 μ g/ml) or both. The controls received equal volume of vehicle buffer (PBS/DTT) alone. Then, the cells were seeded into 24-well plates (1 ml/well) and cultured for 24 h in 5% CO₂ atmosphere at 37 °C. Next, the plates were then centrifuged at 200 \times g for 15 min and the supernatants were collected. The levels of IL1 β , IL4, IL6 and IFN γ in supernatants were determined using commercially available bovine ELISA kits (Thermo Scientific, USA), which were reported to be able to cross-reactive with goat cytokines [26]. The cell viability was assessed by means of the trypan blue exclusion test before and after 24 h incubation of activated PBMC with rHco-gal-m/f. Three individual experiments were performed.

2.16. Cell migration assay

The cell migration assay was performed using a Transwell system (Corning, USA), which allows cells to migrate throughout an 8 μ m pore size polycarbonate membrane [27]. The protocol for each group were as follows: the first group PBMC were incubated with rHco-gal-m/f (20 μ g/ml) at 37 °C for 15 min, the second group were incubated with lactose (30 mM) at 37 °C for 15 min, the third group were preincubated with lactose for 15 min followed by the treatment of rHco-gal-m/f for another 15 min, and the control group was treated with an equal volume of PBS/DTT. After different treatments, 1×10^5 cells of each group were seeded in the upper chamber and cultured in 5% CO₂ atmosphere at 37 °C, respectively. After 2 h of incubation the filters were removed and the cells that migrated through the membrane into the lower chamber were counted with a Neubauer counting chamber in five high-power unrelated fields under a light microscope (magnification 100 \times). The results were presented as percentages of the seeded PBMC. Each experiment was performed in triplicate.

2.17. Statistical analysis

All data are analyzed by SPSS for Windows version 15.0 (SPSS Inc., Chicago, IL, USA). Student's *t* test was used for statistical analysis. Results are expressed as the mean \pm SD and *p* < 0.05 was considered statistically significant.

3. Results

3.1. Purification of rHco-gal-m/f and western blot

After purification, recombinant galectins rHco-gal-m and rHco-gal-f were viewed as single bands with the molecular mass around 32.5 kDa on the SDS-PAGE (Fig. 1A). Western blot analysis indicated that both rHco-gal-m and rHco-gal-f could be identified by the antiserum from goats experimentally infected with *H. contortus* (Fig. 1B).

3.2. Binding of rHco-gal-m/f to PBMC

Goat PBMC were incubated with rHco-gal-m/f and the binding was investigated by an immunofluorescence approach. As depicted in Fig. 2, the emission from the Cy3-labeled rHco-gal-m/f was red, the DAPI-labeled nuclei were blue and DiO-labeled cell membrane was green. No fluorescence was observed under any color channel in the unstained background control (not shown). In the control group, no red fluorescence was observed (Fig. 2 lower panel). Intense red fluorescence was observed when the cells were incubated with rHco-gal-m/f (Fig. 2 upper panel). The red color circled around the green one and partially overlapped with it. It indicated that rHco-gal-m/f could bind to the surfaces of PBMC.

3.3. Differentially expressed proteins in goat PBMC

Representative 2-DE gel images of control and rHco-gal-m/f-treated PBMC are shown in Fig. 3A. After rHco-gal-m/f treatment, significantly differentially expressed protein spots (*p* < 0.05) with

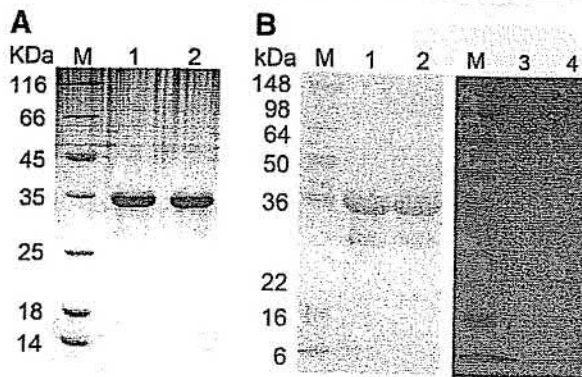


Fig. 1 – Purification of rHco-gal-m/f and western blot. (A) Purified rHco-gal-m/f were resolved by SDS-PAGE on 10% of polyacrylamide gel and stained with Coomassie brilliant blue R250. M: standard protein molecular marker; lane 1: rHco-gal-m; lane 2: rHco-gal-f. (B) Western blot analysis of purified rHco-gal-m (lanes 1 and 3) and rHco-gal-f (lanes 2 and 4). Proteins are recognized by sera from goats as primary antibody. M: standard protein molecular marker; lanes 1 and 2: sera from goats experimentally infected with *H. contortus*; lanes 3 and 4: sera from normal goats. Data are representative of 4 independent experiments.

at least 1.5-fold change in volume as observed in all replicate gels were scored.

Comparing standardized protein abundance data generated from the reference image, 19 protein spots were differentially expressed as indicated by the spots marked with arrows and ID numbers in Fig. 3A and by the expanded plots in Fig. 3B. The average quantity values (%V) and their standard

deviations of the spots, the statistical assay results, and the fold differences are shown in Table 1.

All of these 19 spots, which represented 16 proteins, were successfully identified by MS + MS/MS and are listed in Table 2. Among these 16 proteins, 11 of them were up-regulated while 5 of them were down-regulated in rHco-gal-m/f-treated PBMC. The result of MALDI-TOF MS/MS analysis of spot 1317 is shown in Supplementary data, Fig. S2 as an example. The comprehensive peptide evidence for identification and quantification of goat proteins is provided as Supplementary data, Table S4.

3.4. Bioinformatic analysis

In an attempt to understand the biological functions of the differentially expressed proteins, each identified known protein was classified into cellular component, molecular function and biological process according to its GO functional annotation and hierarchy using Blast2GO.

The cellular components ontology refers to the place in the cell where a gene product is active [28]. Of the differentially expressed proteins, 13 occur in the organelle (GO:0043226), 10 occur in the cytoplasm (GO:0005623), 4 occur in the plasma membrane (GO:0005886) and 10 occur in the nucleus (GO:0005634) with the remainder occurring in the mitochondrion (GO:0005739) and cytoskeleton (GO:0005856) which emphasizes the change of vitality in the rHco-gal-m/f-treated PBMC.

For the molecular function ontology, activities of binding (GO:0005488, 15 proteins, 93.8% of 16 annotated peptides) and catalytic activity (GO:0003824, 9 proteins, 56.3% of 16 annotated peptides) were the two major molecular function categories (Table 2). Most of the assigned binding activity could be assigned to protein binding (GO:0005515), nucleic acid binding (GO:0003676), nucleotide binding (GO:0000166) and, to a lesser extent, lipid binding (GO:0008289). The proteins in the catalytic

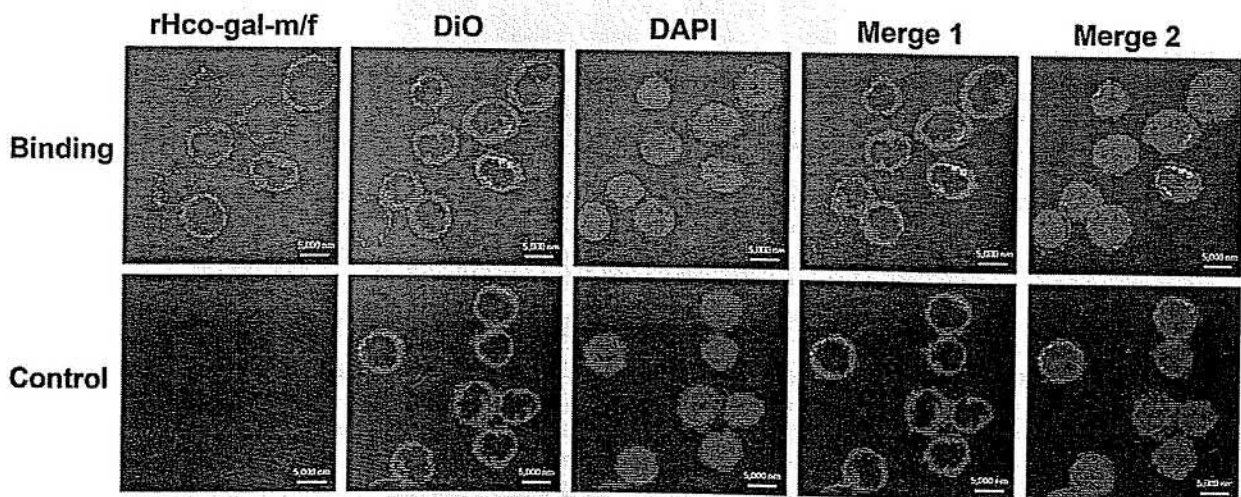


Fig. 2 – Binding of rHco-gal-m/f to PBMC. Goat PBMC were left untreated or incubated with rHco-gal-m/f (5 μ g/ml) for 1 h at 37 $^{\circ}$ C. All cells were fixed and incubated with rat anti-rHco-gal-m/f antibody followed by Cy3 labeled goat anti-rat IgG (red). The nuclei and membranes of the corresponding cells were visualized by DAPI (blue) and DiO (green) staining, respectively. The binding of rHco-gal-m/f to PBMC was visualized with a confocal laser scanning microscopy. Merge 1, overlap of red and green channels; Merge 2, overlap of red, green and blue channels. Bars are 5000 nm. Data are representative of 3 independent experiments.

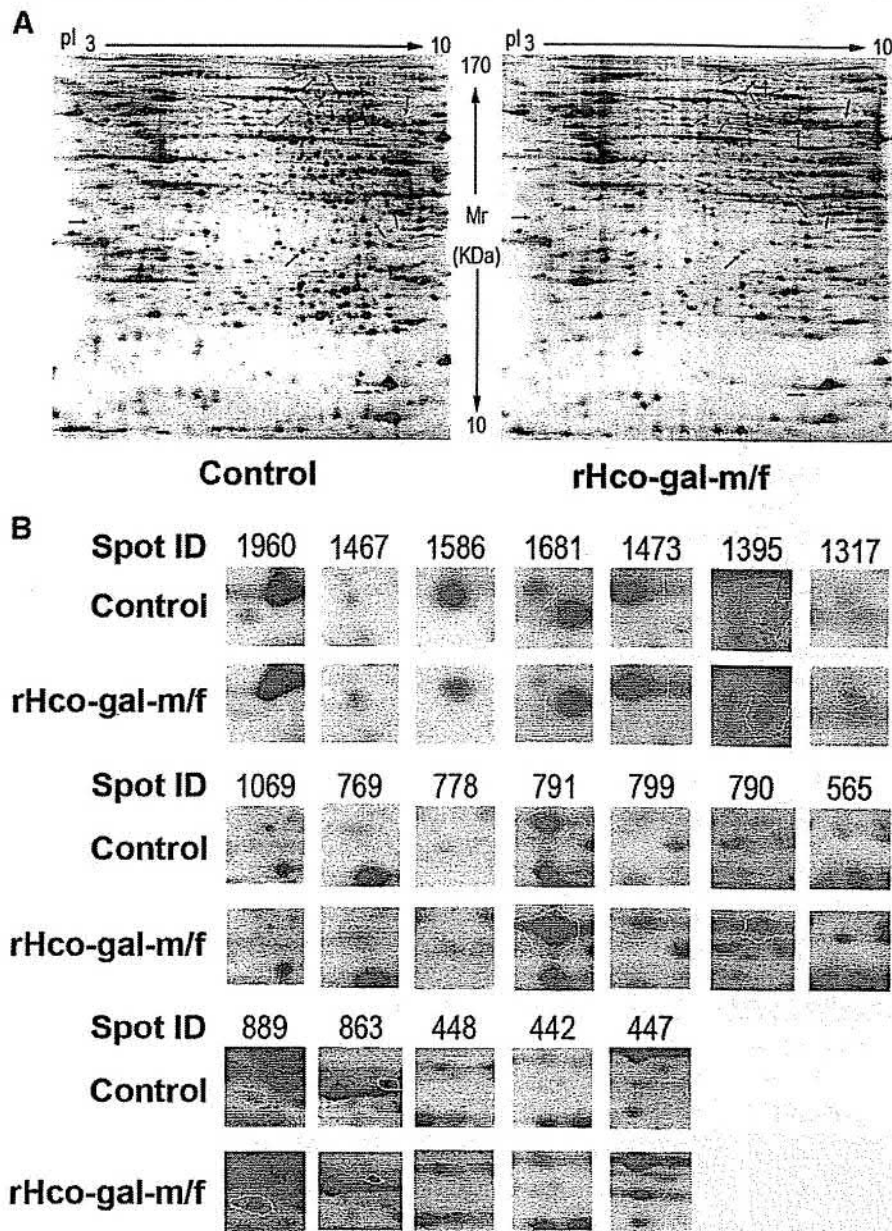


Fig. 3 – The proteome maps (2-DE images) of goat PBMC. **A**, 2-DE images of control (A) and rHco-gal-m/f-treated (B) PBMC. This is a representative of silver stained gel image (n = 3 independent experiments). Differentially expressed spots are shown by the arrows. **B**, the expanded region of differentially expressed protein spots. The proteins within the circles are the differentially expressed proteins.

activity group also can be classified into subgroups based on the specific functions, and hydrolase activity (GO:0016787) is the major subcategory involving 6 proteins (Table 2).

In the biological process category, the proteins were involved in cellular process (GO:0009987), metabolic process (GO:0008152), biological regulation (GO:0065007), response to stimulus (GO:0050896) and localization (GO:0051179) with a small portion related to other terms describing signaling (GO:0023052), death (GO:0016265) and locomotion (GO:0040011).

Simultaneously, the identified proteins were searched against KEGG metabolic pathway database, which contains binary relations that represent molecular interactions and

relations. The identified proteins were mapped into 15 pathways (Supplementary data, Table S5). Based on their close relationship to cell survival and cytokine production, we focused on cell cycle (KEGG Pathway ID: ko04110), calcium signaling pathway (ko04020), nitrogen metabolism (ko00910), phagosome (ko04145) and oxidative phosphorylation (ko00190). The corresponding participators: proliferating cell nuclear antigen (PCNA), vimentin (VIM), voltage-dependent anion-selective channel protein 2 (VDAC2), carbonic anhydrase 2 (CA2), coronin-1A (CORO1A) and NADH dehydrogenase [ubiquinone] 1 beta subcomplex subunit 7 (NDUFB7), were considered as key players in the immunomodulation induced by rHco-gal-m/f (Table 1).

Table 1 – Summary of differentially expressed protein spots in rHco-gal-m/f-treated goat PBMC spot value (%V)

Spot ID ^b	Pairs of gels (n)	Control (mean ± S.D.)	rHco-gal-m/f-treated (mean ± S.D.)	Fold change ^c	p value
1960	3	0.056 ± 0.002	0.031 ± 0.004	-1.58	0.004
1467	3	0.023 ± 0.004	0.065 ± 0.017	1.65	0.004
1586	3	0.087 ± 0.004	0.053 ± 0.001	-1.55	0.000
1681	3	0.064 ± 0.008	0.027 ± 0.012	-1.54	0.012
1473	3	0.016 ± 0.005	0.036 ± 0.007	1.53	0.015
1395	3	0.015 ± 0.004	0.039 ± 0.013	1.55	0.037
1317	3	0.013 ± 0.002	0.027 ± 0.005	1.56	0.009
1069	3	0.041 ± 0.009	0.013 ± 0.004	-2.08	0.007
769	3	0.023 ± 0.004	0.051 ± 0.012	1.56	0.019
778	3	0.009 ± 0.001	0.020 ± 0.002	1.85	0.001
791	3	0.105 ± 0.013	0.189 ± 0.019	1.99	0.003
799	3	0.025 ± 0.003	0.070 ± 0.019	1.77	0.016
790	3	0.019 ± 0.003	0.053 ± 0.017	1.50	0.027
565	3	0.010 ± 0.002	0.025 ± 0.007	1.73	0.018
889	3	0.010 ± 0.003	0.021 ± 0.001	1.60	0.005
863	3	0.066 ± 0.024	0.018 ± 0.002	-2.33	0.028
448	3	0.012 ± 0.001	0.026 ± 0.008	1.6	0.037
442	3	0.013 ± 0.002	0.028 ± 0.005	1.59	0.032
447	3	0.009 ± 0.002	0.026 ± 0.007	1.67	0.014

^a %V: volume percentage.

^b Spot ID was defined at the beginning of images analysis by Image Master 2D Platinum software.

^c The fold change was determined by overlapping measures ratio according to the manual of Image Master 2D Platinum software.

3.5. Real-time PCR analysis of differentially expressed proteins

Six genes corresponding to the protein spots designated 1467, 1317, 1473, 791 (799/790), 1681, 1778, and 1069 were chosen for quantitative real-time PCR analysis to quantify their transcript levels (Fig. 4). Four of them were expressed, at increased levels, namely 1467, 1317, 1473 and 791 (799/790), which had been identified as PCNA, NPM1, VDAC2 and CORO1A. In contrast, the two spots, 1681 (CA2) and 1069 (VIM), were down-regulated. The PCR results were consistent with those of the 2-DE proteomic studies, and suggested that these proteins identified as differentially expressed were regulated at a transcriptional level.

3.6. Changes of key genes related to signal pathways

Although the differentially expressed proteins identified in this study would provide an insight into rHco-gal-m/f regulation of specific cellular processes, only a few proteins relating to signal transduction were detected in the proteomic analysis. This may be explained by the 2-DE bias toward abundant proteins. Signaling proteins of low abundance, such as kinases and transcription factors, often cannot be detected by 2-DE [29,30]. So, gene members of candidate pathways were selected on the basis of relevance to immunomodulation and further analyzed by real-time PCR.

Following treatment of PBMC with rHco-gal-m/f, the transcription of all tested gene members of the VEGF pathway was inhibited, except MMP8 (Fig. 5A). Meanwhile, a decrease of free radical producing genes (CYBA, CYBB, DUOX1, DUOX2, NCF1 and NOS2A) at the transcriptional level was observed with an increase of ARG1 (Fig. 5B). In the TLR signaling pathway, the transcripts of TLR1, 3, 4 and downstream members MYD88 and FADD were up-regulated (Fig. 5C). The expression of DLL4, JAG1 and TBX21, which participate in T cell development pathway, were all decreased (Fig. 5D). Conversely, apoptosis signals (FAS,

CASPASE 3, 7 and 8) (Fig. 5E), anti-inflammatory cytokines (IL10 and TGFβ1) (Fig. 5F), as well as the inhibitor of NF-κB (NFKBIA) (Fig. 5G) were found to be more abundantly expressed in rHco-gal-m/f-treated PBMC. Cytokines, including IFN-γ, IL2, IL6, IL8, and TNFα were all down-regulated in mRNA levels (Fig. 5F). (See the full names of the genes in Supplementary data, Table S6.)

3.7. The alteration of secreted cytokine levels

In the real-time PCR analysis, many cytokine genes were down-regulated. To confirm the expression changes of these genes, the protein level of IL1β, IL4, IL6, and IFN-γ in the culture supernatants were detected by ELISA (Fig. 6). Since the levels of these cytokines in the control and rHco-gal-m/f-treated cultures were below the detection limit of the ELISA kits, the difference between these two groups could not be judged.

This result is reasonable because in the absence of mitogen stimulation, low levels of cytokines would be secreted by the resting PBMC [31], not to mention the result of the real-time PCR that rHco-gal-m/f inhibited the transcription of these cytokines. However, when ConA was employed in the cell culture to activate the PBMC, these cells synthesized detectable levels of IL1β, IL4, IL6 and IFN-γ (Fig. 6) as previously reported [32,33]. rHco-gal-m/f reduced the secretion of IL-1β by 69.80 ± 9.37%, IL-4 by 51.86 ± 6.91%, IL-6 by 42.26 ± 9.22%, IFN-γ by 20.61 ± 6.70% and TNF-α by 23.93 ± 0.59%, respectively (Fig. 6). Meanwhile, the number of living cell ascertained by trypan blue staining was decreased by 4.67 ± 1.65% after 24 h incubation of PBMC with rHco-gal-m/f (not shown).

3.8. Effects on the cell migration

VIM and CORO1A play a critical role in the attachment and migration of lymphocytes [34–36]. In the proteomic study,

Table 2 Identification of total soluble proteins that differentially expressed between untreated and rHco-gal-m/f treated PBMC.

Spot ID ^a	Database ID no.	Identified protein name	Theoretical MW/pi ^b	Protein score	Peptide scout ^c	Sequence coverage (%)	Biological process ^d	Molecular function ^d	Pathway ^e
1960	gi 28603790	NADH dehydrogenase [ubiquinone] 1 betasubcomplex subunit 7	16.6/8.35	100	6	47	Generation of precursor metabolites and energy	Oxidoreductase activity	Oxidative phosphorylation
1467	gi 4505641	Proliferating cell nuclear antigen	29.1/4.57	116	4	12	Cell proliferation	Receptor binding hydrolase activity	Cell cycle
1586	gi 78369458	Proteasome subunit alpha type-1	29.9/6.15	547	17	63	Response stimulus	Protein binding hydrolase activity	Proteasome
1681	gi 118582300	Carbonic anhydrase 2	29.2/6.41	101	5	31	Response stimulus	Protein binding lyase activity	Nitrogen metabolism
1473	gi 47523794	Voltage-dependent anion-selective channel protein 2	32.1/7.49	160	9	36	Apoptosis	Protein binding	Calcium signaling pathway
1395	gi 119614240	Heterogeneous nuclear ribonucleoprotein A2/B1 isoform CRA_a	32.5/8.74	585	15	59	Transport	Nucleic acid binding	
1317	gi 267922645	Nucleophosmin	32.8/4.61	333	8	29	Signal transduction	Nucleic acid binding	
1069	gi 145226795	Vimentin	53.7/5.02	475	24	47	Cell differentiation	Protein binding	
769	gi 301764170	Tryptophanyl-tRNA synthetase cytoplasmic-like Chain B, refined 1.8 Å resolution crystal structure of porcine epsilon-tryptophan	53.5/5.61	131	6	19	Translation	Protein binding ligase activity	
778	gi 999627	Chain B, refined 1.8 Å resolution crystal structure of porcine epsilon-tryptophan	8.9/6.67	117	2	34	Translation initiation	Metal ion binding hydrolase activity	
791/799/790	gi 27806251	Coronin-1A	51.6/6.25	883/211/472	23/13/17	46/18/37	Signal transduction	Protein binding	Phagosome
565	gi 33874520	SYNCRIP protein	46.9/5.85	213	10	26	RNA metabolic process	Nucleic acid binding	
889	gi 296472103	Annexin A11	54.2/8.05	337	12	20	Signal transduction	Protein binding	
863	gi 27807237	ATP synthase subunit alpha, mitochondrial precursor	59.8/9.21	523	21	47	Energy metabolic process	Protein binding hydrolase activity	Oxidative phosphorylation
448/442	gi 335309074	SAM domain and HD domain-containing protein 1-like, partial	59.6/7.36	81/87	5/7	10/12	immune response	nucleic acid binding hydrolase activity	
447	gi 296481142	SAM domain and HD domain-containing protein 1	62.7/6.28	263	11	23	Immune response	nucleic acid binding hydrolase activity	

^a The spot ID was defined at the beginning of analysis of gel images by Image Master 2D Platinum software.
^b MW: molecular weight (kDa); pi: isoelectric points.
^c The peptides found in both PMF and MS/MS.
^d The functions are classified by gene ontology (GO) annotations using Blast2GO.
^e The pathways were determined by searching the protein sequences against KEGG metabolic pathway database.

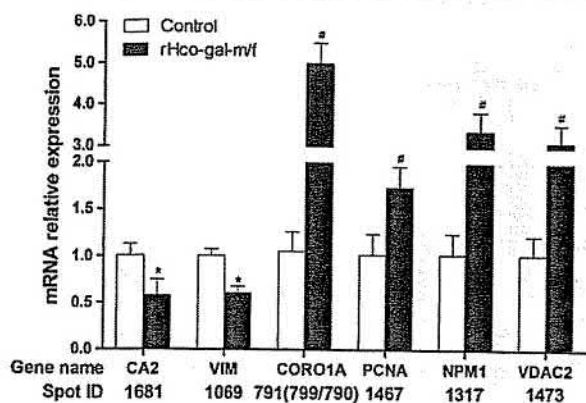


Fig. 4 – Confirmation of transcriptional regulation of differentially expressed proteins by real-time PCR. Transcript levels corresponding to spots (ID: 1681, 1069, 791 (799/790), 1467, 1317 and 1473) out of the 16 differentially expressed proteins were presented relative to those corresponding to GAPDH. Data represent mean \pm SD of three individual experiments; * $p < 0.05$ and # $p < 0.001$ versus the control.

both molecules were detected to be down-regulated (Table 1), suggesting that the rHco-gal-m/f-treated PBMC had a decreased ability to migrate.

To confirm the impact of rHco-gal-m/f-treatment on PBMC migration, a cell migration assay was performed in a Transwell system. In the control group, $28.65 \pm 3.65\%$ PBMC migrated into the lower chambers, the number dramatically decreased to $6.85 \pm 1.44\%$ after the treatment of rHco-gal-m/f (Fig. 7). When PBMC were preincubated with lactose, the inhibitory action of rHco-gal-m/f on cell migration was disrupted, and the percentage of migrated PBMC was up to $27.75 \pm 4.80\%$ in sugar inhibiting group (Fig. 7). No significant difference was observed between control group and lactose-treated group ($31.33 \pm 4.88\%$) or sugar inhibiting group. This result revealed that the rHco-gal-m/f induced suppression of cell migration was in accordance with the down-regulation of VIM and CORO1A.

4. Discussion

The capacity of helminth parasites to modulate the immune system underpins their longevity in the mammalian host [37]. There is consequently an intense interest in understanding the molecular basis of helminth immunomodulation. Galectins have been recognized as significant immune modulators associated with *H. contortus* infection [14–17].

In this research, rHco-gal-m/f could be recognized by the serum of goats experimentally infected with *H. contortus* and were able to bind to the surface of goat PBMC. When combined with previous reports, it suggested that Hco-gal-m/f could enter the host tissues and interact with the host immune system. In the binding assay, however, some cells could not be labeled with Cy3-labeled antibody. The negative binding might be due to the lack of specific receptors on these cells. Which subpopulation of goat PBMC is the primary target of rHco-gal-m/f binding and the identification of cell surface receptors for rHco-gal-m/f still requires further research.

In recent years, the proteomic approach has been successfully applied to the study of host-parasite interactions in mice and sheep [38–41]. Moreover, the combination of proteomic analysis with transcriptomic studies have proved to be a powerful technique for the detection and identification of more novel modulators related to stimulus response [42]. In this study, a proteomic analysis was performed to identify the potential protein regulators that underlie the rHco-gal-m/f-induced immunomodulation and 16 differentially expressed proteins were successfully identified. GO analysis and other bioinformatic techniques were applied to predict their possible functions and plausible pathways. Integrated with a series of transcriptomic studies, the protein and gene profiles revealed that the mechanisms underlying the immunomodulation induced by rHco-gal-m/f might be closely related to pathways as discussed in the succeeding paragraphs.

During the infectious process, a battle for survival takes place between the host and the parasites. A directed migration toward sites of infection is a mandatory process for the efficient involvement of PBMC in the host defense against pathogen stimulus. Vimentin (VIM), an intermediate filament protein, has shown correlation with type I collagens (COL1A1) and other proteins in angiogenesis, attachment and cell migration [34–36]. In the proteomic study, VIM was dramatically down-regulated in rHco-gal-m/f-treated PBMC (Table 1), suggesting that the treated cells appeared to have a decreased ability to migrate. Real-time PCR analysis validated the down-regulation of VIM and COL1A1 (Figs. 4 and 5A) and the Transwell assays additionally proved the decreased mobility of rHco-gal-m/f-treated PBMC (Fig. 7). The decreased capacity of cell migration due to down-regulation of VIM and COL1A1 induced by rHco-gal-m/f suggested a mechanism by which parasitic galectins contribute to the worms evading host immunity.

The VEGF pathway is also known to be associated with angiogenesis, cell migration and cell survival. The key members, VEGFA and MMPs, could work as triggers and promoters of angiogenesis [43], and the activation of HSP27 and CDC42 were essential for cell migration and angiogenesis [44–46]. Therefore, several members of this pathway were selected to be analyzed by real-time PCR. As depicted in Fig. 5A, HSP27, CDC42, VEGFA, MMP2 and MMP9 were down-regulated following rHco-gal-m/f exposure, indicating the disruption of VEGF pathway and potentially contributing to decreased mobility of rHco-gal-m/f-treated PBMC.

Nitric oxide (NO), produced during the metabolism of L-arginine by NO synthases (NOS) and synthesized by many cells involved in the immune response [47], was cytotoxic to a range of parasites, including *H. contortus* [48–51]. In addition to direct toxicity, reactive oxygen species (ROS) or nitrogen intermediates were able to induce pro-inflammatory cytokines, including TNF- α , IL-1, IL-6, and IFN- γ [52]. ROS and nitrogen intermediates can function as second messengers to activate nuclear factor kappa-B (NF- κ B) [53]. On the contrary, carbonic anhydrases (CA) can protect cells from oxidative damage by preventing the apoptosis cascade [54,55]. In the proteomic study, one CA family member, CA2, was down-regulated. This downregulation implies a defective capacity of rHco-gal-m/f-treated PBMC to resist ROS and this dysfunction might be responsible for the apoptosis of goat PBMC induced by rHco-gal-m/f. Real-time PCR analysis was additionally

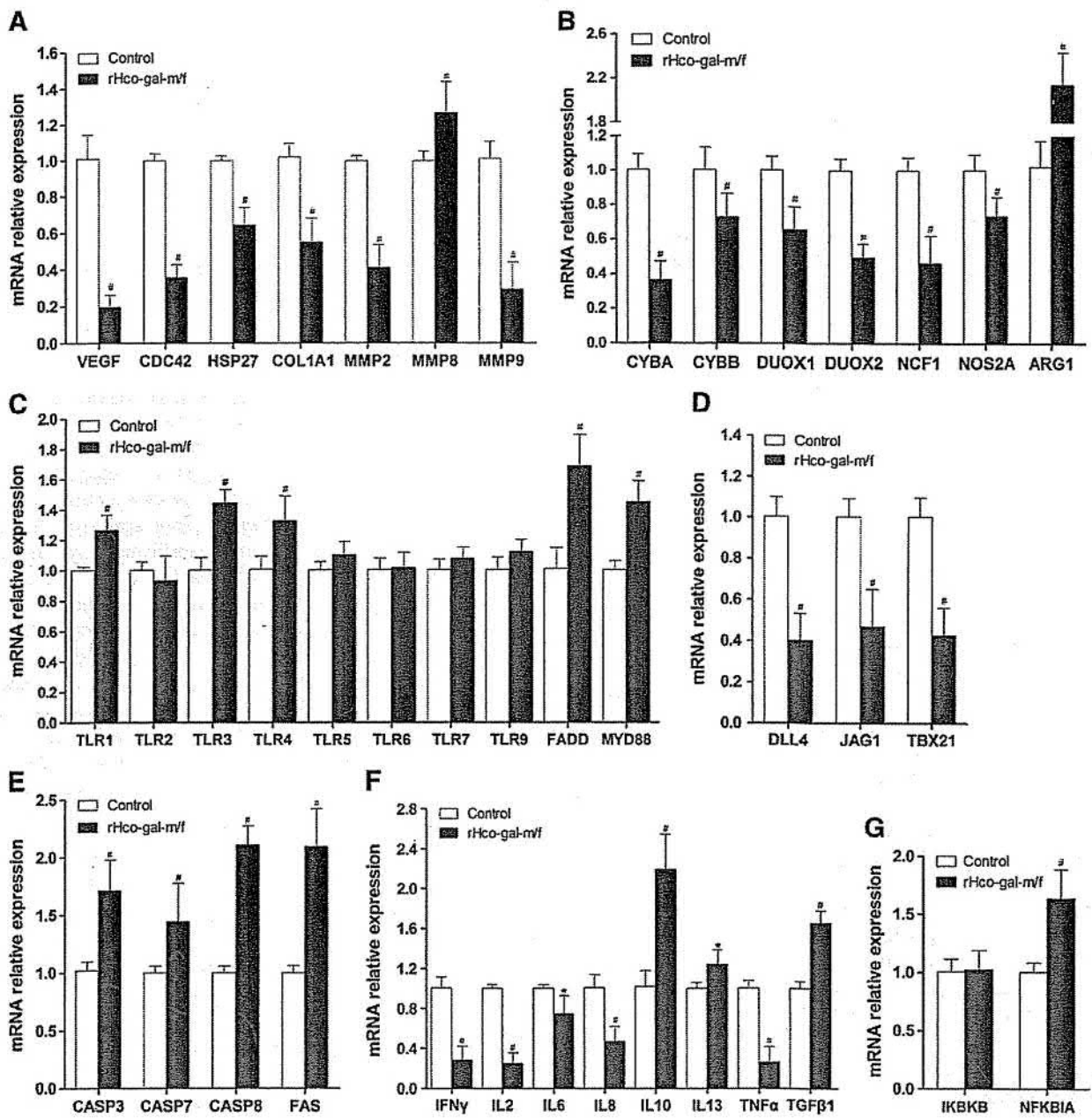


Fig. 5 – Effect of rHco-gal-m/f on the expression profiles of candidate genes belonging to different signal pathways in goat PBMC. Total RNA was purified from PBMC and genes which were grouped with respect to biological function were assayed by real-time PCR. (A) VEGF pathway; (B) free radical producing pathway; (C) TLR pathway; (D) T cell development; (E) apoptosis; (F) cytokines (G) NF- κ B pathway. Data represent mean \pm SD of three individual experiments; * $p < 0.05$ and ** $p < 0.01$ versus the control.

conducted to screen the expression changes of more genes related to free radical production. The results demonstrated that rHco-gal-m/f treatment decreased the transcripts of inducible NOS2A, neutrophil cytosolic factor 1 (NCF1), dual oxidases (DUOX1 and DUOX2) as well as two components of the NADPH oxidase complex (CYBA and CYBB) (Fig. 5B), which functioned in the production of ROS. Recently, a similar result was reported that lec-10, a galectin-encoding gene, showed an ability to reduce oxidative stress in *C. elegans* [56].

The activation of pattern recognition molecules such as TLRs was not only a critical factor in innate immune responses against invading pathogens, but also directed the type and extent of ongoing adaptive immune responses [57]. In turn, helminths have the ability to subvert the TLR signal pathway to facilitate the immune evasion [58]. Meanwhile, mammalian TLRs were implicated in apoptosis [59–62], as well as in the development of immune responses to a number of parasites including trypanosomes [63], malaria [64] and schistosomes

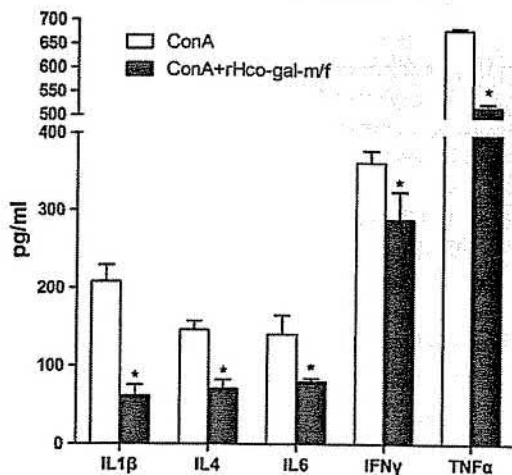


Fig. 6 – rHco-gal-m/f reduced the secretion of pro-inflammatory cytokines. PBMC were stimulated with ConA, or rHco-gal-m/f or both for 24 h to determine the levels of cytokines in culture supernatants. Cells treated with equal volume of PBS/DTT were set as control. Levels of these cytokines in control and rHco-gal-m/f-treated cultures were below the limit of detection of the ELISA kits. Data represent mean \pm SD of three individual experiments; * $p < 0.01$ versus the ConA-treated group.

[65]. Here in this study, the transcripts of TLR1, 3 and 4, as well as the down-stream members, MYD88 and FADD, which were required in TLR-induced apoptosis [66], were up-regulated in

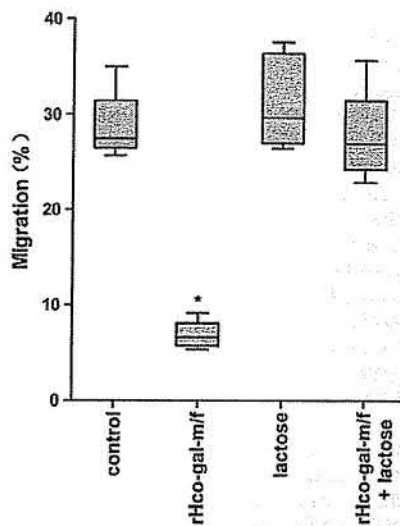


Fig. 7 – Inhibitory activity of rHco-gal-m/f on PBMC migration. PBMC were treated with control buffer, rHco-gal-m/f, lactose, or rHco-gal-m/f + lactose, respectively. Then the random migration was determined. The data are presented as box-and-whiskers blot, with the box containing 50% of the values, and the whiskers showing the highest and the lowest values. The median is indicated by the horizontal bar, the mean value as square. The difference between the mean values was calculated using ANOVA. Data are representative of 4 independent experiments; * $p < 0.01$ versus the control.

rHco-gal-m/f-treated PBMC (Fig. 5C). Coupled with the increased expression of FAS and CASPASE 3, 7 and 8 (Fig. 5E), it seems like TLR expression was not subverted but activated by rHco-gal-m/f. The TLR-CASPASE signaling cascades might participate in the apoptosis induced by rHco-gal-m/f in goat PBMC. In addition, another apoptosis associated protein, VDAC2, was found to be up-regulated in rHco-gal-m/f-treated PBMC. VDAC2 has been demonstrated as a conserved mitochondrial element of death pathways and played an important role in mitochondria-mediated apoptosis [67]. It has been reported that the expression level of VDAC controls life and death of the cell [68]. Overexpression of a rice VDAC (osVDAC4) in the Jurkat T-cell line could induce apoptosis [69].

T cell activation and cytokine secretion plays an important role in immune responses. CORO1A, which has an established role during T lymphocyte activation, migration, survival and calcium signaling [70,71], was up-regulated to the greatest extent on exposure to rHco-gal-m/f in the proteomic analysis. Of particular interest, *coro1a*-deficient mice have reduced peripheral T cells due to both an impaired survival of naive cells and migration defects [70,71]. These findings are consistent with what we observed in the Transwell assays and establish a connection between rHco-gal-m/f-induced apoptosis and the down-regulation of cell migration. Moreover, CORO1A could inhibit both IL17 and IFN γ expression and involved in the inhibition of the Th1 subset [72]. For further detection of the impact of rHco-gal-m/f on cellular homeostasis and cytokine secretion, DLL4, TBX21 and JAG1 as well as 8 cytokine genes were analyzed. DLL4 and TBX21 were implicated in the development of Th1 cells and the promotion of Th1 cytokines [73,74]. JAG1 was required for differentiation of naive CD $^{4+}$ T cells into Th2 cells and expression of Th2 cytokines [75]. Though we did not detect the expression change of IL17, both IFN γ and IL6 were down-regulated (Fig. 5F). Correspondingly, the transcription of DLL4, TBX21 and JAG1 were also decreased (Fig. 5D). The cytokines profile was consistent with previous report [15] and the inhibitory effect of rHco-gal-m/f on Th1 (IFN γ) and Th2 (IL4 and IL6) cytokine secretion was subsequently confirmed by ELISA (Fig. 6).

Modulations of monocyte/macrophage functions were involved in the establishments of immune regulatory environments. One of the modulations of macrophages was alternative activation characterized by high arginase 1 (ARG1) activity, low NO expression, and high IL-10 production [76]. In this research, the macrophage might be alternatively activated, since the transcription of IL10 and ARG1 was increased, while the inducible NOS2A was decreased (Fig. 5B and F). This would facilitate the nematode to persist in the host [77]. Furthermore, a regulatory immune environment due to the activation of T_{reg} cells and alternative activation of monocyte/macrophage are likely to assist pathogen persistence. From the result of real-time PCR, IL10 and TGF β 1 were more abundantly expressed with the stimulation of rHco-gal-m/f (Fig. 5F), indicating the activation of immune suppression T_{reg} cells [78]. Recently, the recombinant galectin of *T. leonina* (rT1-GAL) was also found to be able to inhibit Th1 and Th2 cytokine production by increasing the production of IL10 and TGF β 1 [11].

In eukaryotic cells, the turnover of intracellular proteins is mediated primarily by the ubiquitin-proteasome system (UPS) [79]. The 20S proteasome is a member of ubiquitin-proteasome proteolytic pathway and impacts cell survival through the

regulation of several essential cellular processes, including cell-cycle division, gene repair, differentiation, signal transduction and the elimination of oxidatively damaged proteins [80–82]. Proteasome subunit alpha type-1 (PSMA1) is a core subunit of the 20S proteasome and essential for the proteasome activity [83]. In this study, the down-regulation of PSMA1 (Table 1) would affect the cell-cycle, gene repair and cell survival in the rHco-gal-m/f-treated PBMC through ubiquitin–proteasome pathway.

We also detected the key members of nuclear factor-kappa B (NF- κ B) pathway, whose activation was a hallmark of the inflammatory response [84]. I κ B protein is an inhibitor of NF- κ B and inhibits its associated gene transcription [85]. After the treatment of rHco-gal-m/f, the transcripts for I κ B protein (NFKBIA) were more abundant. This supported evidence in a previous study where the ES products of helminths inhibited NF- κ B activation and thus decreased inflammation and facilitated the survival of parasites [86].

Since rHco-gal-m/f showed an apoptotic effect on goat PBMC [16], the decreased cytokine production may due to a reduced cell number. However, the number of living cell ascertained by trypan blue staining was decreased by $4.67 \pm 1.65\%$ after 24 h incubation of PBMC with rHco-gal-m/f. The drop of living cell was incomparable to that of cytokine production ($20.61 \pm 6.70\% - 69.80 \pm 9.37\%$). Thus, the decreased cytokine productions might be mainly due to multiple intracellular regulations induced by rHco-gal-m/f except for the reduced cell number.

5. Conclusion

In conclusion, our results showed that rHco-gal-m/f could bind to the surface of goat PBMC and behaved as the suppressors of inflammatory response to facilitate the immune evasion of *H. contortus*. Recombinant galectins induced the inhibition of ROS and cytokine production by modulating the free radical producing pathway, T cell development pathway and NF- κ B pathway. Furthermore, they induced cell apoptosis and decreased the capacity of cell migration and the turnover of intracellular proteins through the TLR pathway, CASPASE pathway, VEGF pathway, and ubiquitin–proteasome pathway. The collective results suggested that rHco-gal-m/f are multifunctional molecules that can influence many biological processes, especially those relevant to immune evasion. These findings provided insight into the interactive relationship between parasitic nematode galectins and host PBMC. It also shed new light on the molecular mechanisms of helminthic immune evasion. However, goat PBMC is a mixture of cells, including T cells, B cells, NK cells, monocytes and macrophages. Which subpopulation of goat PBMC is the primary binding target of rHco-gal-m/f and which molecular is the cell surface receptor for rHco-gal-m/f require further research.

Supplementary data to this article can be found online at <http://dx.doi.org/10.1016/j.jprot.2013.12.017>.

Acknowledgments

This work was funded by a grant from the National Natural Science Foundation of P.R. China (No. 31172308) and a project

funded by the Priority Academic Program Development of Jiangsu Higher Education Institutions (PAPD).

We thank XiaoYan Wang from National Institute of Viral Disease Control and Prevention, Chinese Center for Disease Control and Prevention for technical assistance with protein expression and purification. We also thank AnGuo Sun and Rui Wang from Shanghai Applied Protein Technology Co. Ltd. for the technology support.

REFERENCES

- [1] Kasai K, Hirabayashi J. Galectins: a family of animal lectins that decipher glyco-codes. *J Biochem* 1996;119:1–8.
- [2] Cooper DN. Galectinomics: finding themes in complexity. *Biochim Biophys Acta* 2002;1572:209–31.
- [3] Vasta GR. Roles of galectins in infection. *Nat Rev Microbiol* 2009;7:424–38.
- [4] Mercier S, St-Pierre C, Pelletier I, Ouellet M, Tremblay MJ, Sato S. Galectin-1 promotes HIV-1 infectivity in macrophages through stabilization of viral adsorption. *Virology* 2008;371:121–9.
- [5] Mey A, Leffler H, Hmama Z, Normier G, Revillard JP. The animal lectin galectin-3 interacts with bacterial lipopolysaccharides via two independent sites. *J Immunol* 1996;156:1572–7.
- [6] Okumura CY, Baum LG, Johnson PJ. Galectin-1 on cervical epithelial cells is a receptor for the sexually transmitted human parasite *Trichomonas vaginalis*. *Cell Microbiol* 2008;10:2078–90.
- [7] Bowater RJ, Abdelmalik SM, Lilford RJ. The methodological quality of cluster randomised controlled trials for managing tropical parasitic disease: a review of trials published from 1998 to 2007. *Trans R Soc Trop Med Hyg* 2009;103:429–36.
- [8] Kiel M, Josh P, Jones A, Windon R, Hunt P, Kongsuwan K. Identification of immuno-reactive proteins from a sheep gastrointestinal nematode, *Trichostrongylus colubriformis*, using two-dimensional electrophoresis and mass spectrometry. *Int J Parasitol* 2007;37:1419–29.
- [9] Turner DG, Wildblood LA, Inglis NF, Jones DG. Characterization of a galectin-like activity from the parasitic nematode, *Haemonchus contortus*, which modulates ovine eosinophil migration *in vitro*. *Vet Immunol Immunopathol* 2008;122:138–45.
- [10] Wildblood LA, Kerr K, Clark DA, Cameron A, Turner DG, Jones DG. Production of eosinophil chemoattractant activity by ovine gastrointestinal nematodes. *Vet Immunol Immunopathol* 2005;107:57–65.
- [11] Kim JY, Cho MK, Choi SH, Lee KH, Ahn SC, Kim DH, et al. Inhibition of dextran sulfate sodium (DSS)-induced intestinal inflammation via enhanced IL-10 and TGF-beta production by galectin-9 homologues isolated from intestinal parasites. *Mol Biochem Parasitol* 2010;174:53–61.
- [12] Hewitson JP, Grainger JR, Maizels RM. Helminth immunoregulation: the role of parasite secreted proteins in modulating host immunity. *Mol Biochem Parasitol* 2009;167:1–11.
- [13] Li C, Li X-R, X-F WEI, L-X XU. Cloning, characterization and sequence analysis of galectin cDNA of female and male adult worms of *Haemonchus contortus*. *J Agric Biotechnol* 2005;13:86–91.
- [14] Li C, Wei X, Xu L, Li X. Recombinant galectins of male and female *Haemonchus contortus* do not hemagglutinate erythrocytes of their natural host. *Vet Parasitol* 2007;144:299–303.
- [15] Yan-ming S, Ruo-feng Y, Li-xin X, Muleke CI, Xiang-ru L. Recombinant galectins of *Haemonchus contortus* inhibit goat

- cytokine mRNA transcription of peripheral blood mononuclear cells in vitro. *Agric Sci China* 2007;6:1262–8.
- [16] Sun Y, Yan R, Muleke CI, Zhao G, Xu L, Li X. Recombinant galectins of *Haemonchus contortus* parasite induces apoptosis in the peripheral blood lymphocytes of goat. *Int J Pept Res Ther* 2007;13:387–92.
- [17] Yanming S, Ruofeng Y, Muleke CI, Guangwei Z, Lixin X, Xiangrui L. Vaccination of goats with recombinant galectin antigen induces partial protection against *Haemonchus contortus* infection. *Parasite Immunol* 2007;29:319–26.
- [18] Rabinovich GA, Gruppi A. Galectins as immunoregulators during infectious processes: from microbial invasion to the resolution of the disease. *Parasite Immunol* 2005;27:103–14.
- [19] Zhao G, Yan R, Muleke CI, Sun Y, Xu L, Li X. Vaccination of goats with DNA vaccines encoding H11 and IL-2 induces partial protection against *Haemonchus contortus* infection. *Vet J* 2012;191:94–100.
- [20] Han K, Xu L, Yan R, Song X, Li X. Molecular cloning, expression and characterization of enolase from adult *Haemonchus contortus*. *Res Vet Sci* 2012;92:259–65.
- [21] Nicholson IC, Mavrangalos C, Fung K, Ayhan M, Levichkin I, Johnston A, et al. Characterisation of the protein composition of peripheral blood mononuclear cell microsomes by SDS-PAGE and mass spectrometry. *J Immunol Methods* 2005;305:84–93.
- [22] Gotz S, Garcia-Gomez JM, Terol J, Williams TD, Nagaraj SH, Nueda MJ, et al. High-throughput functional annotation and data mining with the Blast2GO suite. *Nucleic Acids Res* 2008;36:3420–35.
- [23] Stahlberg A, Rusnakova V, Forootan A, Anderova M, Kubista M. RT-qPCR work-flow for single-cell data analysis. *Methods* 2013;59:80–8.
- [24] Taylor DL, Zhong L, Begg DJ, de Silva K, Whittington RJ. Toll-like receptor genes are differentially expressed at the sites of infection during the progression of Johne's disease in outbred sheep. *Vet Immunol Immunopathol* 2008;124:132–51.
- [25] Livak KJ, Schmittgen TD. Analysis of relative gene expression data using real-time quantitative PCR and the 2^{-ΔΔCT} method. *Methods* 2001;25:402–8.
- [26] Marinaro M, Tempesta M, Tarsitano E, Camero M, Losurdo M, Buonavoglia C, et al. Antigen-specific IFN-gamma and IL-4 production in caprine herpesvirus infected goats. *Res Vet Sci* 2012;93:662–7.
- [27] Paclik D, Werner L, Guckelberger O, Wiedenmann B, Sturm A. Galectins distinctively regulate central monocyte and macrophage function. *Cell Immunol* 2011;271:97–103.
- [28] Ashburner M, Ball CA, Blake JA, Botstein D, Butler H, Cherry JM, et al. Gene ontology: tool for the unification of biology. The gene ontology consortium. *Nat Genet* 2000;25:25–9.
- [29] Rossignol M. Proteomic analysis of phosphorylated proteins. *Curr Opin Plant Biol* 2006;9:538–43.
- [30] Deng Z, Zhang X, Tang W, Osés-Prieto JA, Suzuki N, Gendron JM, et al. A proteomics study of brassinosteroid response in arabidopsis. *Mol Cell Proteomics* 2007;6:2058–71.
- [31] Bubanovic I. 1α,25-dihydroxy-vitamin-D3 as new immunotherapy in treatment of recurrent spontaneous abortion. *Med Hypotheses* 2004;63:250–3.
- [32] Willheim M, Thien R, Schratlbauer K, Bajna E, Holub M, Gruber R, et al. Regulatory effects of 1α,25-dihydroxyvitamin D3 on the cytokine production of human peripheral blood lymphocytes. *J Clin Endocrinol Metab* 1999;84:3739–44.
- [33] Pichler J, Gerstmayr M, Szeplafalusi Z, Urbanek R, Peterlik M, Willheim M. 1 α,25(OH)2D3 inhibits not only Th1 but also Th2 differentiation in human cord blood T cells. *Pediatr Res* 2002;52:12–8.
- [34] McInroy L, Maatta A. Down-regulation of vimentin expression inhibits carcinoma cell migration and adhesion. *Biochem Biophys Res Commun* 2007;360:109–14.
- [35] Nieminen M, Henttinen T, Merinen M, Marttila-Ichihara F, Eriksson JE, Jalkanen S. Vimentin function in lymphocyte adhesion and transcellular migration. *Nat Cell Biol* 2006;8:156–62.
- [36] Kim BR, Jeon YK, Nam MJ. A mechanism of apigenin-induced apoptosis is potentially related to anti-angiogenesis and anti-migration in human hepatocellular carcinoma cells. *Food Chem Toxicol* 2011;49:1626–32.
- [37] Behnke JM, Barnard CJ, Wakelin D. Understanding chronic nematode infections: evolutionary considerations, current hypotheses and the way forward. *Int J Parasitol* 1992;22:861–907.
- [38] Pemberton AD, Knight PA, Wright SH, Miller HR. Proteomic analysis of mouse jejunal epithelium and its response to infection with the intestinal nematode, *Trichinella spiralis*. *Proteomics* 2004;4:1101–8.
- [39] Wang ZQ, Wang L, Cui J. Proteomic analysis of *Trichinella spiralis* proteins in intestinal epithelial cells after culture with their larvae by shotgun LC-MS/MS approach. *J Proteomics* 2012;75:2375–83.
- [40] Goldfinch GM, Smith WD, Imrie L, McLean K, Inglis NF, Pemberton AD. The proteome of gastric lymph in normal and nematode infected sheep. *Proteomics* 2008;8:1909–18.
- [41] Nagaraj SH, Harsha HC, Reverter A, Colgrave ML, Sharma R, Andronicos N, et al. Proteomic analysis of the abomasal mucosal response following infection by the nematode, *Haemonchus contortus*, in genetically resistant and susceptible sheep. *J Proteomics* 2012;75:2141–52.
- [42] Neave MJ, Stretten-Joyce C, Nouwens AS, Glasby CJ, McGuinness KA, Parry DL, et al. The transcriptome and proteome are altered in marine polychaetes (Annelida) exposed to elevated metal levels. *J Proteomics* 2012;75:2721–35.
- [43] Kim MH. Flavonoids inhibit VEGF/bFGF-induced angiogenesis in vitro by inhibiting the matrix-degrading proteases. *J Cell Biochem* 2003;89:529–38.
- [44] Rousseau S, Dolado I, Beardmore V, Shpiro N, Marquez R, Nebreda AR, et al. CXCL12 and C5a trigger cell migration via a PAK1/2-p38α MAPK-MAPKAP-K2-HSP27 pathway. *Cell Signal* 2006;18:1897–905.
- [45] McMullen ME, Bryant PW, Glembotski CC, Vincent PA, Pumiglia KM. Activation of p38 has opposing effects on the proliferation and migration of endothelial cells. *J Biol Chem* 2005;280:20995–1003.
- [46] Lee JW, Kwak HJ, Lee JJ, Kim YN, Park MJ, Jung SE, et al. HSP27 regulates cell adhesion and invasion via modulation of focal adhesion kinase and MMP-2 expression. *Eur J Cell Biol* 2008;87:377–87.
- [47] Coleman JW. Nitric oxide in immunity and inflammation. *Int Immunopharmacol* 2001;1:1397–406.
- [48] Kotze AC, McClure SJ. *Haemonchus contortus* utilises catalase in defence against exogenous hydrogen peroxide in vitro. *Int J Parasitol* 2001;31:1563–71.
- [49] Ben-Smith A, Lammas DA, Behnke JM. Effect of oxygen radicals and differential expression of catalase and superoxide dismutase in adult *Heligmosomoides polygyrus* during primary infections in mice with differing response phenotypes. *Parasite Immunol* 2002;24:119–29.
- [50] Colasanti M, Gradoni L, Mattu M, Persichini T, Salvati L, Venturini G, et al. Molecular bases for the anti-parasitic effect of NO (review). *Int J Mol Med* 2002;9:131–4.
- [51] Wandurska-Nowak E. The role of nitric oxide (NO) in parasitic infections. *Wiad Parazytol* 2004;50:665–78.
- [52] Guzik TJ, Korb R, Adamek-Guzik T. Nitric oxide and superoxide in inflammation and immune regulation. *J Physiol Pharmacol* 2003;54:469–87.
- [53] Sukkar SG, Rossi E. Oxidative stress and nutritional prevention in autoimmune rheumatic diseases. *Autoimmun Rev* 2004;3:199–206.

- [54] Del Giudice R, Monti DM, Truppo E, Arciello A, Supuran CT, De Simone G, et al. Human carbonic anhydrase VII protects cells from oxidative damage. *Biol Chem* 2013;394:1343–8.
- [55] Zimmerman UJ, Wang P, Zhang X, Bogdanovich S, Forster R. Anti-oxidative response of carbonic anhydrase III in skeletal muscle. *IUBMB Life* 2004;56:343–7.
- [56] Nemoto-Sasaki Y, Kasai K. Deletion of lec-10, a galectin-encoding gene, increases susceptibility to oxidative stress in *Caenorhabditis elegans*. *Biol Pharm Bull* 2009;32:1973–7.
- [57] Schnare M, Barton GM, Holt AC, Takeda K, Akira S, Medzhitov R. Toll-like receptors control activation of adaptive immune responses. *Nat Immunol* 2001;2:947–50.
- [58] Kane CM, Cervi L, Sun J, McKee AS, Masek KS, Shapira S, et al. Helminth antigens modulate TLR-initiated dendritic cell activation. *J Immunol* 2004;173:7454–61.
- [59] Sun R, Zhang Y, Lv Q, Liu B, Jin M, Zhang W, et al. Toll-like receptor 3 (TLR3) induces apoptosis via death receptors and mitochondria by up-regulating the transactivating p63 isoform alpha (TAP63alpha). *J Biol Chem* 2011;286:15918–28.
- [60] Lehner M, Bailo M, Stachel D, Roesler W, Parolini O, Holter W. Caspase-8 dependent apoptosis induction in malignant myeloid cells by TLR stimulation in the presence of IFN-alpha. *Leuk Res* 2007;31:1729–35.
- [61] Arimilli S, Johnson JB, Alexander-Miller MA, Parks GD. TLR-4 and -6 agonists reverse apoptosis and promote maturation of simian virus 5-infected human dendritic cells through NFkB-dependent pathways. *Virology* 2007;365:144–56.
- [62] Fujita Y, Mihara T, Okazaki T, Shitanaka M, Kushino R, Ikeda C, et al. Toll-like receptors (TLR) 2 and 4 on human sperm recognize bacterial endotoxins and mediate apoptosis. *Hum Reprod* 2011;26:2799–806.
- [63] Bafica A, Santiago HC, Goldszmid R, Ropert C, Gazzinelli RT, Sher A. Cutting edge: TLR9 and TLR2 signaling together account for MyD88-dependent control of parasitemia in *Trypanosoma cruzi* infection. *J Immunol* 2006;177:3515–9.
- [64] Coban C, Ishii KJ, Kawai T, Hemmi H, Sato S, Uematsu S, et al. Toll-like receptor 9 mediates innate immune activation by the malaria pigment hemozoin. *J Exp Med* 2005;201:19–25.
- [65] Jenkins SJ, Hewitson JP, Ferret-Bernard S, Mountford AP. Schistosome larvae stimulate macrophage cytokine production through TLR4-dependent and -independent pathways. *Int Immunol* 2005;17:1409–18.
- [66] Imtiyaz HZ, Rosenberg S, Zhang Y, Rahman ZS, Hou YJ, Manser T, et al. The Fas-associated death domain protein is required in apoptosis and TLR-induced proliferative responses in B cells. *J Immunol* 2006;176:6852–61.
- [67] Shoshan-Barmatz V, De Pinto V, Zweckstetter M, Raviv Z, Keinan N, Arbel N. VDAC, a multi-functional mitochondrial protein regulating cell life and death. *Mol Aspects Med* 2010;31:227–85.
- [68] Abu-Hamad S, Sivan S, Shoshan-Barmatz V. The expression level of the voltage-dependent anion channel controls life and death of the cell. *Proc Natl Acad Sci U S A* 2006;103:5787–92.
- [69] Godbole A, Varghese J, Sarin A, Mathew MK. VDAC is a conserved element of death pathways in plant and animal systems. *Biochim Biophys Acta* 2003;1642:87–96.
- [70] Foger N, Rangell L, Danilenko DM, Chan AC. Requirement for coronin 1 in T lymphocyte trafficking and cellular homeostasis. *Science* 2006;313:839–42.
- [71] Mueller P, Massner J, Jayachandran R, Combaluzier B, Albrecht I, Gatfield J, et al. Regulation of T cell survival through coronin-1-mediated generation of inositol-1,4,5-trisphosphate and calcium mobilization after T cell receptor triggering. *Nat Immunol* 2008;9:424–31.
- [72] Kaminski S, Hermann-Kleiter N, Meisel M, Thuille N, Cronin S, Hara H, et al. Coronin 1A is an essential regulator of the TGFbeta receptor/SMAD3 signaling pathway in Th17 CD4(+) T cells. *J Autoimmun* 2011;37:198–208.
- [73] Amsen D, Blander JM, Lee GR, Tanigaki K, Honjo T, Flavell RA. Instruction of distinct CD4 T helper cell fates by different notch ligands on antigen-presenting cells. *Cell* 2004;117:515–26.
- [74] Szabo SJ, Kim ST, Costa GL, Zhang X, Fathman CG, Glimcher LH. A novel transcription factor, T-bet, directs Th1 lineage commitment. *Cell* 2000;100:655–69.
- [75] Lee HJ, Takemoto N, Kurata H, Kamogawa Y, Miyatake S, O'Garra A, et al. GATA-3 induces T helper cell type 2 (Th2) cytokine expression and chromatin remodeling in committed Th1 cells. *J Exp Med* 2000;192:105–15.
- [76] Flynn RJ, Mulcahy G. Possible role for Toll-like receptors in interaction of *Fasciola hepatica* excretory/secretory products with bovine macrophages. *Infect Immun* 2008;76:678–84.
- [77] Donnelly S, O'Neill SM, Sekiya M, Mulcahy G, Dalton JP. Thioredoxin peroxidase secreted by *Fasciola hepatica* induces the alternative activation of macrophages. *Infect Immun* 2005;73:166–73.
- [78] Gigante M, Ranieri E. TGF-beta promotes immune suppression by inhibiting Treg cell apoptosis. *Immunotherapy* 2010;2:608.
- [79] Coux O, Tanaka K, Goldberg AL. Structure and functions of the 20S and 26S proteasomes. *Annu Rev Biochem* 1996;65:801–47.
- [80] Davies KJ. Degradation of oxidized proteins by the 20S proteasome. *Biochimie* 2001;83:301–10.
- [81] Reinstein E, Ciechanover A. Narrative review: protein degradation and human diseases: the ubiquitin connection. *Ann Intern Med* 2006;145:676–84.
- [82] Powell SR, Wang P, Divald A, Teichberg S, Haridas V, McCloskey TW, et al. Aggregates of oxidized proteins (lipofuscin) induce apoptosis through proteasome inhibition and dysregulation of proapoptotic proteins. *Free Radic Biol Med* 2005;38:1093–101.
- [83] Zhang Y, Jia L, Lee SJ, Wang MM. Conserved signal peptide of Notch3 inhibits interaction with proteasome. *Biochem Biophys Res Commun* 2007;355:245–51.
- [84] Karin M, Greten FR. NF-kappaB: linking inflammation and immunity to cancer development and progression. *Nat Rev Immunol* 2005;5:749–59.
- [85] Gilmore TD. The Re1/NF-kappa B/1 kappa B signal transduction pathway and cancer. *Cancer Treat Res* 2003;115:241–65.
- [86] Puneet P, McGrath MA, Tay HK, Al-Riyami L, Rzepecka J, Moochhala SM, et al. The helminth product ES-62 protects against septic shock via Toll-like receptor 4-dependent autophagosomal degradation of the adaptor MyD88. *Nat Immunol* 2011;12:344–51.

RESEARCH ARTICLE

Characterization of a novel mouse model with genetic deletion of CD177

Qing Xie^{1,2}, Julia Klesney-Tait³, Kathy Keck³, Corey Parlet², Nicholas Borcharding², Ryan Kolb², Wei Li², Lorraine Tygrett², Thomas Waldschmidt², Alicia Olivier², Songhai Chen⁴, Guang-Hui Liu^{5,6}, Xiangrui Li^{1,2}, Weizhou Zhang^{2,3}

¹ College of Veterinary Medicine, Nanjing Agricultural University, Nanjing 210095, China

² Department of Pathology, Holden Comprehensive Cancer Center, Carver College of Medicine/University of Iowa, Iowa, IA 52242, USA

³ Department of Internal Medicine, Carver College of Medicine/University of Iowa, Iowa, IA 52242, USA

⁴ Department of Pharmacology, Carver College of Medicine/University of Iowa, Iowa, IA 52242, USA

⁵ National Laboratory of Biomacromolecules, Institute of Biophysics, Chinese Academy of Sciences, Beijing 100101, China

⁶ Beijing Institute for Brain Disorders, Beijing 100069, China

✉ Correspondence: lixiangrui@njau.edu.cn (X. Li), weizhou-zhang@uiowa.edu (W. Zhang)

Received September 1, 2014 Accepted September 25, 2014

ABSTRACT

Neutrophils play an essential role in the innate immune response to infection. Neutrophils migrate from the vasculature into the tissue in response to infection. Recently, a neutrophil cell surface receptor, CD177, was shown to help mediate neutrophil migration across the endothelium through interactions with PECAM1. We examined a publicly available gene array dataset of CD177 expression from human neutrophils following pulmonary endotoxin instillation. Among all 22,214 genes examined, CD177 mRNA was the most upregulated following endotoxin exposure. The high level of CD177 expression is also maintained in airspace neutrophils, suggesting a potential involvement of CD177 in neutrophil infiltration under infectious diseases. To determine the role of CD177 in neutrophils *in vivo*, we constructed a CD177-genetic knockout mouse model. The mice with homozygous deletion of CD177 have no discernible phenotype and no significant change in immune cells, other than decreased neutrophil counts in peripheral blood. We examined the role of CD177 in neutrophil accumulation using a skin infection model with *Staphylococcus aureus*. CD177 deletion reduced

neutrophil counts in inflammatory skin caused by *S. aureus*. Mechanistically we found that CD177 deletion in mouse neutrophils has no significant impact in CXCL1/KC- or fMLP-induced migration, but led to significant cell death. Herein we established a novel genetic mouse model to study the role of CD177 and found that CD177 plays an important role in neutrophils.

KEYWORDS CD177, neutrophil, mouse model, genetic deletion

INTRODUCTION

CD177 is a polymorphic gene that has been linked to several important clinical diseases including polycythemia vera, Wegner's granulomatosis, and immune mediated neonatal neutropenia (Lalezari et al., 1971; Bettinotti et al., 2002; Caruccio et al., 2006). The NB1/CD177 glycoprotein was initially identified in several cases of neonatal neutropenia (Lalezari et al., 1971), where the maternal antibodies react specifically with neonatal neutrophil-specific epitope HNA-2a derived from NB1 glycoprotein. In several cases of transfusion-related acute lung injury, CD177-specific antibodies from donor blood were identified as the primary cause (Bux et al., 1996). CD177 has been established as a diagnostic marker for various myeloproliferative diseases including polycythemia vera, thrombocytopenia, and idiopathic myelofibrosis (Stroncek et al., 2004; Sirhan et al., 2005; Martini et al., 2006; Michiels et al., 2007). This 58–64 kDa

Qing Xie, Julia Klesney-Tait have contributed equally to this work.

Electronic supplementary material The online version of this article (doi:10.1007/s13238-014-0109-1) contains supplementary material, which is available to authorized users.

glycophosphatidylinositol (GPI)-linked N-glycosylated extracellular surface protein (Goldschmeding et al., 1992; Dillon et al., 2008) is expressed on a subpopulation of neutrophils (Matsuo et al., 2000). In general, 20%–80% of circulating neutrophils are CD177 positive, with 3%–5% of population having no CD177⁺ neutrophils (Matsuo et al., 2000).

CD177 belongs to the uPAR/CD59/Ly6 snake toxin superfamily and is conserved in many species (Kissel et al., 2001; Stroncek, 2007). While percentages of CD177⁺ circulating neutrophils are constant in the same individuals (Goldschmeding et al., 1992; Stroncek et al., 1998), CD177 mRNA and protein expression are increased in response to inflammatory stimulation. Granulocyte colony stimulating factor (G-CSF) strongly induces CD177 expression (Stroncek et al., 1998). Expression of CD177 is also altered during pregnancy (Caruccio et al., 2003) and during severe bacterial infections (Gohring et al., 2004). The function of CD177 in neutrophil biology is largely unknown. Recent literature indicates that CD177 mediates the migration of neutrophils across endothelial cells via interactions with proteinase 3 (Kuckleburg et al., 2012; Kuckleburg and Newman, 2013) and PECAM-1 (CD31) (Sachs et al., 2007; Bayat et al., 2010), as well as the degranulation and superoxide generation in a Mac-1-dependent manner (Jerke et al., 2011). These *in vitro* studies suggest a role for CD177 in neutrophil transmigration. However, a recent study indicated that CD177⁻ and CD177⁺ neutrophils accumulate similarly in the peritoneal cavity of human peritonitis patients (Wang et al., 2013), suggesting that CD177 expression in neutrophils provides no transmigration advantage into this site.

Using a murine CD177 knockout model, the present study demonstrates that CD177 plays a crucial role in neutrophil viability, but has no impact on chemotaxis.

RESULTS

CD177 mRNA expression is increased in human neutrophils following pulmonary endotoxin instillation and in neutrophils isolated from septic patients

To understand how neutrophils respond to bacterial stimulus at the transcriptional level, we analyzed a published microarray dataset (GSE2322) (Coldren et al., 2006) using circulating neutrophils before and after bacterial endotoxin (LPS) instillation, and neutrophils from bronchoalveolar lavage (BAL) after endotoxin instillation from human volunteers. Endotoxin treatment alone did not induce CD177 expression in purified blood neutrophils *in vitro* (Fig. 1A). However, CD177 is the most significantly upregulated gene (13 fold induction) in circulating neutrophils among all the genes induced by endotoxin *in vivo* (Table 1 and Fig. 1A). Another 13 genes were co-upregulated with CD177 with a more than two fold increase, and *P* values less than 0.05 (Table 1). The expression of CD177 mRNA was also high after pulmonary endotoxin exposure (Table 1 and Fig. 1A). The significant upregulation of CD177 in both circulating and airway

neutrophils implies an important role for CD177 in neutrophil function in response to bacterial infection in the lung. As expected, pulmonary endotoxin exposure leads to significantly elevated pro-inflammatory pathways identified by gene sets enrichment analysis (GSEA) (Subramanian et al., 2005), including the IL-1R pathway, TH1/TH2 pathway, LPS-induced inflammatory pathway and other pathways related to inflammation (Fig. 1B, Tables S1–3).

To examine the influence of bacterial infection on CD177 expression, we downloaded another dataset GSE5772 (Tang et al., 2007) profiling neutrophil transcripts from normal individuals or septic patients with gram-negative, gram-positive, or mixed bacterial infections. We found that only septic patients with mixed bacterial infections exhibited significantly increased CD177 expression in their neutrophils; whereas septic patients infected with either gram-negative or gram-positive bacteria had a moderate but not significant increase of CD177 expression (Fig. 1C). These data indicate that CD177 expression in neutrophils can be induced by bacterial infection. Induction of CD177, however, is not necessarily mediated through toll-like receptor-mediated signaling since *in vitro* treatment with endotoxin alone failed to induce CD177 expression.

Generation of CD177 genetic knockout mouse models

To understand the physiological role of CD177 in neutrophils, we generated a CD177 genetic knockout mouse by deleting the whole mouse CD177 gene locus via homologous recombination (Fig. 2A). We developed a genotyping protocol to differentiate wild type (wt, CD177^{+/+}), heterozygous (he, CD177^{+/-}), or homozygous (ko, CD177^{-/-}) animals (Fig. 2B). Ly-6G⁺ neutrophils from CD177^{-/-} mice lack mRNA and surface expression of CD177, indicating loss of CD177 at both the RNA and protein levels (Fig. 2C and 2D, P2 gate). As observed in human, neither lymphocytes (R1 gate) nor monocytes (P5 gate) expressed CD177 in wt mice (Fig. 2D). CD177^{-/-} mice were fertile and litters were born at a normal Mendelian ratio without any discernible phenotype (data not shown). We collected various tissues from the CD177^{-/-} mice for histological assessment and found no gross or fine histological differences between wt, CD177^{+/-}, and CD177^{-/-} mice (data not shown). Immunophenotyping of different lineages of immune cells was performed by flow cytometry. There was no significant difference in T and B cell frequencies from all the compartments tested, including bone marrow, blood, thymus (data not shown), and spleen (Fig. 3A). We did not see any major defects in myeloid lineages from the different compartments (Fig. 3A–D). We did observe a significant decrease of CD11b⁺Ly-6C⁺Ly-6G⁺ circulating neutrophils from CD177^{-/-} mice relative to WT and CD177^{+/-} mice (Fig. 3B), but no difference could be detected in the spleen (Fig. 3A), lymph nodes (Fig. 3C), and bone marrow (Fig. 3D). Our results indicate that CD177 is dispensable for normal neutrophil development in mouse bone marrow or distribution within secondary lymphoid tissues,

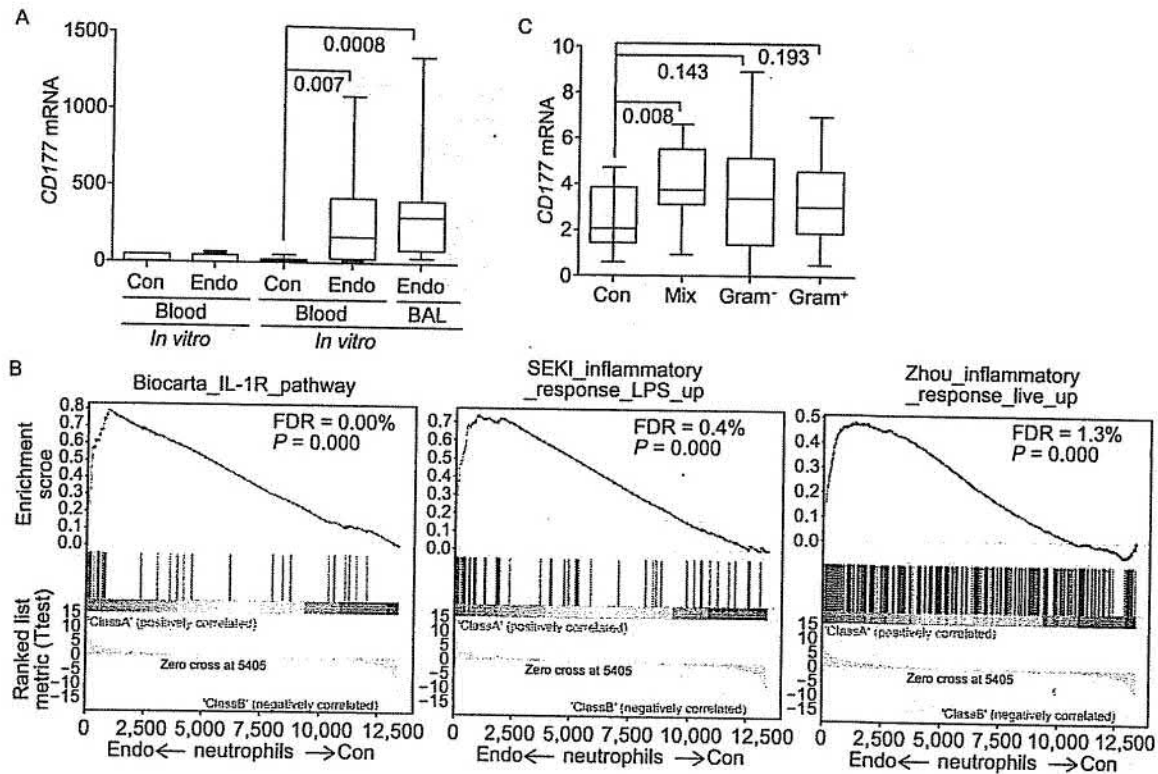


Figure 1. Pulmonary endotoxin instillation induces CD177 expression in circulating and airway neutrophils. (A) GEO dataset GSE2322 was downloaded and analyzed for endotoxin-induced CD177 mRNA expression from purified neutrophils before and after *in vitro* endotoxin treatment, circulating neutrophils before *in vivo* endotoxin treatment, or circulating neutrophils and airway neutrophils after *in vivo* endotoxin treatment. $n = 14$ for circulating neutrophils prior to endotoxin treatment; $n = 17$ for circulating neutrophils post endotoxin treatment; $n = 17$ for airway neutrophils post endotoxin treatment. (B) Gene Set Enrichment Analysis (GSEA) was performed to compare biological pathways that are different between circulating neutrophils before and after endotoxin instillation, or between circulating neutrophils before endotoxin instillation and airway neutrophils after endotoxin treatment. Both distinct pathways and common pathways are summarized in supplemental Tables 1–3. Common pathways are shown including IL-1R signaling, LPS-induced inflammatory pathway, and live *Porphyromonas gingivalis*-induced inflammatory pathway. (C) GEO dataset GSE5772 was downloaded including 17 non-infected normal controls, 25 septic patients infected with gram-negative bacteria, 18 septic patients infected with gram-positive bacteria, and 12 septic patients with both gram-negative and gram-positive bacterial infections; CD177 expression is in \log_2 . (A and C) P values are shown; (B) Both P values and false discovery rate (FDR) are shown.

which agrees with the observation that up to 5% of individuals have normal neutrophil counts and function with no detectable CD177 expression (Matsuo et al., 2000).

CD177-deficiency leads to decreased neutrophil accumulation early after infection

To examine the role of CD177 in a bacterial infection model, we used a mouse model of *Staphylococcus aureus* skin infection. WT and *CD177*^{-/-} mice were infected with bacteria at day 0. Skin was collected from infected mice, and CD11b⁺Ly-6C⁺Ly-6G⁺ neutrophils were quantitated by flow cytometry at different days after infection. We found an initial significant decrease of neutrophils in wounded skin of *CD177*^{-/-} mice at day one after administration of *Staphylococcus aureus* (Fig. 4A). The trend was maintained at three

days after infection, but the difference was not statistically significant between infected WT or *CD177*^{-/-} mice (Fig. 4A). After seven days of infection when the wound was already recovered, there was no difference in neutrophil counts between the two groups (Fig. 4A). We also observed a significant decrease of CD11b⁺Ly-6C⁺Ly-6G⁺ monocytes in the wounded skin of *CD177*^{-/-} mice at day one after infection (Fig. 4B) and there was no difference after 3 or 7 days of infection (Fig. 4B), which may reflect the importance of neutrophils in initial recruitment of monocytes. In the same model, we did not identify any significant difference in wound healing (Fig. 4C) and body weight recovery (Fig. 4D) after infection.

Since it was reported that *CD177*⁻ and *CD177*⁺ neutrophils accumulate similarly in the peritoneal cavity of human peritonitis patients (Wang et al., 2013), we included a

Table 1. Genes were induced by pulmonary endotoxin treatment

Probe_ID	Gene symbol	Blood Neu after/before endotoxin		BAL Neu/Blood Neu	
		Fold change	P value	Fold change	P value
219669_at	CD177	12.98	4.11×10^{-3}	20.34	4.34×10^{-3}
203021_at	SLPI	3.48	1.28×10^{-3}	9.11	1.49×10^{-5}
207500_at	CASP5	3.25	5.98×10^{-3}	15.66	1.29×10^{-4}
204860_s_at	NAIP	3.05	8.37×10^{-4}	4.03	1.33×10^{-2}
209369_at	ANXA3	2.97	2.71×10^{-3}	4.48	6.84×10^{-6}
208771_s_at	LTA4H	2.58	6.06×10^{-4}	4.20	1.79×10^{-3}
200985_s_at	CD59	2.55	7.02×10^{-3}	3.94	3.44×10^{-5}
210166_at	TLR5	2.55	2.80×10^{-4}	2.99	4.67×10^{-3}
200984_s_at	CD59	2.53	1.40×10^{-3}	3.60	2.48×10^{-5}
203233_at	IL4R	2.51	1.28×10^{-4}	2.34	6.66×10^{-4}
201554_x_at	GYG1	2.45	1.49×10^{-3}	3.60	2.60×10^{-7}
217823_s_at	UBE2J1	2.27	7.10×10^{-4}	2.30	1.19×10^{-4}
209835_x_at	CD44	2.22	2.53×10^{-3}	21.12	5.31×10^{-10}
206697_s_at	HPR	2.14	8.11×10^{-3}	2.61	2.89×10^{-2}
212135_s_at	ATP2B4	2.09	4.05×10^{-5}	2.29	1.78×10^{-3}
204232_at	FCER1G	2.05	6.75×10^{-4}	4.07	1.47×10^{-7}
212136_at	ATP2B4	2.01	3.80×10^{-3}	2.32	5.98×10^{-3}

GEO dataset GSE2322 was downloaded including transcripts from circulating neutrophils and bronchoalveolar lavage neutrophils obtained from human volunteers before and after endotoxin instillation. Genes that were significantly induced by endotoxin treatment are listed, with at least two-fold change and *P* values less than 0.05. *n* = 14 for circulating neutrophils prior to endotoxin treatment; *n* = 17 for circulating neutrophils post endotoxin treatment; *n* = 17 for airway neutrophils post endotoxin treatment.

thioglycollate-induced peritonitis model to examine the effect of CD177 on neutrophil accumulation into the peritoneal cavity. Congruently, we did not find a significant difference in total peritoneal CD11b⁺Ly6C⁺Ly6G⁺ neutrophils or CD11b⁺Ly6C⁺Ly6G⁻ monocytes between WT and CD177^{-/-} mice (Fig. 5A and 5B), confirming that CD177 has no role in peritoneal accumulation of neutrophils in peritonitis.

CD177-deficiency leads to increased neutrophil cell death

Since CD177 is reported to be involved in neutrophil chemotaxis and transmigration, we examined the impact of CD177 on neutrophil chemotaxis and found that CD177-deficiency have no significant impact on CXCL1- and fMLP-induced chemotaxis when using naïve bone marrow cells (Fig. 6A), or using activated neutrophils present in thioglycollate-induced peritoneal exudate cells (Fig. 6B).

To identify the potential reason why CD177-deficiency resulted in significantly fewer neutrophils in the skin early after bacterial infection, we searched GEO profiles and found that deletion of IKK β led to a significant increase in CD177 expression from neutrophils (Fig. 6C). IKK β is a well-known factor whose inactivation leads to neutrophilia in the mouse and human due to increased neutrophil survival (Hsu

et al., 2011). Curiously, we found that CD177-deficiency led to increased cell death of bone marrow neutrophils when cultured *ex vivo* (Fig. 6D), suggesting that CD177 could be the downstream effector of IKK β deletion leading to increased neutrophil survival.

DISCUSSION

Here we established a novel CD177 genetic deletion model to study its role in neutrophil biology. We found that CD177 is only expressed on neutrophils but not monocytes or lymphocytes (Fig. 2), similar to the expression patterns in human. Although CD177 had been suggested to serve as an adhesive molecule mediating migration towards chemokine gradients in human neutrophils (Sachs et al., 2007; Bayat et al., 2010; Jerke et al., 2011), we did not find any role for CD177 in promoting mouse neutrophil migration in response to CXCL1 and fMLP. Instead, we found decreased neutrophil counts in blood and infected skin from the CD177 ko animals. The CD177-deficiency led to decreased survival of bone marrow neutrophils *ex vivo*, which could potentially be used to explain the decreased neutrophil phenotype in CD177 ko mice. Among the many factors that have been shown to be involved in neutrophil death, IKK β has attracted attention given its role in inflammatory diseases and cancer

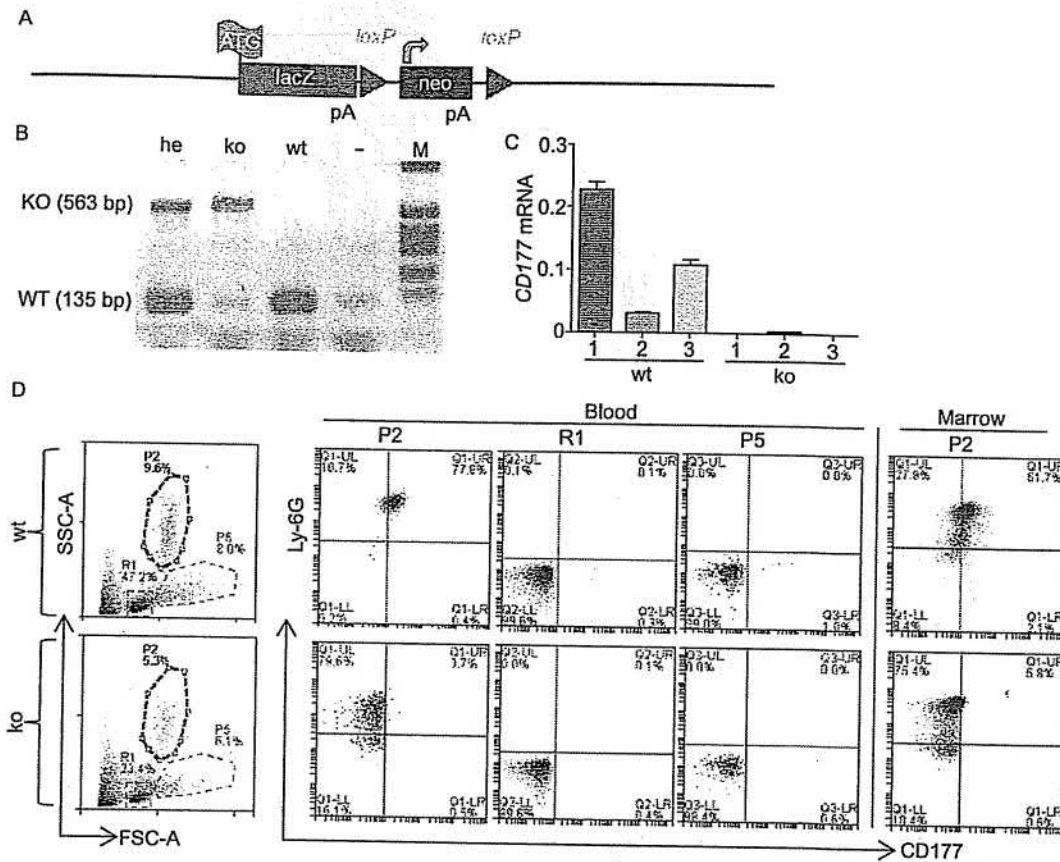


Figure 2. Genetic deletion of *CD177* in mice. (A) Schematic depiction of the *CD177* targeting construct. The entire *CD177* locus was replaced by *LacZ* and *Neomycin* by homologous recombination. (B) Image representative for genotyping *CD177* genetic knock out mice. Genomic DNA was purified from tail clips and amplified with specific primers listed in the Materials and Methods. he: heterozygous knock out; ko: homozygous knock out; wt: wild type. (C) mRNA expression of *CD177* in bone marrow cells from WT or *CD177*^{-/-} mice, analyzed by real-time PCR, $n = 3$. (D) Surface expression of *CD177* in blood and bone marrow cells (marrow) were collected and stained with anti-Ly-6G-FITC, and anti-*CD177*-PE antibodies, followed by flow cytometry, $n = 3$.

(Hsu et al., 2011). However, one of the common complications for IKK β inhibition in patients is neutrophilia (Hsu et al., 2011), which is also observed in mice when IKK β is deleted in the myeloid lineage. The IKK β deletion was found to increase neutrophil life span by inducing pro-survival molecules (Hsu et al., 2011). *CD177* is upregulated in neutrophils with IKK β deletion and at the same time is involved in neutrophil survival (Fig. 6), suggesting that *CD177* could be one of the factors mediating IKK β -inhibition-induced survival and neutrophilia.

Another interesting observation is that *CD177*-deletion only impacts neutrophil numbers in blood and bacteria-infected skin, but not in bone marrow or secondary lymphoid tissues. These results suggest that the role of *CD177* in neutrophil survival depends on the context where neutrophils are located and if other survival signals exist. It is known that neutrophils are adhesive and interact with many cell types (Geering et al.,

2013). Some of the cell-cell interactions provide strong survival signal for neutrophils (Geering et al., 2013). Upon infection, however, neutrophils are recruited from the bone marrow microenvironment and lose these pro-survival signals. Importantly, certain infections lead to an upregulation of *CD177* on human neutrophils (Fig. 1), leading to potentially prolonged neutrophil survival for efficient clearance of the bacteria. It is worth noting that *CD177* may facilitate but is not required for survival, since there are still significant numbers of neutrophils in the blood of *CD177* ko mice. Human *CD177*-negative neutrophils may also utilize alternative survival signals since 3%–5% of individuals who lack *CD177* expression on their neutrophils have normal neutrophil counts and a normal defense towards bacteria (Stroncek et al., 2004). An interesting future avenue would be if the deletion of *CD177* in human *CD177*-positive neutrophils has an impact on their survival under physiological or pathological conditions.

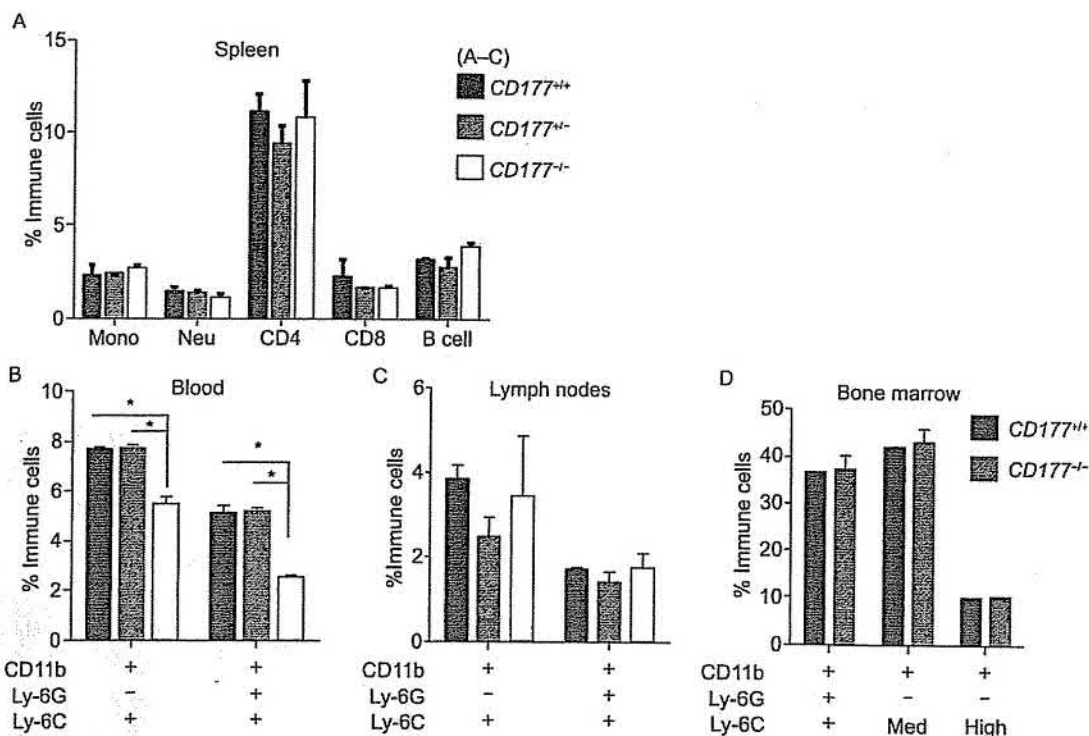


Figure 3. Normal development of myeloid cell lineages in *CD177*^{-/-} mice. (A) Splenic cells from seven-week-old mice were stained with anti-CD45, anti-Ly-6C, anti-Ly-6G, anti-CD11b, anti-CD11c, anti-CD3, anti-CD4, anti-CD8, and anti-B220 antibodies, followed with flow cytometry ($n = 4-5$). (B-D) Seven-week old mice were euthanized and different organs were collected. Single cell suspensions were prepared for immunolabelling with different antibodies and analyzed with flow cytometry. Blood cells (B), single cells from lymph nodes (C), or bone marrow cells (D) were labeled anti-CD45, anti-Ly-6C, anti-Ly-6G, anti-CD11b, anti-CD11c, followed with flow cytometry. $CD45^+CD11b^+Ly-6C^+Ly-6G^+$ cells are defined as neutrophils; $CD45^+CD11b^+Ly-6C^+Ly-6G^-$ cells are defined as monocytic cells. $n = 4-5$. * $P < 0.05$.

The skin infection model clearly shows that *CD177* ko mice have an early decrease in neutrophils in infected skin, but the initial neutrophil defect has no significant impact on bacterial clearance as reflected by the normal wound size and body weight recovery (Fig. 5). It has been acknowledged that neutrophils, and as well as other leukocytes, need to maintain a critical threshold concentration for efficient clearance of infection (Li et al., 2002, 2004). This could explain the normal recovery in *CD177* ko mice where reduced neutrophil numbers are still in sufficient quantity to eliminate *Staphylococcus aureus*.

A role for *CD177* in neutrophil survival could be dependent upon particular physiological or pathological conditions. Ramirez-Velazquez et al. showed that *CD177*⁺ neutrophils co-expressing IL-17 are increased in moderate to severe allergic asthma (Ramirez-Velazquez et al., 2013). Our analysis based on published datasets demonstrated that *CD177* expression is increased in circulating and BAL neutrophils when human volunteers were instilled with endotoxin (Fig. 1), a condition mimicking bacterial infection. All together, we believe that in certain respiratory diseases, especially those that can be exacerbated by secondary bacterial

infection and involve neutrophilic inflammation (Simpson et al., 2007; Simpson et al., 2008; Essilfie et al., 2011), *CD177* could be a potential contribution to the accumulation of neutrophils in the lung airway. This process, if uncontrolled, could lead to tissue damage and more severe disease. Thus *CD177* may provide a target to treat respiratory diseases that are worsened by uncontrolled neutrophilic inflammation.

MATERIALS AND METHODS

CD177 knockout mice construction

All animals were maintained under specific pathogen-free conditions according to the IACUC guidelines. The *CD177* knockout mouse strain used for this research project was created from ES cell clone (12120a-B11), obtained from the KOMP Repository (www.komp.org) and generated by Regeneron Pharmaceuticals, Inc (Valenzuela et al., 2003). We purchased mouse sperm carrying the *CD177* deletion allele from the UC Davis KOMP Repository and sent it to Jackson Laboratories for *in vitro* fertilization. Seven mice were obtained with 3 carrying a heterozygous deletion of *CD177*. Mice were backcrossed to C57BL/6 for 6 generations. Genotyping of the *CD177* knockout mice was

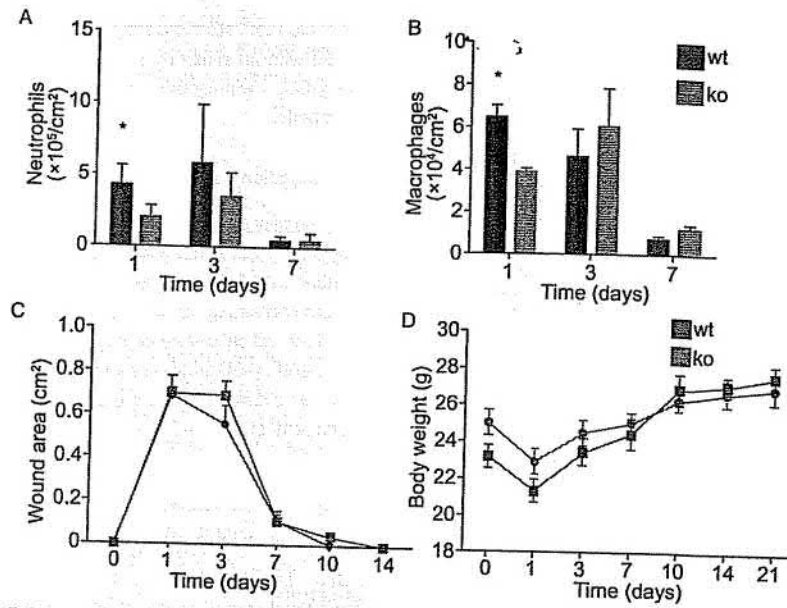


Figure 4. CD177 deficiency leads to decreased neutrophil accumulation in infected skin. (A) CD45⁺CD11b⁺Ly-6C⁺Ly-6G⁺ neutrophils in the wounded skin of *Staphylococcus Aureus*-infected mice at different days. (B) CD11b⁺F4/80⁺ macrophages in the wounded skin of *Staphylococcus Aureus*-infected mice. Wounded area (C) and body weight (D) after *Staphylococcus Aureus* infection. *P values < 0.05.

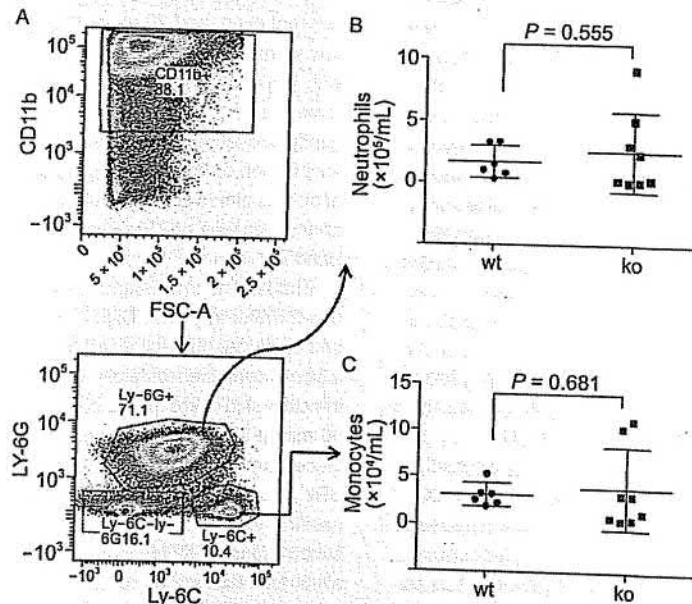


Figure 5. CD177 deficiency has no impact on peritoneal accumulation of neutrophils in thioglycolate-induced peritonitis. (A) Schematic showing flow cytometry to determine neutrophil numbers. Peritoneal cells were stained with antibodies, followed by flow cytometry to determine the total numbers of neutrophils and monocytes. (B) CD45⁺CD11b⁺Ly-6C⁺Ly-6G⁺ neutrophils were counted and graphed. (C) CD45⁺CD11b⁺Ly-6C⁺Ly-6G⁻ monocytes were graphed. n = 6 in WT group and n = 8 in CD177^{-/-} group. P values were indicated.

performed through standard PCR procedures. Primers used for genotyping are: WT allele (135 bp): forward primer 5'-GGTGATCTGG CTCAGGACAG-3' and reverse primer 5'-CACCTGTGGGTAGGT

AGC-3'; mutant allele (563 bp): forward primer 5'-ATTCGGCTATGA CTGGGCAC-3' and reverse primer 5'-TGAATCCAGAAAAGCGGC CA-3'.

Protein & Cell

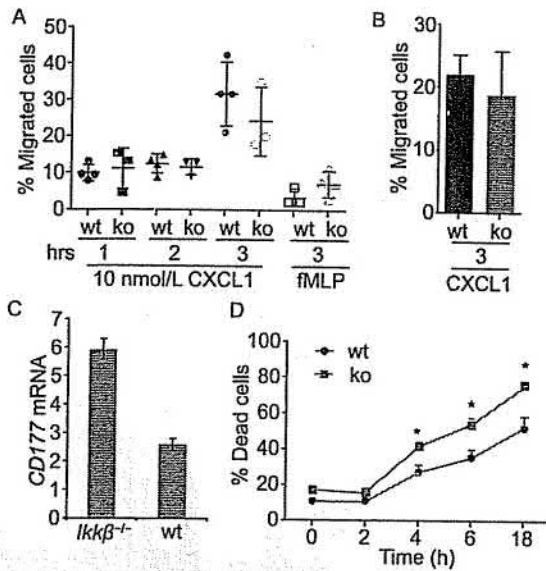


Figure 6. CD177 deletion leads to neutrophil cell death. (A and B) CD177 did not impact chemotaxis *ex vivo*. Bone marrow cells (A) or thioglycollate-induced peritoneal cells (B) were isolated from WT or *CD177*^{-/-} mice. These cells were measured for their transmigration in response to 10 nmol/L of CXCL1/KC or 100 nmol/L of fMLP at the indicated time points. Ly-6G⁺Ly-6C⁺ neutrophils counts were determined by flow cytometry. *n* = 3–4 mice per group. (C) GEO dataset GSE25211 was downloaded and analyzed for CD177 mRNA expression from purified neutrophils with (WT) or without IKK β -deletion (*Ikk β* ^{-/-}). *n* = 2 per group. (D) Primary bone marrow cells from WT or *CD177*^{-/-} mice were collected and cultured in medium. At the indicated time points, cells were stained with propidium iodide, and dead cells were enumerated by flow cytometry at each time point. *n* = 4 mice per group. **P* < 0.05.

Flow cytometric analysis

Single-cell suspensions were prepared from spleen, bone marrow, thymus and blood, and red blood cells were lysed with red blood lysis buffer containing 155 mmol/L NH₄Cl, 12 mmol/L NaHCO₃ and 0.1 mmol/L EDTA. Cells were stained with different isotype controls or antibodies with different fluorophores, supplemented with CD16/CD32 FcR blockers. After being stained for 30 min, cells were washed twice and fixed in PBS containing 1% paraformaldehyde. Labeled cells were collected on a FACS Canto II (BD Biosciences) or LSR II (BD Biosciences) using Diva acquisition software, and analyzed using FlowJo (TreeStar, Stanford, CA, USA). The following antibodies were used: anti-CD3 (145-2C11, Ebiosciences), anti-CD4 (GK1.5, Ebiosciences), anti-CD8 (53-6.7, Ebiosciences), anti-B220 (RA3-6B2, Ebiosciences), CD45 (30-F11, Ebiosciences), Ly-6C (HK1.4, Ebiosciences), Ly-6G (1A8, BD Pharmingen), CD11b (M170, Ebiosciences), and the rat anti-mouse CD177 mAb was developed in our own laboratory.

Thioglycollate-induced peritonitis

Eight-week old WT or *CD177*^{-/-} mice were injected i.p. with 1 mL of 4% sterile thioglycollate. Four hours later, mice were anesthetized

and peritoneal cells were recovered using 10 mL of ice cold PBS and stained with an antibody cocktail including anti-CD45, anti-CD11b, anti-Ly-6C, anti-Ly-6G antibodies to quantitate peritoneal neutrophils.

Transmigration assay

Bone marrow cells or peritoneal cells harvested after thioglycollate stimulation were seeded into the top chamber of a modified Boyden chamber with 0.5 μ m pore size filter. The lower chamber included medium containing 10 nmol/L of CXCL1/KC or left untreated. Three hours later, all cells were collected and stained with anti-CD11b, anti-Ly-6C, anti-Ly-6G antibodies to quantitate neutrophil migration into the lower chamber by flow cytometry. Random neutrophil transmigration was subtracted from the CXCL1-treated chambers.

Staphylococcus aureus skin infection model

A USA 100, methicillin sensitive, spa type 002 *Staphylococcus aureus* clinical isolate (347) was grown in TSB medium (1.7% enzymatic digest of casein, 0.3% enzymatic digest of soybean meal, 0.5% NaCl, 0.25% K₂HPO₄, 0.25% dextrose, pH 7.3) overnight at 37°C at 200 rpm. Mid-logarithmic phase bacteria were obtained after 2.5 h subculture of a 1:100 dilution of the overnight culture. Bacterial cells were pelleted and resuspended in PBS. Spectrophotometric readings of absorbance at 600 nm were used to estimate bacterial concentration, and 20 μ L of *Staphylococcus aureus* at 5×10^7 colony forming units was used for inoculations. Mice were anesthetized with isoflurane, abdominal skin was shaved with Accuedge microtome blades (CardinalHealth, Dublin, OH) and exposed skin was gently stroked 15 times with 200 grit sandpaper. 20 μ L of bacterial suspension or PBS was applied to this surface and a gentle stream of air was aimed at the inoculation site until the inoculum suspension on the skin was dry. Finally, infected skin sites were covered with a Band Aid for 1 h.

The lesions and weight were recorded at day 0, 1, 3, 7, 10, 14 and 21 after infection. Digital photos of skin lesions were recorded and analyzed for lesion area using the Image J Software. Skin lesions were then carefully excised. Single-cell suspensions from infected skin were prepared by incubating with 0.6% trypsin for 90 min at 37°C. Trypsin-digested skin was then chopped into small pieces and incubated with 500 μ g/mL collagenase type II (Gibco BRL, Grand Island, NY, USA) for 90 min at 37°C and dissociated by passing through 16, 18 and 20 gauge needles. The resulting cell suspensions were incubated for an additional 90 min at 37°C to allow for recovery of surface antigens. All samples were passed through a 70 μ m filter and single cells were stained with a cocktail of antibodies including anti-CD45, anti-CD11b, anti-Ly-6C, anti-Ly-6G, anti-F4/80 antibodies and analyzed by flow cytometry. The total cell recovery of various populations was divided by the area of lesion skin and the resulting quotient was represented as cells/cm².

Microarray analysis

GEO datasets GSE2322 (Coldren et al., 2006) and GSE5772 (Tang et al., 2007) were downloaded. Expression levels of CD177 were analyzed and compared in different patient groups. GSE2322 contains 58 samples representing transcript profiles from neutrophils

under different *in vitro* and *in vivo* treatments. GSE5772 has 94 samples of neutrophil transcripts from patients without sepsis, or patients with infections of gram-negative, gram-positive or mixed bacterial infections.

Statistics

Statistical significance was determined using non-parametric Two-tailed Mann-Whitney test without assuming Gaussian distribution.

ACKNOWLEDGEMENTS

We sincerely thank Drs. Tang and Coldren for sharing the microarray datasets. The CD177 mouse strain used for this research project was created from an ES cell clone (12120a-B11) obtained from the KOMP Repository (www.komp.org) and generated by Regeneron Pharmaceuticals, Inc.

This work was supported by NIH grant CA158055 (W.Z.) and NIH T32 GM007337 (N.B.). Additionally, W.Z. was supported by departmental start up funds, and seed grants from the Department of Pathology at the University of Iowa Carver College of Medicine and from the American Cancer Society. G.H.L. was supported by the National Basic Research Program (973 Program) (Nos. 2015CB964800 and 2014CB964600), the Strategic Priority Research Program of the Chinese Academy of Sciences (XDA01020312), the National Natural Science Foundation of China (Grant Nos. 81271266, 31222039, 81330008, 31201111, and 81300677), Beijing Natural Science Foundation (7141005), and the Thousand Young Talents program of China, and State Key Laboratory of Drug Research (SIMM1302KF-17). Q.X. was supported by a scholarship from the China Scholarship Council.

COMPLIANCE WITH ETHICS GUIDELINES

Qing Xie, Julia Klesney-Tait, Kathy Keck, Corey Parlet, Nicholas Borchering, Ryan Kolb, Wei Li, Lorraine Tygrett, Thomas Waldschmidt, Alicia Olivier, Songhai Chen, Guang-Hui Liu, Xiangrui Li, and Weizhou Zhang declare that they have no conflict of interest.

This article does not contain any studies with human subjects performed by the any of the authors. For studies with animals, all institutional and national guidelines for the care and use of laboratory animals were followed.

OPEN ACCESS

This article is distributed under the terms of the Creative Commons Attribution License which permits any use, distribution, and reproduction in any medium, provided the original author(s) and the source are credited.

REFERENCES

Bayat B, Werth S, Sachs UJ, Newman DK, Newman PJ, Santoso S (2010) Neutrophil transmigration mediated by the neutrophil-specific antigen CD177 is influenced by the endothelial S536 N dimorphism of platelet endothelial cell adhesion molecule-1. *J Immunol* 184:3889–3896

- Bettinotti MP, Olsen A, Stroncek D (2002) The use of bioinformatics to identify the genomic structure of the gene that encodes neutrophil antigen NB1, CD177. *Clin Immunol* 102:138–144
- Bux J, Becker F, Seeger W, Kilpatrick D, Chapman J, Waters A (1996) Transfusion-related acute lung injury due to HLA-A2-specific antibodies in recipient and NB1-specific antibodies in donor blood. *Br J Haematol* 93:707–713
- Caruccio L, Bettinotti M, Matsuo K, Sharon V, Stroncek D (2003) Expression of human neutrophil antigen-2a (NB1) is increased in pregnancy. *Transfusion* 43:357–363
- Caruccio L, Bettinotti M, Director-Myska AE, Arthur DC, Stroncek D (2006) The gene overexpressed in polycythemia rubra vera, PRV-1, and the gene encoding a neutrophil alloantigen, NB1, are alleles of a single gene, CD177, in chromosome band 19q13.31. *Transfusion* 46:441–447
- Coldren CD, Nick JA, Poch KR, Woolum MD, Fouty BW, O'Brien JM, Gruber MP, Zamora MR, Svetkauskaite D, Richter DA et al (2006) Functional and genomic changes induced by alveolar transmigration in human neutrophils. *Am J Physiol Lung Cell Mol Physiol* 291:L1267–L1276
- Dillon M, Minear J, Johnson J, Lannutti BJ (2008) Expression of the GPI-anchored receptor Prv-1 enhances thrombopoietin and IL-3-induced proliferation in hematopoietic cell lines. *Leuk Res* 32:811–819
- Essilfie AT, Simpson JL, Horvat JC, Preston JA, Dunkley ML, Foster PS, Gibson PG, Hansbro PM (2011) Haemophilus influenzae infection drives IL-17-mediated neutrophilic allergic airways disease. *PLoS Pathog* 7:e1002244
- Geering B, Stoeckle C, Conus S, Simon HU (2013) Living and dying for inflammation: neutrophils, eosinophils, basophils. *Trends Immunol* 34:398–409
- Gohring K, Wolff J, Doppl W, Schmidt KL, Fenchel K, Pralle H, Sibelius U, Bux J (2004) Neutrophil CD177 (NB1 gp, HNA-2a) expression is increased in severe bacterial infections and polycythaemia vera. *Br J Haematol* 126:252–254
- Goldschmeding R, van Dalen CM, Faber N, Calafat J, Huizinga TW, van der Schoot CE, Clement LT, von dem Borne AE (1992) Further characterization of the NB 1 antigen as a variably expressed 56-62 kD GPI-linked glycoprotein of plasma membranes and specific granules of neutrophils. *Br J Haematol* 81:336–345
- Hsu LC, Enzler T, Seita J, Timmer AM, Lee CY, Lai TY, Yu GY, Lai LC, Temkin V, Sinzig U et al (2011) IL-1beta-driven neutrophilia preserves antibacterial defense in the absence of the kinase IKKbeta. *Nat Immunol* 12:144–150
- Jerke U, Rolle S, Dittmar G, Bayat B, Santoso S, Sporbert A, Luft F, Kettritz R (2011) Complement receptor Mac-1 is an adaptor for NB1 (CD177)-mediated PR3-ANCA neutrophil activation. *J Biol Chem* 286:7070–7081
- Kissel K, Santoso S, Hofmann C, Stroncek D, Bux J (2001) Molecular basis of the neutrophil glycoprotein NB1 (CD177) involved in the pathogenesis of immune thrombocytopenias and transfusion reactions. *Eur J Immunol* 31:1301–1309
- Kuckleburg CJ, Newman PJ (2013) Neutrophil proteinase 3 acts on protease-activated receptor-2 to enhance vascular endothelial cell barrier function. *Arterioscler Thromb Vasc Biol* 33:275–284
- Kuckleburg CJ, Tilkens SB, Santoso S, Newman PJ (2012) Proteinase 3 contributes to transendothelial migration of NB1-positive neutrophils. *J Immunol* 188:2419–2426

- Lalezari P, Murphy GB, Allen FH Jr (1971) NB1, a new neutrophil-specific antigen involved in the pathogenesis of neonatal neutropenia. *J Clin Invest* 50:1108–1115
- Li Y, Karlin A, Loike JD, Silverstein SC (2002) A critical concentration of neutrophils is required for effective bacterial killing in suspension. *Proc Natl Acad Sci U S A* 99:8289–8294
- Li Y, Karlin A, Loike JD, Silverstein SC (2004) Determination of the critical concentration of neutrophils required to block bacterial growth in tissues. *J Exp Med* 200:613–622
- Martini M, Teofili L, Larocca LM (2006) Overexpression of PRV-1 gene in polycythemia rubra vera and essential thrombocythemia. *Methods Mol Med* 125:265–273
- Matsuo K, Lin A, Procter JL, Clement L, Stroncek D (2000) Variations in the expression of granulocyte antigen NB1. *Transfusion* 40:654–662
- Michiels JJ, Bemema Z, Van Bockstaele D, De Raeye H, Schroyens W (2007) Current diagnostic criteria for the chronic myeloproliferative disorders (MPD) essential thrombocythemia (ET), polycythemia vera (PV) and chronic idiopathic myelofibrosis (CIMF). *Pathol Biol (Paris)* 55:92–104
- Ramirez-Velazquez C, Castillo EC, Guido-Bayardo L, Ortiz-Navarrete V (2013) IL-17-producing peripheral blood CD177 + neutrophils increase in allergic asthmatic subjects. *Allergy Asthma Clin Immunol* 9:23
- Sachs UJ, Andrei-Selmer CL, Maniar A, Weiss T, Paddock C, Orlova VV, Choi EY, Newman PJ, Preissner KT, Chavakis T et al (2007) The neutrophil-specific antigen CD177 is a counter-receptor for platelet endothelial cell adhesion molecule-1 (CD31). *J Biol Chem* 282:23603–23612
- Simpson JL, Grissell TV, Douwes J, Scott RJ, Boyle MJ, Gibson PG (2007) Innate immune activation in neutrophilic asthma and bronchiectasis. *Thorax* 62:211–218
- Simpson JL, Powell H, Boyle MJ, Scott RJ, Gibson PG (2008) Clarithromycin targets neutrophilic airway inflammation in refractory asthma. *Am J Respir Crit Care Med* 177:148–155
- Sirhan S, Lasho TL, Elliott MA, Tefferi A (2005) Neutrophil polycythemia rubra vera-1 expression in classic and atypical myeloproliferative disorders and laboratory correlates. *Haematologica* 90:406–408
- Stroncek DF (2007) Neutrophil-specific antigen HNA-2a, NB1 glycoprotein, and CD177. *Curr Opin Hematol* 14:688–693
- Stroncek DF, Jaszcz W, Herr GP, Clay ME, McCullough J (1998) Expression of neutrophil antigens after 10 days of granulocyte-colony-stimulating factor. *Transfusion* 38:663–668
- Stroncek DF, Caruccio L, Bettinotti M (2004) CD177: a member of the Ly-6 gene superfamily involved with neutrophil proliferation and polycythemia vera. *J Transl Med* 2:8
- Subramanian A, Tamayo P, Mootha VK, Mukherjee S, Ebert BL, Gillette MA, Paulovich A, Pomeroy SL, Golub TR, Lander ES et al (2005) Gene set enrichment analysis: a knowledge-based approach for interpreting genome-wide expression profiles. *Proc Natl Acad Sci U S A* 102:15545–15550
- Tang BM, McLean AS, Dawes IW, Huang SJ, Lin RC (2007) The use of gene-expression profiling to identify candidate genes in human sepsis. *Am J Respir Crit Care Med* 176:676–684
- Valenzuela DM, Murphy AJ, Frendewey D, Gale NW, Economides AN, Auerbach W, Poueymirou WT, Adams NC, Rojas J, Yasenchak J et al (2003) High-throughput engineering of the mouse genome coupled with high-resolution expression analysis. *Nat Biotechnol* 21:652–659
- Wang L, Ge S, Agustian A, Hiss M, Haller H, von Vietinghoff S (2013) Surface receptor CD177/NB1 does not confer a recruitment advantage to neutrophilic granulocytes during human peritonitis. *Eur J Haematol* 90:436–437

RESEARCH ARTICLE

Identification and Molecular Characterization of Microneme 5 of *Eimeria acervulina*

ZhenChao Zhang, JingWei Huang, MengHui Li, YuXia Sui, Shuai Wang, LianRui Liu, LiXin Xu, RuoFeng Yan, XiaoKai Song, XiangRui Li*

College of Veterinary Medicine, Nanjing Agricultural University, Nanjing, Jiangsu, PR China

*Lixiangrui@njau.edu.cn



CrossMark
click for updates

 OPEN ACCESS

Citation: Zhang Z, Huang J, Li M, Sui Y, Wang S, et al. (2014) Identification and Molecular Characterization of Microneme 5 of *Eimeria acervulina*. PLoS ONE 9(12): e115411. doi:10.1371/journal.pone.0115411

Editor: Paulo Lee Ho, Instituto Butantan, Brazil

Received: March 14, 2014

Accepted: November 23, 2014

Published: December 22, 2014

Copyright: © 2014 Zhang et al. This is an open-access article distributed under the terms of the Creative Commons Attribution License, which permits unrestricted use, distribution, and reproduction in any medium, provided the original author and source are credited.

Data Availability: The authors confirm that all data underlying the findings are fully available without restriction. All relevant data are within the paper.

Funding: This work was funded by a grant from the National Natural Science Foundation of P.R. China (No. 31372428) and a project funded by the Priority Academic Program Development of Jiangsu Higher Education Institutions (PAPD). The funders had no role in study design, data collection and analysis, decision to publish, or preparation of the manuscript.

Competing Interests: The authors have declared that no competing interests exist.

Abstract

In the present study, the microneme 5 gene of *Eimeria acervulina* (*E. acervulina*) (EaMIC5) was cloned and characterized. Specific primers for the rapid amplification of cDNA ends (RACE) were designed based on the expressed sequence tag (EST, GenBank Accession No. EH386430.1) to amplify the 3'- and 5'-ends of EaMIC5. The full length cDNA of this gene was obtained by overlapping the sequences of 3'- and 5'-extremities and amplification by reverse transcription PCR. Sequence analysis revealed that the open reading frame (ORF) of EaMIC5 was 336 bp and encoded a protein of 111 amino acids with 12.18 kDa. The ORF was inserted into pET-32a (+) to produce recombinant EaMIC5. Using western blotting assay, the recombinant protein was successfully recognized by the sera of chicks experimentally infected with *E. acervulina*, while the native protein in the somatic extract of sporozoites was as well detected by sera from rats immunized with the recombinant protein of EaMIC5. Immunofluorescence analysis using antibody against recombinant protein EaMIC5 indicated that this protein was expressed in the sporozoites and merozoites stages of *E. acervulina*. Animal challenge experiments demonstrated that the recombinant protein of EaMIC5 could significantly increase the average body weight gains, decrease the mean lesion scores and the oocyst outputs of the immunized chickens, and presented anti-coccidial index (ACI) more than 160. All the above results suggested that the EaMIC5 was a novel *E. acervulina* antigen and could be an effective candidate for the development of a new vaccine against this parasite.

Introduction

E. acervulina is one of the seven *Eimeria* spp which infect the chicken. This parasite infects the intestinal epithelial cells of chicken and can cause intense damage to duodenum, result in malabsorption and poor feed utilization, and reduced body weight gain [1–3]. Chicken coccidiosis exists worldwide and is economically the most important parasitic disease of the poultry industry. So far, the main measures of controlling *Eimeria* infection are applications of anti-coccidial drugs and live vaccines. However, the emergence of drug resistance, the potential reversion to virulence and high production expenses of live vaccines have driven the developments of new control strategies [4].

Recent efforts are committed to find recombinant antigen or DNA vaccines against coccidiosis [5–7]. Some studies have proved that the recombinant antigen or DNA vaccines can induce both humoral and cell-mediated immune responses [8–10]. Meanwhile, cytokines as adjuvants have been considered to enhance the potential of DNA vaccines or recombinant antigen to induce broad and long-lasting humoral and cellular immunity [11, 12].

Microneme organelles are present in all apicomplexan protozoa and contain proteins critical and multifunctional for parasite motility and host cell invasion [13]. So far, nine microneme proteins have been reported in *Eimeria*. They are microneme protein 1–7 (MIC1–7) and apical membrane antigen 1, 2 (AMA1,2) [14]. The functions of MICs during host cell invasion suggest they might be potential candidates for vaccines development against the infection of *Eimeria*. The gene sequences of *E. tenella* MIC1 (AF032905.1), MIC2 (KC333870.1), MIC3 (AY512382.1), MIC4 (AJ306453.2), MIC5 (AJ245536.1) and AMA1 (JN032081.1), *E. maxima* MIC2 (FR718971.1), MIC3 (FR718972.1), MIC5 (FR718974.1) and MIC7 (FR718975.1) and *E. necatrix* MIC5 (EU335049.1) were published in GenBank.

The EtMIC5 is a micronemal glycoprotein and has eleven cysteine-rich receptor-like regions with striking similarity to the Apple domains (A-domains) of the binding regions of blood coagulation factor XI (FXI) [15] and plasma prekallikrein (PK) [16]. When sporozoites were in contact with host cell, EtMIC5 was secreted by the sporozoite [17]. Saouros et al [18] demonstrated the C-terminal region of TgMIC5, the MIC5 of *Toxoplasma gondii*, was responsible for inhibition of TgSUB1, while Periz et al [19] suggested EtMIC4 and EtMIC5 formed an oligomeric, ultrahigh molecular mass protein complex that interacted with target host cells during invasion.

Until now, few genes of *E. acervulina* have been reported and tested for their immunogenicity, and no MIC of it is reported and characterized although there is EST in GenBank.

In this study, the gene of EaMIC5 was obtained, characterized and the immunogenicity of the recombinant protein of EaMIC5 was checked through chicken challenge experiments.

Materials and Methods

Animals and parasites

New-hatched Chinese Yellow chickens were reared in clean brooder cages under coccidian-free conditions and were screened periodically for their *Eimeria* infection status by microscopic examination of feces. The birds were provided with coccidiostat-free feed and water ad libitum. The birds were shifted to animal containment facility prior to challenge with virulent oocysts. The study was conducted following the guidelines of the Animal Ethics Committee, Nanjing Agricultural University, China. All experimental protocols were approved by the Science and Technology Agency of Jiangsu Province. The approval ID is SYXK (SU) 2010-0005.

E. acervulina JS strain was propagated and maintained in the Laboratory of Veterinary Parasite Disease, Nanjing Agricultural University, China. Sporulated oocysts of *E. acervulina* JS strain were stored in 2.5% potassium dichromate solution at 4°C and passed through chickens every 5 months interval.

Sporozoites from *E. acervulina* oocysts were purified on DE-52 anion-exchange columns using a protocol described previously [20]. *E. acervulina* merozoites were harvested from the duodenal loops of chickens 54 h post-infection (p.i.) and purified using standard methods [21, 22] before being pelleted and frozen in liquid nitrogen.

Soluble antigens of *E. acervulina*

A total of 5×10^9 *E. acervulina* sporozoites were washed three times by centrifugation with 0.1 M PBS (pH 7.2) at $2000 \times g$ for 10 min at 4°C. The pellet was dissolved respectively in 2 ml of PBS and PBS containing 0.5% TritonX-100 and was disrupted by ultrasound in ice bath (200 W, work time 5 s, interval time

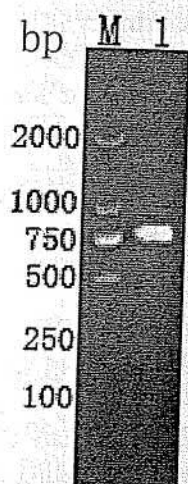


Fig. 1. The ORF of EaMIC5 PCR. (Lane M) DNA Mark (ordinate values in bp); (Lane 1) the ORF of EaMIC5.

doi:10.1371/journal.pone.0115411.g001

10 s, 50 cycles). After high-speed centrifugation, the supernatant proteins were separated and estimated spectrophotometrically, adjusted to 1 mg/ml with PBS and stored at -20°C until to be used.

The soluble antigen dissolved by PBS containing Triton X-100 was used for western blot to analyze the native protein of the EaMIC5.

Cloning of EaMIC5 gene

RNA extraction

Total RNA was extracted from *E. acervulina* sporozoites using TRIZOL reagent (TaKaRa) according to the manufacturer's instructions. RNA samples were resuspended in diethyl pyrocarbonate (DEPC) treated water in the presence of ribonuclease inhibitor (TaKaRa). All RNA samples were treated with RNase-free DNase I (TaKaRa) before processing reverse transcription to eliminate genomic DNA contamination. The quantity of RNA was estimated by measuring the optical density at 260 nm (OD_{260}) using a spectrophotometry and the quality was determined by $\text{OD}_{260}/\text{OD}_{280}$ ratio. The samples with ratio $\text{OD}_{260}/\text{OD}_{280}$ between 1.9 and 2 were used.

3'- and 5'-rapid amplification of cDNA ends

A 3'-end of the cDNA was amplified by 3'-full RACE kit (TaKaRa Biotech, Dalian, PR China) using the forward gene specific primers EaMIC5-3-F1 and EaMIC5-3-F2 (Table 1) designed based on EaMIC5 EST (GenBank Accession No. EH386430.1) in combination with the 3' outer and 3' inner primers provided in the RACE kit (Table 1). The primary PCR system and condition were set as the manufacturer's protocol described. The EaMIC5 3'-end fragment was then obtained and sequenced.

The 5'-end of the cDNA was amplified by 5'-RACE PCR using the same method as the 3'-RACE PCR. The primary PCR was performed using EaMIC5-5-R1 and 5' outer primer, with EaMIC5-5-R2 and 5' inner primer in the Nest PCR.

Both of the products of the second PCRs for 3'-end and 5'-end were cloned into the pMD18-T vector (TaKaRa Biotech, Dalian, PR China) and sequenced by Invitrogen Biotech (Shanghai, PR China).

All oligonucleotides used in this research were synthesized by Invitrogen Biotechnology Co. Ltd. (Shanghai, PR China).

The amplification of the EaMIC5 ORF

The complete sequence of the EaMIC5 cDNA was deduced from the overlapping sequences of both 3'-end and 5'-end amplification products using BioEdit Version 7.0.1 (T.A. Hall, North Carolina State University, USA). Open Reading Frame Finder (ORF Finder) was used to predict the ORF of MIC5. The ORF was amplified from cDNA of sporozoites by PCR with the following restriction enzyme-anchored (underlined) and protective bases-anchored primers (*EcoRI* anchored forward primer, 5'-CCGGAATTCGAGCTCTGCTACAAACACCCG-3',

Table 1. Oligonucleotide primer sequences used for PCR in this research.

Name	Sequences (5'-3')	Description
EaMIC5-3-F1	ATCCAGATACTTTGCCTTGTTTT	Forward primer specific for 3'-end of EaMIC5 in primary PCR
EaMIC5-3-F2	ACATCGGGTGTGGTAGCAGA	Forward primer specific for 3'-end of EaMIC5 in second PCR
3'outer primer	TACCGTCGTTCCACTAGTGATTT	Reverse primer for 3'-end of EaMIC5 in primary PCR (in RACE kit)
3'inner primer	CGCGGATCCTCCACTAGTGATTTCACTATAGG	Reverse primer for 3'-end of EaMIC5 in second PCR (in RACE kit)
EaMIC5-5-R1	AACCTCCTCAAGACTATTCCG	Reverse primer specific for 5'-end of EaMIC5 in primary PCR
EaMIC5-5-R2	ATGCCAATACGAGAGCAACTG	Reverse primer specific for 5'-end of EaMIC5 in second PCR
5'outer primer	CATGGCTACATGCTGACAGCCTA	Forward primer for 5'-end of EaMIC5 in primary PCR (in RACE kit)
5'inner primer	CGCGGATCCACAGCCTACTGATGATCAGTCGATG	Forward primer for 5'-end of EaMIC5 in second PCR (in RACE kit)
EaMIC5F	CCGGAATTC GAGCTCTGCTACAAACACCCG	Forward primer containing an <i>EcoRI</i> site for cloning into pET32a-EaMIC5
EaMIC5R	CCCAAGCTT GCCGTTATTAATGCATGCG	Reverse primer containing a <i>HindIII</i> site for cloning into pET32a-EaMIC5

doi:10.1371/journal.pone.0115411.t001

HindIII anchored reverse primer, 5'-CCCAAGCTT GCCGTTATTAATGCATGCG-3'). PCR products were cloned into pMD18-T vector (TaKaRa Biotech, Dalian, PR China) and transformed into *E. coli* (DH5a) competent cells (Invitrogen). Recombinant pMD18-T-MIC5 clone was identified by PCR amplification and endonuclease digestion. Three positive clones were further confirmed by sequence analysis. The complete nucleotide sequence data inserted in recombinant plasmid was analyzed for homology to known sequences in GenBank databases using a basic alignment search tool (BLAST) (<http://www.ncbi.nlm.nih.gov/BLAST/>).

All oligonucleotides used in this research were synthesized by Invitrogen Biotechnology Co. Ltd. (Shanghai, PR China).

Sequence analysis

Sequence similarity was studied using the BLASTP and BLASTX (<http://www.blast.ncbi.nlm.nih.gov/Blast.cgi>). Microneme protein sequences were aligned using CLUSTALW1.8. The signal peptide, secondary structure and protein motifs were predicted using approaches accessible on the Internet: SignalP (<http://www.cbs.dtu.dk/services/SignalP/>), TMHMM (<http://www.cbs.dtu.dk/services/TMHMM/>), GPI Modification Site Prediction (http://mendel.imp.ac.at/sat/gpi/gpi_server.html), PSIPred (<http://www.bioinf4.cs.ucl.ac.uk:3000/psipred/>), Motifscan (http://www.myhits.isb-sib.ch/cgi-bin/motif_scan), respectively.

Expression and purification of MIC5 recombinant protein and pET-32a protein

The identified recombinant plasmid pMD18-T-MIC5 was digested with *EcoRI* and *HindIII*. The target fragment of MIC5 was purified and cloned into frame of digested expression vector pET-32a (+) (Novagen, USA) to generate plasmid pET-32a-MIC5. The recombinant plasmid was sequenced to confirm that the MIC5 insert was in the proper reading frame. The correct recombinant pET-32a-MIC5

plasmid was transferred into competent *E. coli* BL21 (DE3) cells and the recombinant protein expression in *E. coli* was induced by addition of 0.8 mM Isopropyl- β -D-thiogalactopyranoside (IPTG; Sigma-Aldrich, USA) to the cell culture after the OD₆₀₀ of the culture reached 0.6 at 37°C. The cells were incubated at 37°C for 5 h and harvested by centrifugation after the addition of IPTG. The cell pellet was lysed using lysozyme (10 μ g/ml) (Sigma-Aldrich, USA) followed by sonication and then the cell lysates were analyzed by 12% (w/v) sodium dodecyl sulfate polyacrylamide gel electrophoresis (SDS-PAGE).

The recombinant protein was purified by Ni²⁺-nitrilotriacetic acid (Ni-NTA) column (GE Healthcare, USA) according to the manufacturer's instructions. Purity of the protein was detected by 12% SDS-PAGE and refolded by renaturation buffer (20 mmol/L Tris-Cl, 500 mmol/L NaCl, 1 mmol/L GSH, 0.1 mmol/L GSSG, pH 8.0) containing different concentrations of urea (8, 6, 4, 2, 0 mol/L). The concentration of refolded protein was determined according to the Bradford procedure [23], using bovine serum albumin (BSA) as a standard. The protein was stored at -20°C for later use.

The pET-32a protein was obtained by induction of *E. coli* BL21 transformed with pET-32a (+) plasmid using the same methods to the recombinant protein.

Antisera against recombinant MIC5 protein and against *E. acervulina*

To generate polyclonal antibodies, about 0.3 mg of the purified recombinant MIC5 protein were mixed with Freund's complete adjuvant as a 1:1 mixture and injected into SD rats (Qualified Certificate: SCXK 2008-0004; Experimental Animal Center of Jiangsu, PR China) subcutaneously in multiple places. Two weeks later, a booster was given in the same conditions by using protein which was mixed with Freund's incomplete adjuvant as a 1:1 mixture. And then, the rats were re-boostered three times at intervals of 1 week. Finally, the serum was collected and stored until used. Sera collected before protein injection were used as negative sera [24].

The antisera against *E. acervulina* (chicken antisera) were collected from chickens experimentally infected with *E. acervulina* 1 week post-infection.

Immunoblotting analysis for the recombinant and native EaMIC5

Samples including crude somatic extracts of *E. acervulina* sporozoites and the recombinant protein of MIC5 were separated by SDS-PAGE. Then the proteins were transferred to nitrocellulose membrane (Millipore, USA). After being blocked with 5% (w/v) skimmed milk powder in TBS (Tris-buffer saline)-Tween 20 (TBST), the membranes were incubated with the primary antibody (rat antisera and chicken antisera, respectively) for 1 h at 37°C (dilutions 1:100 to rat antisera, 1:100 to chicken antisera). Then the membranes were washed 3 times and were incubated with horseradish peroxidase (HRP)-conjugated goat anti-rat IgG and HRP-conjugated donkey anti-chick IgG (Sigma, USA) at 37°C for 1 h,

Table 2. Effects of recombinant EaMIC5 protein against *E. acervulina* challenge on different parameters.

Groups	Average body weight gains (g)	Mean lesion scores (difference in rank sum)	Oocyst out (fg) (mean \pm SD)put	Oocyst decrease ratio(%)	Anti-coccidial index
Unchallenged control	140.07 \pm 1.27 ^a	0 ^a	— ^a	100 ^a	200
pET-32a protein control	68.95 \pm 4.51 ^c	98.57 ^c	5.43 \pm 0.02 ^c	1.26 ^c	82.64
PBS control	68.24 \pm 4.61 ^c	101.8 ^c	5.43 \pm 0.02 ^c	1.50 ^c	81.03
Recombinant MIC5 protein	121.55 \pm 2.81 ^b	49.23 ^b	4.88 \pm 0.03 ^b	72.26 ^b	161.24
Challenged control	67.27 \pm 4.37 ^c	104.4 ^c	5.44 \pm 0.03 ^c	0.00 ^c	79.86

Note: in each column, significant difference ($p < 0.05$) between means and ranks with different letters and no significant difference ($p > 0.05$) between means and ranks with the same letter; the oocyst output was zero (designated as "—") in the unchallenged control group.

doi:10.1371/journal.pone.0115411.t002

respectively. Finally, the bound antibody was detected using 3,3'-diaminobenzidine tetrahydrochloride (DAB) kit (Boster Bio-technology) according to the manufacturer's instructions.

Expression analysis of EaMIC5 in sporozoite and merozoite of *E. acervulina* by immunofluorescence

Purified sporozoites and merozoites were smeared and air-dried on a poly-L-lysine treated glass slide before fixation. Sporozoites and merozoites were fixed with 4% paraformaldehyde in TBS for 10 min at RT, permeabilized with 1% TritonX-100 in TBS for 10 min, washed 3 times in TBS containing 0.05% Tween-20 (TBST), and blocked with TBST containing 5% (w/v) BSA for 2 h at 37°C. After 3 times washing in TBST, rat antisera against EaMIC5 (1:100 dilution) were added respectively and allowed to incubate at 4°C overnight. After 3 washes in TBST, the coverslips were maintained in darkness for 40 min in goat anti-rat IgG antibody (Beyotime) labeled with Cy3 diluted at 1:1000. After washing with TBST, fluorescent mounting medium (Beyotime) was added and cells were examined by fluorescent microscopy (Olympus).

Immunization and challenge infection

Two-week-old chickens were randomly divided into five groups of 30 each as shown in Table 2 according to the permission for inoculating the chickens with the recombinant protein vaccine issued by the Animal Care and Ethics Committee of Nanjing Agricultural University. Experimental group was inoculated with 200 μ g EaMIC5 recombinant protein without any adjuvant, the pET-32a protein control group was given 200 μ g of pET-32a protein without adjuvant, and the PBS control group was given the same volume of PBS alone each chicken at the same injection site. The chickens of challenged control and unchallenged control groups were not injected. A booster immunization was given 1 week later with the same amount of components as the first immunization. Seven days post second injection, the chickens in each group except the unchallenged control group were

challenged orally with 1.2×10^5 sporulated oocysts of *E. acervulina*. Unchallenged control chickens were given PBS orally. All of the chickens were euthanized following protocols approved by the Animal Care and Ethics Committee of Nanjing Agricultural University to determine the effects of immunization on the 6th day post-challenge.

Evaluation of immune protection

The efficacy of immunization was evaluated on the basis of lesion score, body weight gain, oocyst output, oocyst decrease ratio and anti-coccidial index (ACI) [25, 26]. Body weight gain of chickens in each group was determined by weighing the chickens at the end of the experiments subtracting the body weight at the time of challenge. Lesion scores were observed and recorded according to the system described by Reid and Johnson [27]. The duodenal content for each group was collected separately and oocysts per gram of content (OPG) were determined using McMaster's counting technique. Oocyst decrease ratio was calculated as described by Rose and Mockett [28] and Talebi and Mulcahy [29] as follows: (the number of oocysts from the challenged control chickens – vaccinated chickens)/the challenged control chickens $\times 100\%$.

ACI was a synthetic criterion for assessing the protective effect of a medicine or vaccine and calculated as follows: (survival rate + relative rate of weight gain) – (lesion value + oocyst value). Whereas, survival rate was estimated by the number of surviving chickens divided by the number of initial chicken. Relative rate of weight gain of the chickens in each group was determined by subtracting the body weight of the chickens at the time of challenge from the body weight at the end of the experiments. Lesion score of the chickens from each group was investigated according to the method of Johnson and Reid [27] and oocyst value was calculated using the formula described by Peek and Landman [30, 31]. According to Merck Sharp & Dohme Company Ltd [32], ACI value of ≥ 180 was considered high performance, ACI value of 160–179 was considered as effective, and ACI value of < 160 was considered as ineffective.

Determination of serum antibody level and cytokine concentration

Preparation of the serum

Two-week-old chickens were randomly divided into three groups of 10 chickens each. The chickens in groups were respectively immunized with 200 μg recombinant protein of EaMIC5 without any adjuvant, pET-32a protein and the same PBS volume. One week later, a booster immunization was given with the same amount of components as the first immunization. After 10 days of booster immunization, the blood sample was collected, incubated at 37°C for 1 h and centrifugated at 5000 rpm for 5 min at 4°C to isolate the serum. The sera were used for the detection of antibody, cytokines and serum CD4, CD8.

Determination of serum antibody level by enzyme-linked immunosorbent assay (ELISA)

The IgG antibody levels against EaMIC5 in the serum samples were determined by ELISA as described previously [33]. Briefly, flat-bottomed 96-well plates (Maxi-Sorp, Nunc, Denmark) were coated overnight at 4°C with 100 µl solution per well of recombinant EaMIC5 (50 µg/ml) in 0.05 M carbonate buffer, pH 9.6. The plates were washed with 0.01 M PBS containing 0.05% Tween-20 (PBS-T) and blocked with 5% skim milk powder (SMP) in PBS-T for 2 h at 37°C. The plates were incubated for 2 h at 37°C with 100 µl of the serum samples diluted 1:50 in PBS-T with 1% SMP in duplicate. After three washes, the plates were incubated for 1 h at room temperature with 100 µl/well of horseradish peroxidase-conjugated donkey anti-chicken IgG anti-body (Sigma) diluted 1:1000 in 2% SMP in PBS-T. Color development was carried out with 3,3',5,5'-tetramethylbenzidine (TMB) (Sigma), and the optical density at 450 nm (OD₄₅₀) was determined with a microplate spectrophotometer. All serum samples were investigated by ELISA at the same time under the same conditions and were included on one plate.

Determination of serum CD4, CD8 and cytokine concentrations

The concentration of soluble cluster of differentiation 4 (sCD4), soluble cluster of differentiation 8 (sCD8), interferon-γ (IFN-γ), interleukin-4 (IL-4), interleukin-10 (IL-10), interleukin-17 (IL-17), and tumor growth factor-β (TGF-β) in serum were detected by utilizing an indirect ELISA with the "chick cytokine ELISA Quantitation Kits" (catalog numbers: CSB-E13114C, CSB-E14317C, CSB-E08550Ch, CSB-E06756Ch, CSB-E12835C, CSB-E0467Ch, and CSB-E09875Ch for sCD4, sCD8, IFN-γ, IL-4, IL-10, IL-17 and TGF-β respectively; CUSABIO, China) in duplicate, according to manufacturer's instructions.

Statistical analysis

One way analysis of variance (ANOVA) with Duncan's multiple range tests were used for the determination of statistical significance by using the SPSS statistical package (SPSS for Windows 16, SPSS Inc., Chicago, IL, USA) after all data in this paper was test by Levene (F)-Test by using SPSS. Differences among groups were tested and $p < 0.05$ was considered to indicate a significant difference.

Results

Cloning and sequence analysis of EaMIC5

By overlapping the 3'- and 5'-RACE fragments, a transcript of 877 bp was obtained, which have been submitted to NCBI (GenBank Accession No. KF922373). A 178 bp 5'-untranslated region (5'-UTR) was detected before the ATG initiation codon and a 336 bp open reading frame (ORF) (Fig.1) was found that terminated with the TAA stop codon. On the 3'-end, the cDNA had a 363 bp 3'-UTR in the frame. By analysis with the sequence, the ORF was found to encode a protein of 111 amino acids with a molecular mass of 12.18 kDa. The

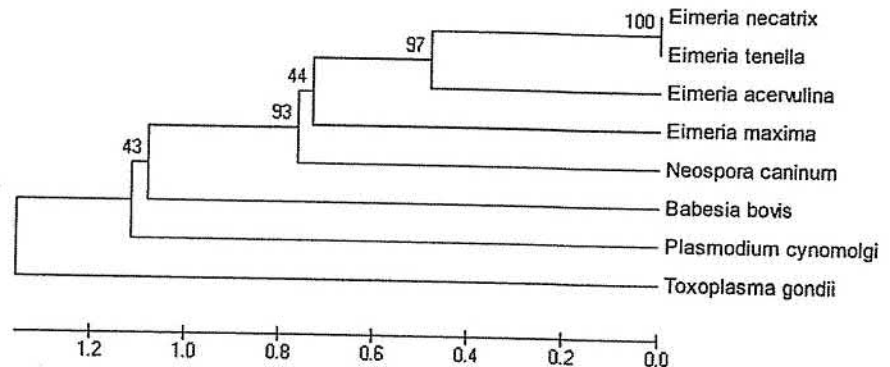


Fig. 2. The phylogenetic tree of amino acid sequences between EaMIC5 and those of MIC5 from other species.

doi:10.1371/journal.pone.0115411.g002

theoretical pI of the protein was 9.44. No signal peptide, GPI anchor and transmembrane domain were found in the deduced protein, but one O-glycosylation site and twelve phosphorylation sites could be detected. The protein had six hydrophilicity regions including 7–17, 24–35, 38–56, 59–76, 82–90 and 96–111, and four high antigenic index and consecutive regions including 9–23, 25–57, 69–77 and 83–111. It also contained two Apple Factor XI like-regions.

EaMIC5 multiple sequence alignment and cladogram

When compared with the known microneme nucleotide and protein sequences on the NCBI database (<http://www.blast.ncbi.nlm.nih.gov/blast.cgi/>) and on the GeneDB database (http://www.genedb.org/blast/submitblast/GeneDB_Eacervulina), the identity of EaMIC5 nucleotide sequence was 99% to *E. acervulina* hypothetical protein (EAH_00034850.1) and 60% to *E. acervulina* hypothetical protein (EAH_00013920.1) in GeneDB, and was lower than 15% to any other nucleotide sequence in NCBI. The amino acid sequence of EaMIC5 had 100% homology to the C-terminus of *E. acervulina* hypothetical protein (CDI78535.1) in NCBI. It also had 89% identity to *E. acervulina* hypothetical protein (EAH_00034850.1) in GeneDB, 42% identity to *E. necatrix* microneme protein 5 (ABY53156.1) and 40% identity to *E. tenella* microneme protein 5 (CAB52368.1) in NCBI. The phylogenetic tree of amino acid sequences was built by using MEGA4.0 and the result of cladogram (Fig. 2) showed that the kinship of EaMIC5 protein between *Eimeria* spp was highly related when compared with other species (*Neospora caninum*, *Babesia bovis*, *Plasmodium cynomolgi*, *Toxoplasma gondii*) of apicomplexan parasites.

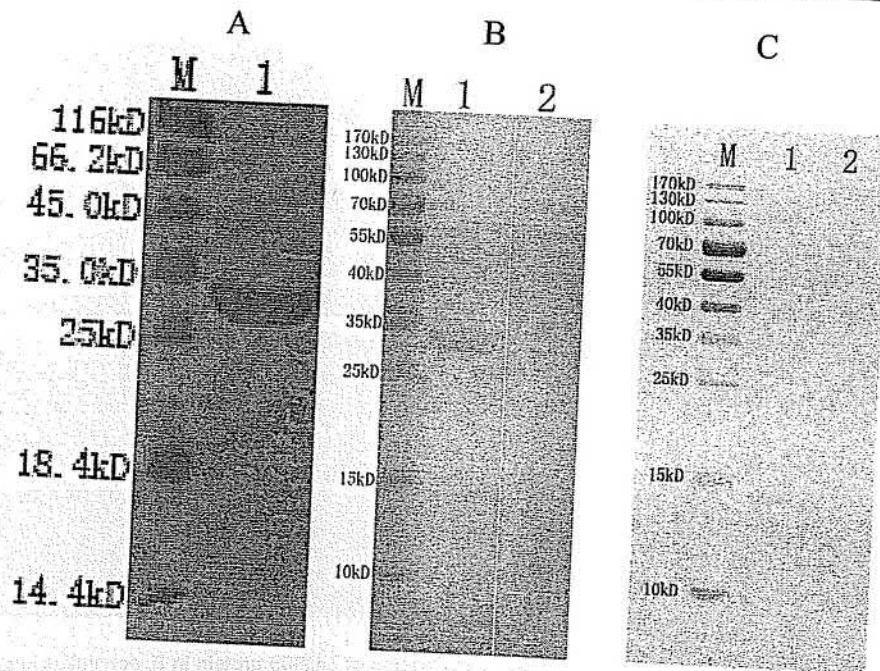


Fig. 3. A: SDS-PAGE of recombinant protein purified. (Lane M) protein Mark (ordinate values in kDa); (Lane 1) MIC5 protein; B: Immunoblot for the recombinant EaMIC5. (Lane M) protein Mark (ordinate values in kDa); (Lane 1) Recombinant protein MIC5 probed by serum from chickens experimentally infected with *E. acervulina* as primary antibody; C: Immunoblot for crude somatic extracts of *E. acervulina* sporozoites. (Lane M) protein Mark (ordinate values in kDa); (Lane 1) crude somatic extracts of *E. acervulina* sporozoites probed by serum of normal rat without immunizing as primary antibody. (Lane 2) crude somatic extracts of *E. acervulina* sporozoites probed by serum of normal rat immunized by EaMIC5.

doi:10.1371/journal.pone.0115411.g003

Expression, purification and renaturation of recombinant EaMIC5
 SDS-PAGE showed that the recombinant protein was mostly found in the sonicated bacteria inclusion bodies. After purification from the inclusion bodies by chromatography on the Ni-NTA and renaturation, the protein was seen as a single band with the molecular mass 30 kDa on the SDS-PAGE gel (Fig.3A). Subtracted the 18 kDa fused protein in the vector, the recombinant protein molecular weight was consistent with the deduced size of 12.18 kDa.

Immunoblot for the recombinant and native protein of EaMIC5
 The results of the immunoblot assay indicated that the recombinant EaMIC5 protein was recognized by immune sera of chickens infected with *E. acervulina*, but could not be recognized by the serum of normal chickens (Fig.3B). Western blot analysis also showed that rat anti-EaMIC5 antiserum recognized the native EaMIC5 as a band of about 14 kDa in the somatic extract of *E. acervulina* sporozoites (Fig.3C), slightly larger than the deduced one.

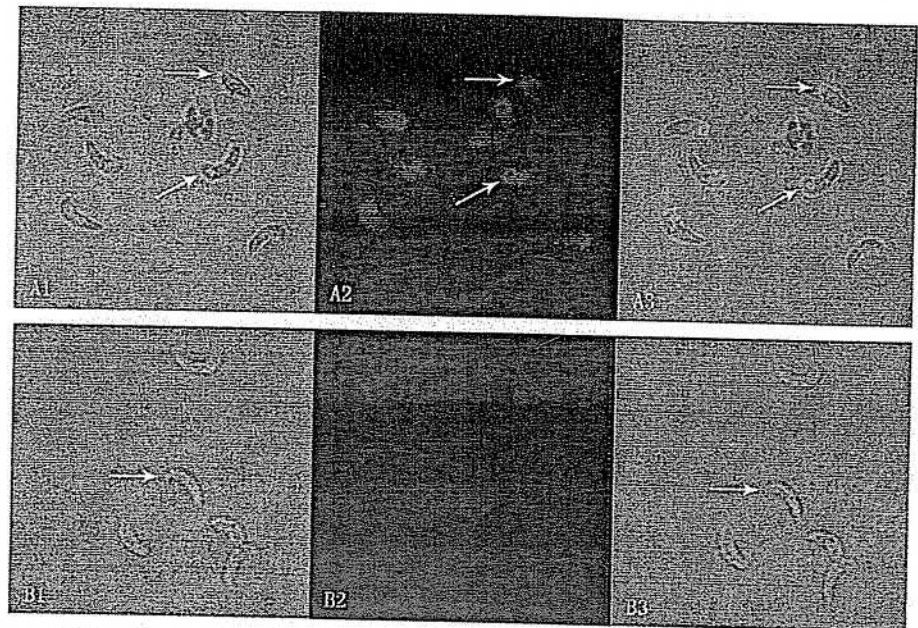


Fig. 4. Expression of EaMIC5 protein in *E. acervulina* sporozoites by immunofluorescence assay ($\times 100$ magnification). Panel A: *E. acervulina* sporozoites. The white arrows indicate sporozoites. (A1) Differential interference contrast (DIC). (A2) Immunofluorescence localization using Cy3. (A3) DIC and Immunofluorescence combined. Panel B: Negative control, the sporozoites were probed by serum of normal rat without immunizing as primary antibody. (B1) DIC. (B2) Cy3. (B3) Combined.

doi:10.1371/journal.pone.0115411.g004

Expressions of EaMIC5 in sporozoites and merozoites

Using anti-rEaMIC5 serum, EaMIC5 protein expression was investigated in sporozoites (Fig.4) and merozoites. The results showed that greater staining intensity was seen in sporozoites but in case of the merozoites the staining intensity was weak. No staining was seen in the negative control sections.

Protective effects of vaccination on *E. acervulina* challenge

The immunization efficacies of EaMIC5 are described in Table 2. No chicken died from coccidial challenge in any group in this study. Body weight gains were significantly reduced in challenged control group, PBS control group and pET-32a protein control group compared with unchallenged control group ($p < 0.05$). Chickens immunized with recombinant EaMIC5 protein displayed significantly enhanced weight gains relative to chickens in challenged control group, PBS control group and pET-32a protein control group ($p < 0.05$). The oocyst counts of EaMIC5 immunized chickens were significantly lower than that of challenged control group, PBS control group and pET-32a protein control group ($p < 0.05$). Significant alleviations in duodenal lesions were observed in EaMIC5 immunized chickens compared to that of challenged control group, PBS control group and pET-32a protein control group ($p < 0.05$). Group of chickens immunized with recombinant protein resulted in ACI more than 160.

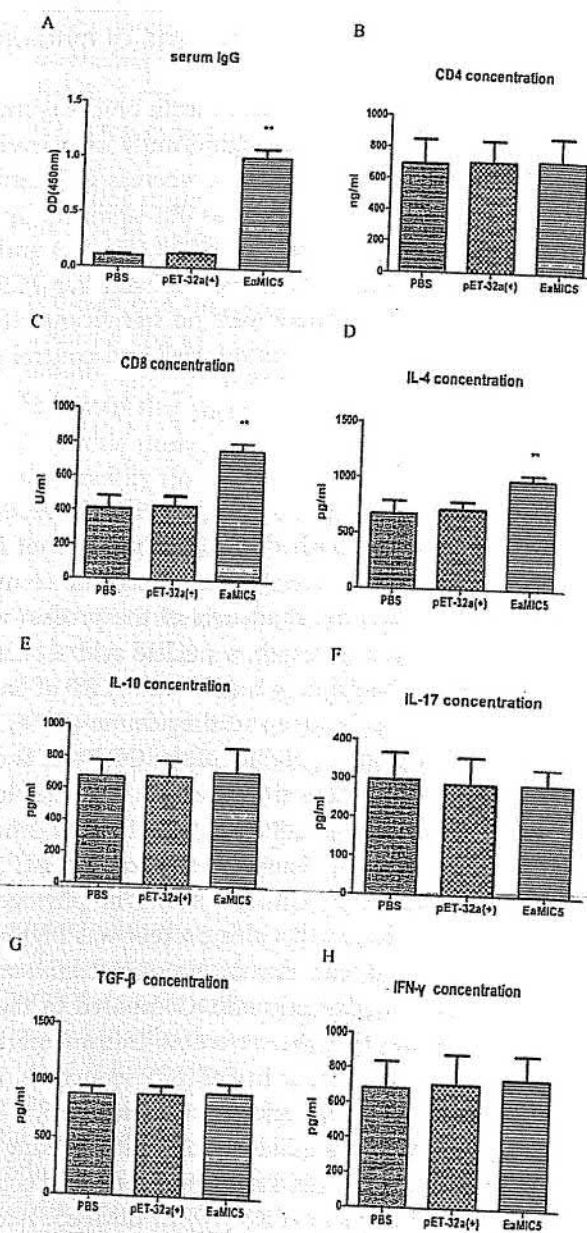


Fig. 5. Serum EaNIC5-specific IgG, the concentrations of CD4, CD8 and cytokine levels in chickens. Chickens were immunized intramuscularly with PBS (negative control), pET-32a protein (pET-32a control), recombinant EaNIC5 protein. The IgG titers and the concentration CD4, CD8 and cytokine are expressed as mean \pm SD with respect to absorbance at 450 nm. One star on the bar is slightly different from others, and two stars are significantly different ($p < 0.05$), otherwise no different ($p > 0.05$). A: IgG; B: CD4; C: CD8. D: IL-4; E: IL-10; F: IL-17; G: TGF- β and H: IFN- γ .

doi:10.1371/journal.pone.0115411.g005

IgG titers and concentrations of cytokines, CD4 and CD8 in sera of immunized chickens

As depicted in Fig. 5A, serum from chickens immunized with recombinant EaMIC5 protein showed significantly high level of IgG antibody ($p < 0.05$) compared to that of controls, whereas IgG antibody of chicken immunized with pET-32a protein and PBS was not significantly induced ($p > 0.05$). Meanwhile significantly higher levels of sCD8 (Fig. 5C) and IL-4 (Fig. 5D) were observed in chickens immunized with recombinant EaMIC5 protein compared to the control groups ($p < 0.05$). There were no significant differences of the sCD4 and other cytokines between the immunized and control groups.

Discussion

So far, complete sequences of MIC5 of *E. tenella* [17], *E. necatrix* and *E. maxima* [34] have been published in NCBI, but none of *E. acervulina* has been reported. In this research, we successfully obtained the complete sequence of MIC5 of *E. acervulina* and some characters of the protein were clarified.

In our current research, a nucleic acid sequence of 877 bp was obtained by RACE using the primers based on the EST of EaMIC5 in GenBank. This sequence contained a 336 bp open reading frame (ORF). The molecular mass of the deduced translation product of the ORF was about 12.18 kDa. The ORF included the start codon at the site 179–181 and the stop codon at the site 512–514. Compared with the sequences of MIC 5 of other *Eimeria* spp, the product was found to have 42% identity to *E. necatrix* MIC 5 (ABY53156.1) and 40% identity to *E. tenella* MIC 5 (CAB52368.1). The phylogenetic analysis of amino acid sequences indicated that this protein was highly related to the MIC 5 of *Eimeria* when compared with that of *Neospora caninum*, *Babesia bovis*, *Plasmodium cynomolgi*, *Toxoplasma gondii*. Compared to the EtMIC5 sequences published [17], we found that there were no transmembrane region and signal region for GPI anchor attachment in EaMIC5 sequences. BLASTP analysis revealed two Apple Factor XI like regions in the EaMIC5, which were similar to the eleven cysteine-rich receptor-like regions with striking similarity to the Apple domains (A-domains) of the binding regions of blood coagulation factor XI (FXI) [15] and plasma pre-kallikrein (PK) [16] in EtMIC5. According to Brown et al [17] and Saouros et al [18], EaMIC5, similar to EtMIC5 and TgMIC5, was located mainly at the apical tip of the sporozoite. In the current research, immunofluorescence analysis using serum against the recombinant protein showed that the native protein of EaMIC5 also mainly located at the apical end of the sporozoite. All of the above results suggested that the gene we obtained should be the MIC5 of *E. acervulina*. However, we found that TgMIC5, EtMIC5, EmMIC5 and EnMIC5 were larger than EaMIC5 in size and, compared to TgMIC5, the MIC5 proteins of *Eimeria* had no leader peptide. This indicated that MIC5s of different species might be different in size.

We found that EaMIC5 also had 100% homology to the C-terminus of *E. acervulina* hypothetical protein (CDI78535.1). However, the relationship between EaMIC5 and this hypothetical protein and whether the MIC5 was truncated from the same gene to the hypothetical protein in *E. acervulina* need to be further researched.

In this study, the sera against recombinant EaMIC5 recognized a band of about 14 kDa in the somatic extract of *E. acervulina* sporozoites. It indicated that the native EaMIC5 was 14 kDa in size. Comparison of the native EaMIC5 with the deduced one suggested that the native EaMIC5 was slightly larger than the deduced one of 12.18 kDa. It might be resulted from post-translational modification, such as glycosylation and phosphorylation. The sequence analysis indicated that there were glycosylation and phosphorylation sites in EaMIC5.

In this study, western blot assay revealed that recombinant EaMIC5 could be detected by the sera of chicken experimentally infected with *E. acervulina*. It indicated that EaMIC5 could be recognized by host immune system and induce the antibody response.

Identification of genes expressed in the life cycle of coccidian is very critical to understand the developmental biology of these parasites and MIC proteins including MIC5 are generally considered to be involved in cellular invasion. In this research, we demonstrated that MIC5 could be detected in sporozoite and merozoite stages of the life cycle. However, in sporozoite and merozoite the location of EaMIC5 differs. EaMIC5 is located mainly at the apical tip of the sporozoite and is similar to EtMIC2 in *E. acervulina* sporozoite [35], while in the merozoite EaMIC5 is diffused and located mainly at both poles. The reason for this difference maybe because the protein is confined to an intracellular location in resting sporozoites but is translocated to the parasite surface when it comes in contact with the cells [17].

This result proclaimed that the protein was conserved in the life cycle of this parasite, but the expression of this protein in other stages of *E. acervulina* and its detailed localization are worthy of further researches.

IL-4 is known to be a marker cytokine for Th2 cells, and it can promote B cell generation, differentiation, maturation, CD4⁺ cells differentiation to Th2 cells and the production of antibody [36]. In this study, EaMIC5 was found to be able to induce significant release of IL-4 and high levels of IgG antibody, indicating that EaMIC5 could enhance humoral response.

CD4⁺ and CD8⁺ cells have been shown to release a soluble forms known as sCD4 and sCD8 [37] and the sCD8 has long been used as a marker for the identification of active cytotoxic and suppressor cells [38]. The levels of sCD4 and sCD8 in serum are consistent with the count of CD4⁺ and CD8⁺ cell [39]. In this study, the concentration of sCD8 was significantly increased, suggesting that EaMIC5 was able to stimulate the recruitment of this T cell subpopulation. IFN- γ is the marker cytokine of Th1 type and the CD8⁺ cells are also well known for their ability to simultaneously produce high levels of IFN- γ in response to the parasite [40]. In this research, we attempted to investigate the involvement of IFN- γ in the immune response during immunization with EaMIC5. However, no

significant IFN- γ was detected. The inconsistency of sCD8 with IFN- γ need to be further researched. In this study, it was also found that the concentrations of sCD4 did not differ significantly between EaMIC5 group and control groups. This also needs to be further investigated.

Zhu et al [9, 41] reported that antigen cSZ-JN1 could induce significant level of IL-4 and TGF- β , and cSZ-JN2 could stimulate significant level of IL-2 10 days post second injection. They also found neither cSZ-JN1 nor cSZ-JN2 could incite significant level of the IFN- γ at the same time point. In our study, we measured the level of cytokines at 10 days post booster injection and found that EaMIC5 could induce significant level of IL-4, but not incite significant level of the IFN- γ at the time point. These were consistent with Zhu's results. In addition, our results showed that EaMIC5 could not result in significant level of IL-10, IL-17 and TGF- β . Song et al [8] indicated none of pVAX-LDH, pVAX-LDH-IFN- γ and pVAX-LDH-IL-2 could induce the increment of CD4⁺ and CD8⁺ at 7 days post primary and booster immunization. But we found EaMIC5 could incite significant level of sCD8 while the level sCD4 could not be promoted 10 days post booster. Moreover, Qi et al [42] found that EtMIC1 induced significant level of the IFN- γ transcript profiles at first immunization (at days 14), and reached the peak at third immunization (at days 28). All of the above results indicated that different antigens might induce different cytokine and CD4⁺ or CD8⁺ cells at different time points. Thus, the profiles of cytokines and T cells stimulated by EaMIC5 at different time points should be further investigated.

In our research, recombinant EaMIC5 resulted in an ACI more than 160 in the animal protective experiment, suggesting that EaMIC5 might be an effective vaccine candidate against *E. acervulina*. Recent reports demonstrated that DNA vaccine or co-delivery of cytokines as adjuvants could enhance the efficiency of vaccines to induce strong humoral and cellular immune responses [43, 44]. So the possibilities of the DNA vaccine of EaMIC5 or co-delivery with cytokines and other molecular adjuvants to enhance the immunity of EaMIC5 is worthy of further researches.

In recent studies, dual immunofluorescence staining of EtMIC3 and EtMIC5 on fixed and permeabilized sporozoites of *E. tenella* and the parasites apically attached to host cells showed that EtMIC3 located mainly at the apical tip of the sporozoite, whilst the majority of EtMIC5 labeling was detected just posterior to this region [45]. EtMIC3 could bind to sialic acid-bearing molecules on the epithelial cell surface of the host, and played key roles in the invasion of the sporozoite [45, 46]. However, it was reported that the eleven cysteine-rich receptor-like regions similar to the Apple domains of EtMIC5 was associated with the parasites membrane and provided a crucial link between cytoskeletal elements of the parasite and receptors on the surface of the host cell [47]. TgMIC5 was also retained on the parasite plasma membrane via its physical interaction with the membrane-anchored toxoplasma subtilisin 1 (TgSUB1) and directly regulated MPP2 activity or influenced MPP2's ability to access substrate cleavage sites on the parasite surface [48]. In our current research, we demonstrated that EaMIC5 was located mainly at the apical tip of the sporozoite and could be translocated to

the merozoite surface, and EaMIC5 could induce partial protection against the challenge of *E. acervulina*. All of these results suggested that EaMIC5 might also be involved in the cell invasion of *E. acervulina*. However, the exact role of EaMIC5 during cell invasion is still unclear and need further investigation.

In conclusion, we successfully obtained EaMIC5 full sequence based on the EST published on GenBank by the method of RACE. This protein was expressed in sporozoite and merozoite stages of the coccidian and could stimulate humoral and cellular responses to induce partial protection against the challenge of *E. acervulina*. Its location on sporozoite and merozoite and its protective function also indicated that EaMIC5 might be involved in the cell invasion. However, the exact roles of EaMIC5 in cell invasion need to be further studied.

Author Contributions

Conceived and designed the experiments: ZCZ XRL. Performed the experiments: ZCZ JWH MHL YXS SW LRL LXX RFY XKS. Analyzed the data: ZCZ. Contributed reagents/materials/analysis tools: ZCZ. Wrote the paper: ZCZ XRL.

References

1. Lillehoj HS, Jenkins MC, Bacon LD (1990) Effects of major histocompatibility genes and antigen delivery on induction of protective mucosal immunity to *E. acervulina* following immunization with a recombinant merozoite antigen. *Immunology* 71: 127–132.
2. Peek H, Landman W (2003) Resistance to anticoccidial drugs of Dutch avian *Eimeria* spp. field isolates originating from 1996, 1999 and 2001. *Avian Pathology* 32: 391–401.
3. Graat EAM, van der Kooij E, Frankena K, Henken AM, Smeets JFM, et al. (1998) Quantifying risk factors of coccidiosis in broilers using on-farm data based on a veterinary practice. *Preventive Veterinary Medicine* 33: 297–308.
4. Shah MA, Yan R, Xu L, Song X, Li X (2010) A recombinant DNA vaccine encoding *Eimeria acervulina* cSZ-2 induces immunity against experimental *E. tenella* infection. *Vet Parasitol* 169: 185–189.
5. Song H, Song X, Xu L, Yan R, Shah MAA, et al. (2010) Changes of cytokines and IgG antibody in chickens vaccinated with DNA vaccines encoding *Eimeria acervulina* lactate dehydrogenase. *Veterinary parasitology* 173: 219–227.
6. Xu Q, Song X, Xu L, Yan R, Shah MAA, et al. (2008) Vaccination of chickens with a chimeric DNA vaccine encoding *Eimeria tenella* TA4 and chicken IL-2 induces protective immunity against coccidiosis. *Veterinary parasitology* 156: 319–323.
7. Song X, Xu L, Yan R, Huang X, Shah MAA, et al. (2009) The optimal immunization procedure of DNA vaccine pcDNA-TA4-IL-2 of *Eimeria tenella* and its cross-immunity to *Eimeria necatrix* and *Eimeria acervulina*. *Veterinary parasitology* 159: 30–36.
8. Song H, Yan R, Xu L, Song X, Shah MAA, et al. (2010) Efficacy of DNA vaccines carrying *Eimeria acervulina* lactate dehydrogenase antigen gene against coccidiosis. *Experimental parasitology* 126: 224–231.
9. Zhu H, Xu L, Yan R, Song X, Tang F, et al. (2012) Identification and characterization of a cDNA clone-encoding antigen of *Eimeria acervulina*. *Parasitology* 139: 1711–1719.
10. Shah MAA, Song X, Xu L, Yan R, Song H, et al. (2010) The DNA-induced protective immunity with chicken interferon gamma against poultry coccidiosis. *Parasitology research* 107: 747–750.
11. Lee SH, Lillehoj HS, Jang SI, Lee KW, Kim DK, et al. (2012) Evaluation of novel adjuvant *Eimeria* profilin complex on intestinal host immune responses against live *E. acervulina* challenge infection. *Avian Diseases* 56: 402–405.

12. Kim DK, Lillehoj HS, Lee SH, Dominowski P, Yancey RJ, et al. (2012) Effects of novel vaccine/adjuvant complexes on the protective immunity against *Eimeria acervulina* and transcriptome profiles. *Avian Diseases* 56: 97–109.
13. Bansal A, Singh S, More KR, Hans D, Nangalia K, et al. (2013) Characterization of *Plasmodium falciparum* calcium-dependent protein kinase 1 (PfCDPK1) and its role in microneme secretion during erythrocyte invasion. *Journal of Biological Chemistry* 288: 1590–1602.
14. Carruthers VB, Tomley FM (2008) Microneme proteins in apicomplexans. *Molecular mechanisms of parasite invasion*: Springer. pp. 33–45.
15. Fujikawa K, Chung DW, Hendrickson LE, Davie EW (1986) Amino acid sequence of human factor XI, a blood coagulation factor with four tandem repeats that are highly homologous with plasma prekallikrein. *Biochemistry* 25: 2417–2424.
16. Chung DW, Fujikawa K, McMullen BA, Davie EW (1986) Human plasma prekallikrein, a zymogen to a serine protease that contains four tandem repeats. *Biochemistry* 25: 2410–2417.
17. Brown PJ, Billington KJ, Bumstead JM, Clark JD, Tomley FM (2000) A microneme protein from *Eimeria tenella* with homology to the Apple domains of coagulation factor XI and plasma pre-kallikrein. *Mol Biochem Parasitol* 107: 91–102.
18. Saouros S, Dou Z, Henry M, Marchant J, Carruthers VB, et al. (2012) Microneme protein 5 regulates the activity of *Toxoplasma* subtilisin 1 by mimicking a subtilisin prodomain. *J Biol Chem* 287: 36029–36040.
19. Periz J, Gill AC, Hunt L, Brown P, Tomley FM (2007) The microneme proteins EtMIC4 and EtMIC5 of *Eimeria tenella* form a novel, ultra-high molecular mass protein complex that binds target host cells. *J Biol Chem* 282: 16891–16898.
20. Klotz C, Gehre F, Lucius R, Pogonka T (2007) Identification of *Eimeria tenella* genes encoding for secretory proteins and evaluation of candidates by DNA immunisation studies in chickens. *Vaccine* 25: 6625–6634.
21. Gadde U, Chapman H, Rathinam T, Erf G (2011) Cellular immune responses, chemokine, and cytokine profiles in turkey poult following infection with the intestinal parasite *Eimeria adenoeides*. *Poultry Science* 90: 2243–2250.
22. Martin A, Awadalla S, Lillehoj H (1995) Characterization of cell-mediated responses to *Eimeria acervulina* antigens. *Avian diseases*: 538–547.
23. Bradford MM (1976) A rapid and sensitive method for the quantitation of microgram quantities of protein utilizing the principle of protein-dye binding. *Analytical biochemistry* 72: 248–254.
24. Yanming S, Ruofeng Y, Muleke C, Guangwei Z, Lixin X, et al. (2007) Vaccination of goats with recombinant galectin antigen induces partial protection against *Haemonchus contortus* infection. *Parasite immunology* 29: 319–326.
25. Chapman H, Shirley M (1989) Sensitivity of field isolates of *Eimeria* species to monensin and lasalocid in the chicken. *Research in veterinary science* 46: 114–117.
26. Morehouse NF, Baron RR (1970) Coccidiosis: evaluation of coccidiostats by mortality, weight gains, and fecal scores. *Experimental parasitology* 28: 25–29.
27. Johnson J, Reid WM (1970) Anticoccidial drugs: lesion scoring techniques in battery and floor-pen experiments with chickens. *Exp Parasitol* 28: 30–36.
28. Rose ME, Mocket A (1983) Antibodies to coccidia: detection by the enzyme-linked immunosorbent assay (ELISA). *Parasite immunology* 5: 479–489.
29. Talebi A, Mulcahy G (2005) Partial protection against *Eimeria acervulina* and *Eimeria tenella* induced by synthetic peptide vaccine. *Experimental parasitology* 110: 342–348.
30. Chapman H (1998) Evaluation of the efficacy of anticoccidial drugs against *Eimeria* species in the fowl. *International journal for parasitology* 28: 1141–1144.
31. Jeffers T (1974) *Eimeria acervulina* and *E. maxima*: incidence and anticoccidial drug resistance of isolants in major broiler-producing areas. *Avian diseases*: 331–342.
32. Merck Sharp & Dohme Company Ltd. (1998) The control of coccidiosis. MSD Technical Booklet. pp. 2–4.

33. Lillehoj HS, Ding X, Quiroz MA, Bevenssee E, Lillehoj EP (2005) Resistance to intestinal coccidiosis following DNA immunization with the cloned 3-1E *Eimeria* gene plus IL-2, IL-15, and IFN- γ . *Avian diseases* 49: 112–117.
34. Blake DP, Alias H, Billington KJ, Clark EL, Mat-Isa MN, et al. (2012) EmaxDB: Availability of a first draft genome sequence for the apicomplexan *Eimeria maxima*. *Mol Biochem Parasitol* 184: 48–51.
35. Sasai K, Fetterer RH, Lillehoj H, Matsuura S, Constantinoiu CC, et al. (2008) Characterization of Monoclonal Antibodies that Recognize the *Eimeria tenella* Microneme Protein MIC2. *Journal of Parasitology* 94: 1432–1434.
36. Kaplan MH, Schindler U, Smiley ST, Grusby MJ (1996) Stat6 is required for mediating responses to IL-4 and for the development of Th2 cells. *Immunity* 4: 313–319.
37. Zajkowska J, Hermanowska-Szpakowicz T, Swierzbinska T (2001) Concentration of soluble CD4, CD8 and CD25 receptors in early localized and early disseminated Lyme borreliosis. *Infection* 29: 71–74.
38. Tomkinson BE, Brown MC, Ip SH, Carrabis S, Sullivan JL (1989) Soluble CD8 during T cell activation. *The Journal of Immunology* 142: 2230–2236.
39. Willsie SK, Herndon BL, Miller L, Dew M (1996) Soluble versus cell-bound CD4, CD8 from bronchoalveolar lavage: correlation with pulmonary diagnoses in human immunodeficiency virus-infected individuals. *Journal of leukocyte biology* 59: 813–816.
40. Lu TX, Hartner J, Lim E-J, Fabry V, Mingler MK, et al. (2011) MicroRNA-21 limits in vivo immune response-mediated activation of the IL-12/IFN- γ pathway, Th1 polarization, and the severity of delayed-type hypersensitivity. *The Journal of Immunology* 187: 3362–3373.
41. Zhu H, Yan R, Wang S, Song X, Xu L, et al. (2012) Identification and molecular characterization of a novel antigen of *Eimeria acervulina*. *Molecular and Biochemical Parasitology*.
42. Qi NS, Wang YY, Liao SQ, Wu CY, Lv MN, et al. (2013) Partial protective of chickens against *Eimeria tenella* challenge with recombinant EtMIC-1 antigen. *Parasitol Res* 112: 2281–2287.
43. Shah MAA, Song X, Xu L, Yan R, Li X (2011) Construction of DNA vaccines encoding *Eimeria acervulina* cSZ-2 with chicken IL-2 and IFN- γ and their efficacy against poultry coccidiosis. *Research in veterinary science* 90: 72–77.
44. Shah MAA, Xu L, Yan R, Song X, Li X (2010) Cross immunity of DNA vaccine pVAX1-cSZ2-IL-2 to *Eimeria tenella*, *E. necatrix* and *E. maxima*. *Experimental parasitology* 124: 330–333.
45. Lai L, Bumstead J, Liu Y, Garnett J, Campanero-Rhodes MA, et al. (2011) The role of sialyl glycan recognition in host tissue tropism of the avian parasite *Eimeria tenella*. *PLoS pathogens* 7: e1002296.
46. Friedrich N, Santos JM, Liu Y, Palma AS, Leon E, et al. (2010) Members of a novel protein family containing microneme adhesive repeat domains act as sialic acid-binding lectins during host cell invasion by apicomplexan parasites. *Journal of biological chemistry* 285: 2064–2076.
47. Carruthers VB, Sibley LD (1999) Mobilization of intracellular calcium stimulates microneme discharge in *Toxoplasma gondii*. *Mol Microbiol* 31: 421–428.
48. Brydges SD, Zhou XW, Huynh MH, Harper JM, Mital J, et al. (2006) Targeted deletion of MIC5 enhances trimming proteolysis of *Toxoplasma* invasion proteins. *Eukaryot Cell* 5: 2174–2183.

荣誉证书

宋小凯同志的的学术报告《Induction of protective immunity against *Eimeria tenella*, *Eimeria necatrix*, *Eimeria maxima* and *Eimeria acervulina* infections using multivalent epitope DNA vaccines》被评为中国畜牧兽医学
会兽医寄生虫学分会第十三次学术研讨会优秀学术报告壹等奖。

特颁此证



荣誉证书

宋小凯教师

在2010—2011学年中，工作认真，成绩突出，
荣获森楠奖教金。

特发此证，以资鼓励！



森楠(江苏)生物技术研究有限公司
南京林业大学动物医学院
二〇一一年十一月

荣誉证书

宋小凯同志在动物医学院二〇一二年青年
教师授课竞赛中，荣获三等奖，特发此状，
以资鼓励。



南京农业大学动物医学院
二〇一二年四月十二日

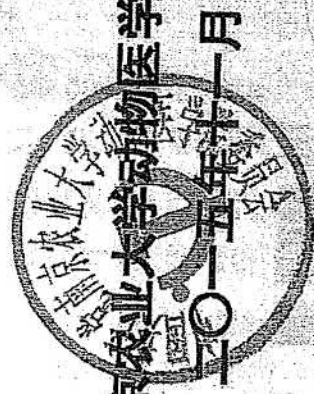
荣誉证书

宋小凯 老师在2014-2015学年中工作优秀，
表现突出，荣获 武汉回盛奖教金。

特发此证，以资鼓励！

武汉回盛生物技术有限公司

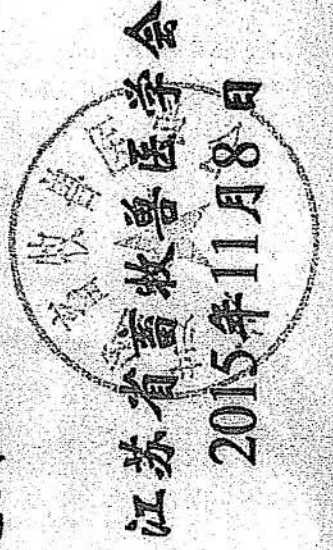
南京农业大学动物医学院



荣誉证书

宋小凯 同志：

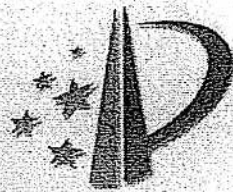
你撰写的《Induction of protective immunity against *Eimeria tenella*, *Eimeria necatrix*, *Eimeria maxima* and *Eimeria acervulina* infections using multivalent epitope DNA vaccines》一文在江苏省畜牧兽医学会60周年庆典暨学术年会上荣获优秀论文奖。



江苏省畜牧兽医学会

2015年11月8日

证书号第988205号



发明专利证书

发明名称：预防鸡巨型艾美耳球虫的免疫调节型DNA疫苗

发明人：李祥瑞；宋小凯；严若峰；徐立新；雷晨昱；宋鸿雁

专利号：ZL 2008 1 0234982.5

专利申请日：2008年11月12日

专利权人：南京农业大学

授权公告日：2012年07月04日

本发明经过本局依照中华人民共和国专利法进行审查，决定授予专利权，颁发本证书并在专利登记簿上予以登记。专利权自授权公告之日起生效。

本专利的专利权期限为二十年，自申请日起算。专利权人应当依照专利法及其实施细则规定缴纳年费。本专利的年费应当在每年11月12日前缴纳。未按照规定缴纳年费的，专利权自应当缴纳年费期满之日起终止。

专利证书记载专利权登记时的法律状况。专利权的转移、质押、无效、终止、恢复和专利权人的姓名或名称、国籍、地址变更等事项记载在专利登记簿上。

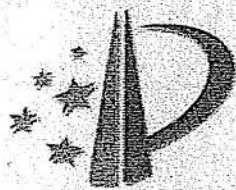


局长

田力普



证书号第984577号



发明专利证书

发明名称：预防鸡雏型艾美耳球虫的免疫调节型DNA疫苗

发明人：李祥瑞；徐立新；宋小凯；严岩峰；宋鸿雁

专利号：ZL 2008 1 0155079. X

专利申请日：2008年11月03日

专利权人：南京农业大学

授权公告日：2012年07月04日

本发明经过本局依照中华人民共和国专利法进行审查，决定授予专利权，颁发本证书并在专利登记簿上予以登记。专利权自授权公告之日起生效。

本专利的专利权期限为二十年，自申请日起算。专利权人应当依照专利法及其实施细则规定缴纳年费。本专利的年费应当在每年11月03日前缴纳。未按照规定缴纳年费的，专利权自应当缴纳年费期满之日起终止。

专利书记载专利权登记时的法律状况。专利权的转移、质押、无效、终止、恢复和专利权人的姓名或名称、国籍、地址变更等事项记载在专利登记簿上。



局长

田力善



证书号第1792697号



发明专利证书

发明名称：一种用于弓形虫感染的诊断抗原的应用

发明人：李祥瑞；徐立新；严若峰；宋小凯；李锐

专利号：ZL 2013 1 0124956.8

专利申请日：2013年04月11日

专利权人：南京农业大学

授权公告日：2015年09月16日

本发明经过本局依照中华人民共和国专利法进行审查，决定授予专利权，颁发本证书并在专利登记簿上予以登记。专利权自授权公告之日起生效。

本专利的专利权期限为二十年，自申请日起算。专利权人应当依照专利法及其实施细则规定缴纳年费。本专利的年费应当在每年04月11日前缴纳。未按照规定缴纳年费的，专利权自应当缴纳年费期满之日起终止。

专利证书记载专利权登记时的法律状况。专利权的转移、质押、无效、终止、恢复和专利权人的姓名或名称、国籍、地址变更等事项记载在专利登记簿上。

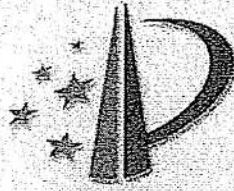


局长
申长雨

申长雨



证书号第 771411 号



发明专利证书

发明名称：一种鸡柔嫩艾美耳球虫复合免疫调节型 DNA 疫苗

发明人：李祥瑞；宋小凯；严若峰；徐立新

专利号：ZL 2007 1 0191695.6

专利申请日：2007 年 12 月 14 日

专利权人：南京农业大学

授权公告日：2011 年 05 月 04 日

本发明经过本局依照中华人民共和国专利法进行审查，决定授予专利权，颁发本证书并在专利登记簿上予以登记。专利权自授权公告之日起生效。

本专利的专利权期限为二十年，自申请日起算。专利权人应当依照专利法及其实施细则规定缴纳年费。本专利的年费应当在每年 12 月 14 日前缴纳。未按照规定缴纳年费的，专利权自应当缴纳年费期满之日起终止。

专利证书记载专利权登记时的法律状况。专利权的转移、质押、无效、终止、恢复和专利权人的姓名或名称、国籍、地址变更等事项记载在专利登记簿上。



局长

田力善



证书号第 1476513 号



发明专利证书

发明名称：一种鸡艾美耳球虫免疫调节型多价多表位 DNA 疫苗

发明人：李祥瑞；宋小凯；严若峰；徐立新；任喆

专利号：ZL 2011 1 0307305.3

专利申请日：2011 年 10 月 10 日

专利权人：南京农业大学

授权公告日：2014 年 09 月 03 日

本发明经过本局依照中华人民共和国专利法进行审查，决定授予专利权，颁发本证书并在专利登记簿上予以登记。专利权自授权公告之日起生效。

本专利的专利权期限为二十年，自申请日起算。专利权人应当依照专利法及其实施细则规定缴纳年费。本专利的年费应当在每年 10 月 10 日前缴纳。未按照规定缴纳年费的，专利权自应当缴纳年费期满之日起终止。

专利书记载专利权登记时的法律状况。专利权的转移、质押、无效、终止、恢复和专利权人的姓名或名称、国籍、地址变更等事项记载在专利登记簿上。



局长
申长雨

申长雨



证书号第 1588992 号



发明专利证书

发明名称：一种鸡球虫多价重组蛋白亚单位疫苗及其应用

发明人：李祥瑞；严若峰；徐立新；宋小凯；高云路

专利号：ZL 2013 1 0273603.4

专利申请日：2013 年 07 月 01 日

专利权人：南京农业大学

授权公告日：2015 年 02 月 18 日

本发明经过本局依照中华人民共和国专利法进行审查，决定授予专利权，颁发本证书并在专利登记簿上予以登记。专利权自授权公告之日起生效。

本专利的专利权期限为二十年，自申请日起算。专利权人应当依照专利法及其实施细则规定缴纳年费。本专利的年费应当在每年 07 月 01 日前缴纳。未按照规定缴纳年费的，专利权自应当缴纳年费期满之日起终止。

专利证书记载专利权登记时的法律状况。专利权的转移、质押、无效、终止、恢复和专利权人的姓名或名称、国籍、地址变更等事项记载在专利登记簿上。



局长
申长雨

申长雨



